NASA TECHNICAL TRANSLATION

NASA TT F-684

PHYSICAL PROPERTIES OF ROCKS AT HIGH TEMPERATURES

by A. P. Dmitriyev, L. S. Kuzyayev, Yu. I. Protasov, and V. S. Yamshchikov

"Nedra" Press, Moscow, 1969

NATIONAL AERONAUTICS AND SPACE ADMINISTRATION • WASHINGTON, D. C. • JUNE 1972

PHYSICAL PROPERTIES OF ROCKS AT HIGH TEMPERATURES

By A. P. Dmitriyev, L. S. Kuzyayev, Yu. I. Protasov,
and V. S. Yamshchikov

Translation of "Fizicheskiye svoystva gornykh
porod pri vysokikh temperaturakh."
"Nedra" Press, Moscow, 1969

NATIONAL AERONAUTICS AND SPACE ADMINISTRATION

For sale by the National Technical Information Service, Springfield, Virginia 22151
$3.00

ANNOTATION

This monograph sets forth the results of theoretical and experimental studies of the strength, elastic, acoustic, thermal, and electromagnetic properties of rocks as a function of temperature.

The authors give a detailed description of methods for investigating the physical properties of rocks at high temperatures and give examples of the use of the dependence of physical properties of rocks on temperature for solving mining problems.

The book is intended for scientific workers, engineers and technicians engaged in the mining and processing of minerals and may also be useful to college students concerned with problems in the geology, mineralogy, chemistry and physics of rocks, and the methods and equipment employed in extracting and processing minerals.

Tables 38, illustrations 67, bibliography 57 items.

INTRODUCTION

The considerable increase in industrial production and the need for increasing work productivity called for in the Directives of the Twenty-Third Congress of the Communist Party Soviet Union set the principal tasks in the field of mineral extraction and processing.

New, highly productive engineering methods and equipment for working mineral deposits, based on advances in modern physics, chemistry, hydro- and thermodynamics, geophysics, geochemistry, electronics, and other sciences, have been broadly developed during recent years.

Thermal, electrophysical and other methods for destroying and strengthening rocks and acoustic and electromagnetic methods for studying and monitoring the rock mass are being introduced in mining work and physicochemical methods of mineral extraction are being developed.

Thermodynamics will play a significant role in solving many problems in the mining industry and the possibilities of its application are expanding.

Thermal methods for rock fracturing are already being used in industry. The thermal ("fire") and low-frequency electrophysical methods have exhibited a high efficiency in the drilling and fragmenting of hard rocks. Rocks have been experimentally fractured by electromagnetic fields of different frequencies, electric arc torches, and other methods.

Investigations of the behavior of directed change in mechanical, electric and magnetic properties occupy a special role. These investigations were the basis for developing methods for the thermomechanical fracturing of rocks and methods for thermal and electrophysical strengthening of rocks and physicochemical methods and equipment for the extraction of sulfur, copper, coal and fuel shales. Some laws of change in the properties of rocks (electric, elastic and magnetic) in a high-temperature field can be used for obtaining information on change in state of a rock mass.

At the same time, solution of the examined problems and accordingly, the broad introduction of new technical solutions in industry are being held back to a certain degree by an inadequate use of mathematics, physics and computers.

This can be attributed to a poor knowledge of the physical properties of rocks and the conditions for the occurrence of physicochemical processes in them.

A study of the physical properties of rocks and the patterns of their change under the influence of different factors will create conditions for formulating appropriate control algorithms and the extensive use of methods for mathematical and physical modeling of processes in rocks.

Many studies have been devoted to the multisided investigation of the physical properties of rocks; these have been published in the Soviet and foreign literature. However, inadequate attention has been given to the dependence of the physical properties of rocks on temperature applicable to mining industry methods.

The material in this book is based for the most part on experiments and theoretical investigations made during recent years in the rock physics problem laboratory at the Moscow Mining Institute.

The book consists of three chapters, incorporating the results of the strength and elastic, thermal and electric properties of some rocks. Each chapter discusses theory and research methods and changes in rock properties in a high-temperature field; each describes original experimental apparatus based on the use of advances in physics and electronics and developed in our laboratory.

Analysis of the accumulated material made possible an attempt at some systematization of rocks on the basis of the patterns in change in their physical properties for the specific conditions of interaction with a temperature field.

Particular attention is devoted to problems relating to the practical application of the research results; these are fundamental in a study of the mechanisms of thermal and electric fracturing.

The book was written by specialists in the Department of Rock Physics at the Moscow Mining Institute. Chapter I was written by V. S. Yamshchikov and A. P. Dmitriyev; Chapter II was written by A. P. Dmitriyev and L. S. Kuzyayev; Chapter III was written by Yu. I. Protasov.

The authors express deep appreciation to the specialists in the Rock Physics Department and Problems Laboratory at the Moscow Mining Institute for assistance rendered in preparing the book for publication.

TABLE OF CONTENTS

Chapter I

STRENGTH AND ELASTIC PROPERTIES OF ROCKS AT HIGH TEMPERATURES

1. Strength Properties of Rocks

/5*

The effectiveness and field of rational applicability of electrophysical, thermal, and thermomechanical methods for destroying rocks are determined to a great extent by the physicomechanical properties of the latter and primarily by their strength, elastic and viscoelastic properties. In addition to the absolute values of the properties, their dependence on temperature is also taken into account in the computations.

Among the strength properties determining the resistance of rocks to destruction under the influence of different factors are compression strength, tensile strength, shear strength, bending strength, and hardness.

The values of the strength indices are dependent on porosity, micro- and macrofissuring, strength of the minerals making up the rocks, and the bonds between them. These same factors determine the strength properties of rocks as a function of temperature.

Since ancient times, researchers have been interested in the possibility of controlling the strength properties of rocks (strengthening or weakening) under the influence of a temperature field. Man probably first came face to face with the possibility of changing the strength of rocks when firing clay and kaolin. With heating of these rocks to a temperature of 600°C their strength is increased by several times with a simultaneous decrease in plasticity.

The phenomena of strengthening and weakening rocks under the influence of high temperatures were also observed in studies of other types of rocks. However, a systematic study of this matter was only recently initiated in relation to the development of new destruction methods and study of rock behavior at great depths.

---

* Numbers in the margin indicate pagination in the foreign text.

Methods and Equipment for Investigating Rocks

Methods for determining the compression strength and tensile strength and the indices of rock hardness have come into the widest use in studying the strength properties of rocks in a high-temperature field.

The testing of rocks under uniaxial compression (crushing) is the simplest method for evaluating rock strength. In this case the compression strength is defined as the maximum compressive stress acting on the sample at the time of its destruction. /6

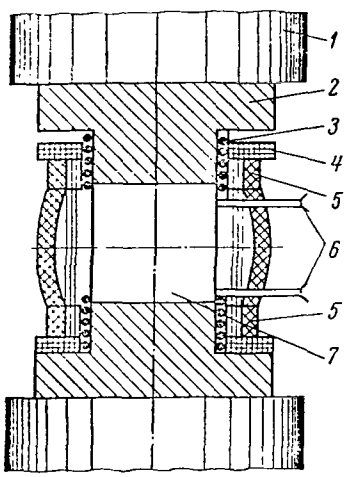

Figure 1. Diagram of testing of apparatus for investigating compression strength of rocks during heating: 1- press punches; 2- working punches; 3- asbestos cord; 4- rings; 5- electric furnace; 6- thermocouples; 7- sample.

The method for testing the compressive strength of rocks at high temperatures is as follows.

Prior to the tests the samples are heated to the initial temperatures in special apparatus which can be situated both in the press and outside it. In the latter case [1, 2], an electric muffle furnace is used for these purposes. With heating to the required temperature the rock samples (with the thermometers inserted in them) are removed from the furnace by manual manipulators and placed under the test press. The temperature decrease in the sample is registered with thermocouples. In order to reduce heat exchange between the sample surface and the surrounding medium during the tests its lateral surfaces are insulated with asbestos cement linings.

The experiments show that this variant for heating samples prior to tests (for standard rates of loading) makes it possible to determine the qualitative dependence of strength on temperature.

A special apparatus is used [3] (Figure 1) when heating rock samples in a press. An electric furnace surrounding the sample is cut into the network through an autotransformer. The sample is heated uniformly and is held at the stipulated temperature for not less than 20 minutes. Then the sample is loaded until destructive fractures appear.

Loads and deformations must be continuously measured in order to evaluate the elastic and plastic deformations developing under the influence of temperature during the tests of rocks for compression and dilatation. However, it is impossible to use for this purpose wire resistance detectors (strain gauges) cemented to the lateral surfaces of the sample when high temperatures are involved. An apparatus making it possible to measure deformations without cementing strain gauges to the sample [5] can be used for automatically recording deformations and loads during rock compression tests. Figure 2 is a diagram of this apparatus. Loads during compression of the sample, 1, with the press, 2, are registered with a slide-wire potentiometer, 3, and deformations are registered using strain gauges. /7

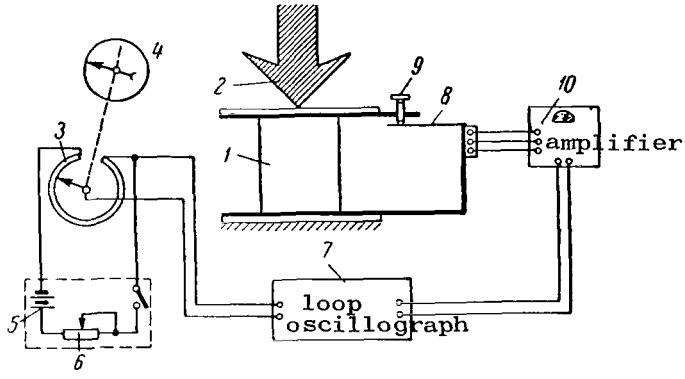

Figure 2. Diagram of apparatus for automatically recording loads and deformations.

The slide-wire potentiometer is rigidly connected to the scale of the indicator, 4, of press load and receives current from a battery, 5, with a voltage of 6 to 15 V. For selecting an electric signal corresponding to the maximum compressive load the control panel has an adjustable potentiometer, 6. The signal characterizing the load, imparted to the slide wire, is fed to a multi-loop oscillograph, 7, on which the changes in the axial load are registered.

A cantilever apparatus was used for measuring deformations using strain gauges without cementing them to the sample. A support with a spring plate, 8, (grade 12KhN3A steel) is rigidly attached to the fixed base plate of the press. The upper moving plate is rigidly attached to a steel cantilever plate on which there is a micrometer screw, 9, which comes into contact with the spring plate.

Working and compensating strain gauges, parts of the general bridge measuring system, are glued on the plate. The signal from bridge imbalance, caused by change in sample length under the press, is fed to the strain gauge amplifier 10, type TA-5, and then to a loop oscillograph. Before beginning the experiments the system must be calibrated using a two-micron mechanical strain gauge indicator. The site for gluing the working strain gauge on the spring plate is selected taking into account the possibilities of signal amplification.

Thus, this system makes possible automatic registry of the axial force and deformations. The results of the experiments are presented in the form of oscillograms. Comparison with the results of measurements made with other measurement systems (for example, when using a dynamometer-type ring with strain gauges /8 for registering the load force) indicates their good agreement.

Further processing of the registered oscillograms makes it possible to construct "stress-strain" diagrams from which by well-known graph analysis methods it is possible to determine the compression strength, elastic limit, elastic modulus of the first kind, plasticity coefficient, etc.

Tensile strength tests of rocks can be made by direct and indirect methods.

When using the direct method based on the dilatation of the sample (rod) in the direction of its axis it is difficult to ensure a uniform stressed state in the middle of the sample. In addition, bending stresses can arise during the tests.

The indirect method (core fracturing) makes it possible to determine the index of resistance of rocks to dilatation in a different way. In this case the rock sample is placed under the press plate along the diametral (in a case when cylindrical samples are used) plane and compressive load is tested. The method is based on solution of the Hertz problem in elasticity theory concerning the distribution of stresses in a thin circular disk compressed along the diameter by two forces. In determining the tensile strength for fracturing of rocks

having a Poisson coefficient 0.1 to 0.25 the following formula is used [6]:

$$\sigma_{ten} = \frac{P}{F}, \text{ kg/cm}^3; \qquad (I.1)$$

where

P is the force at which the sample is fractured, kg;

F is the area of the diametral plane of the sample (the product of the length and diameter of the sample), cm^2.

Heating of the sample prior to the test is by one of the two variants described above.

The indentation of a punch can be used in studying the effect of temperature on rock hardness. In this case the test method described in detail in [1] is as follows.

The punch is placed on the rock sample and the press ram is raised to the stop in the lower base of the upper press support. Then the sample is loaded and the penetration of the punch is registered.

In this case the index of rock hardness is the maximum force on the punch related to a unit surface of its end plane at the time of the first chipping off of the rock:

$$P_{punch} = \frac{P}{S}, \qquad (I.2)$$

where

P_{punch} is hardness under the punch, kg/mm^2;

P is the load at the time of chipping off of the rock, kg;

S is the punch area, mm^2.

In testing samples by the punch indentation method it is best to use a UMTP-3 instrument for which the "stress-strain" curves are automatically registered. Hard alloy cylindrical or conical punches are used, depending on the rock hardness. The resulting deformation curves are used in determining indentation hardness, yield stress and the conventional plasticity coefficient [1]. /9

An important problem in testing rock samples at high temperatures is the choice of a rational time for holding the sample, heated to a definite temperature, in the furnace for the purpose of creating a uniform temperature distribution within it. Experimental investigations revealed that the time

dependence of compression strength of rock samples heated to a definite temperature changes sharply (up to 30 to 50%) during the initial heating period (up to 20 to 30 minutes); with further heating the strength remains almost constant. Accordingly, it is recommended that the sample be held in a heating device for 20 minutes or more prior to testing, with the provision that the heating temperature be kept constant [7].

Analysis of Strength Properties of Rocks as a Function of Temperature

The experimental results show that the nature of change in the strength properties of rocks is not common for all types of rocks. Depending on the peculiarities of the mineralogical composition and structural bonds in the rocks the change in the strength properties during heating occurs in accordance with different laws. In this case the nature of the dependence on temperature for different strength indices (compression and tensile strength, hardness, etc.) obtained for the same rock usually coincides.

Study of the effect of high temperatures on strength indices makes it possible to classify all rocks into groups on the basis of the nature of temperature dependence:

rocks in which the strength indices increase to some maximum with a temperature increase and then decrease;

rocks in which with a temperature increase the strength indices immediately decrease or change little to certain temperatures and then decrease.

It should be noted that in rocks in the first group during the initial period (to a temperature of 100 to 160°C) some decrease in strength indices is also usually observed.

For example, the first group includes quartzite, sandstone and serpentinite; the second group includes limestone, sulfurized ores, apatite ore, etc.

Rock tests for hardness [1] with a temperature change from 20 to 400-600°C revealed that the hardness of Shokshinskiy quartzite, quartzy sandstone, and microclinic granite increases somewhat, whereas the hardness of microgabbro remains almost unchanged.

It was also established that the relative increase in the hardness of monomineral rocks (Shokshinskiy quartzite) was somewhat higher than for polymineral rocks. /10

Figure 3 shows that for rocks in the first group there is a characteristic "critical" temperature region in which the strength indices attain a maximum value. For example, for sandstones the tensile strength increased by a factor of approximately 1.6 with a temperature change to 800°C in comparison with room temperature and then decreased. A marked strength increase is observed at temperatures 600 to 800°C. At still higher temperatures plastic deformations appear in the rocks, resulting in fracturing. One of the factors indicating a plastic nature of destruction is the absence of the characteristic cracking and breaking away of pieces at the time of destruction.

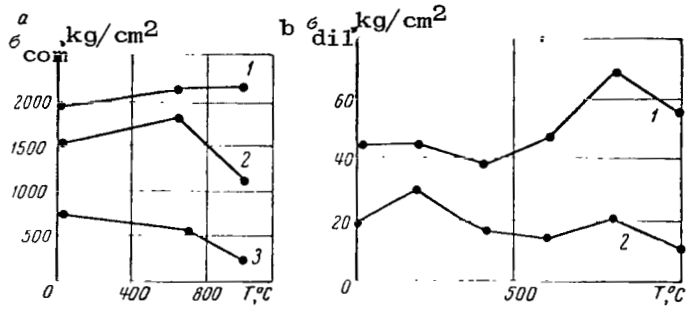

Figure 3. Graphs of dependence of change in compression strength (a) and tensile strength (b) on temperature: 1- sandstone; 2- gabbro; 3- marble.

TABLE 1. CHANGE IN COMPRESSION STRENGTH WITH HEATING OF ROCKS FROM THE ROZDOL'SKOYE DEPOSIT

Rocks	Density γ, g/cm^3	Porosity P, %	Compression strength (kg/cm2) at temperature	
			20°	150°
Hard sulfurized limestone, ore type - druse-phenocrystic perpendicular to stratification	2.49	5.36	270	90
Hard unsulfurized limestone, perpendicular to stratification	2.72	14.0	796	461
Hard gray unsulfurized banded limestone, parallel to stratification	2.51	5.95	357.1	> 20
Hard gray sulfurized limestone, parallel to stratification	2.38	8.41	248	> 20

In the second group of rocks the decrease in strength with heating can be attributed in part to chemical transformations in the presence of admixtures which are slightly resistant to heating. For example, limestone, consisting for the most part of $CaCO_3$, loses strength as a result of decomposition and release of CO_2: /11

$$CaCO_3 = CaO + CO_2. \qquad (I.3)$$

The presence of sulfur admixtures in limestones leads to a decrease in strength even with heating of 130 to 150°C (Table 1).

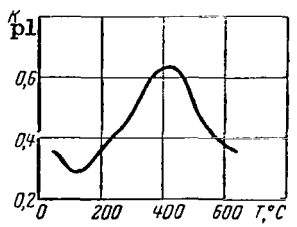

Figure 4. Graph of dependence of change in plastic deformations of marble on temperature.

A major role in reducing the strength indices of rocks with heating is also played by the natural plasticity of rocks preventing an increase in the breaking points and developing under the influence of high temperatures. Figure 4 shows the dependence of plastic deformations of marble on temperature. In this case plasticity is estimated from the plasticity coefficient, equal to the ratio of

work in the region of plastic deformations to the total work of deformations on the "load-deformation" diagram obtained during simultaneous registry of loads and deformations by the method described above.

This nature of the development of plastic deformations in marble during heating corresponds to the nature of change in elasticity in this same temperature range.

Reasons for Change in Rock Strength at High Temperatures

The nature of change in the strength characteristics of rocks at high pressures is influenced by external and internal factors, among which mineralogical composition, properties of structural bonds and bedding conditions are decisive. However, in most cases it is impossible to isolate any single decisive factor even for rocks of the same type (Table 2)[1].

The nature of change in rock strength with a temperature increase is dependent on their structural characteristics, thermal stability of minerals and cements constituting the rock, and other factors.

In the case of holocrystalline rocks the mechanism of decrease in strength with heating can be attributed to a change in the role of different factors in the structure accompanying a temperature increase (Figure 5).

Assuming that during the heating of rocks their strength changes as a function of the hardening or softening of minerals and their boundaries, the entire heating scale can be divided into three regions with the initial boundary temperatures T_0, T_1 and T_2. According to the results of numerous experiments, /12 each of the regions can be characterized as follows:

first temperature region (T_0-T_1): the dependence of rock strength on temperature is determined by the thermal stability of minerals;

second temperature region (T_1-T_2): the dependence of rock strength on temperature is determined by the state of the boundary between the minerals;

third temperature region ($T_2 \rightarrow \infty$): the nature of the change in rock strength is determined by the change in mineral strength.

1. The experimental data in Tables 1 and 2 were provided by Engineer O. N. Tret'yakov.

The possible nature of changes in the strength indices of different rock types can be postulated on the basis of this classification.

If the change in rock strength during heating is examined with this hypothesis in mind, the rocks in which the strength of the component minerals decreases sharply in the first temperature region should already be destroyed at a relatively low temperature and the boundaries between the minerals should exhibit a very slight resistance. For example, such a mechanism can explain the decrease in strength with the heating of limestones in which the decomposition of minerals occurs at relatively low temperatures.

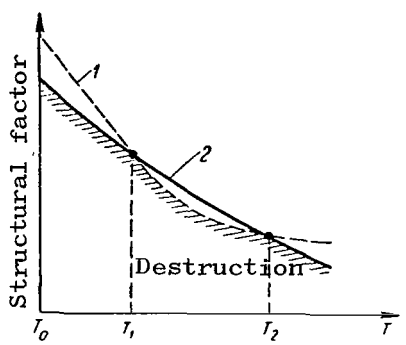

Figure 5. Diagram of effect of different factors on rock strength during heating: 1- boundary between minerals; 2- mineral.

However, if the strength of rocks with heating to temperatures corresponding to the boundary of the first temperature region does not decrease and the component minerals have a high thermal stability, with a further temperature increase, that is, in the second temperature region, the nature of strength change will be determined for the most part by the state of the boundary between the minerals. The following phenomena are characteristic for rocks whose strength in a high-temperature field is determined by factors corresponding to /13

TABLE 2. CHANGE IN COMPRESSION STRENGTH OF APATITE ORES FROM THE KHIBINSKOYE DEPOSIT DURING HEATING

Rock	Density γ, g/cm^3	Porosity P, %	Heating temperature, °C			
			20	100	200	300
Urtite	2.92	12.6	298	227	283	353
Poor ore parallel to stratification	2.87	5.55	904	606	385	270
Poor ore perpendicular to stratification	2.93	14.6	935	535	418	-
Rich ore	3.1	9.6	643	1051	837	418

the second temperature region. With a temperature increase there is thermal expansion of minerals having dissimilar values of the coefficient of linear thermal expansion in different crystallographic directions. Volume expansion of the minerals forming the rock leads to a decrease in the distance between the interfaces of the individual minerals and an increase in their mutual attraction. In this case the strength of the bonds increases and therefore the strength properties of rocks also are increased to a definite limit. At the same time, anisotropy of the minerals leads to a gradual development of relaxation phenomena at the boundary between the minerals. Nonuniformly increasing with a temperature increase, these phenomena become fundamental at a definite stage and lead the rock to destruction. However, the effect of thermal oscillation of atoms at these temperatures is still too small to break the bonds within the minerals.

A similar mechanism determines the nature of strength change in such minerals as granites and quartzites. However, for cemented rocks the mechanism explaining the nature of change in the temperature dependence is far more complex.

Effect of Cooling on the Strength of Preheated Rocks

This matter is of great practical interest because it is characteristic for the thermal and electrothermal fracturing of rocks in flooded boreholes and also for the thermomechanical fracturing methods.

The following cases of change in the strength of preheated rocks during their subsequent cooling can be distinguished:

1) cooling in air;

2) cooling in water.

It was established that slow cooling of a preheated rock in the air does not significantly reduce its strength increase acquired during the heating process. This can be attributed to the fact that the bond between minerals increasing during heating is also partially retained in a gradually cooled rock.

During rapid cooling of a rock, and particularly with cooling in the water, the following phenomenon is observed. Abrupt cooling of a heated rock in a stressed state leads to an instantaneous ("dynamic") compression of the minerals in the surface layers. The nonuniformity of the stressed field is intensified and as a result the intercrystalline bonds are broken, that is, microcracks

appear and these lessen the strength properties of the rocks.

The strength of preheated rocks is more intensively reduced under the influence of abrupt cooling by water. In this process microcracking develops as a result of rapid cooling, and in addition there is an additional destruction due to wetting and adsorption. /14

The adsorption fluid (water) penetrates through minute microcracks in the surface layer into the depths of the rock and produces a wedge effect, thereby weakening the intermolecular bonds between the interfaces. The microcracking forming during abrupt cooling, in combination with the water wedge and adsorption effect, results in a considerable weakening in rock strength.

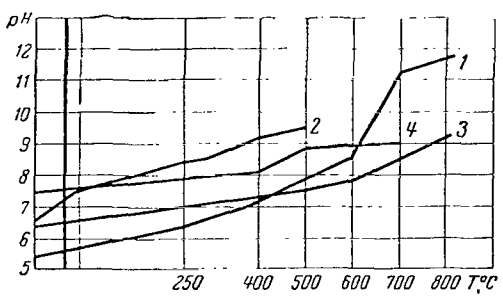

Figure 6. Effect of rock heating on change in pH of cooling medium: 1- feldspathic horneblende; 2- marble; 3- granite; 4- granodiorite.

The experiments reveal [8] that with abrupt water cooling of rocks preheated to a temperature of 600°C their strength properties are reduced by a factor of two or more.

It should be noted that during interaction between water and heated rock the physical process of strength weakening is accompanied by a chemical process leading to the formation of alkaline solutions. The formation of solutions occurs more rapidly with an increase in heating temperature of different rocks (marble, granite, granodiorite, and others). Figure 6 is a graph showing the dependence of pH, an evaluation of the degree of formation of an alkaline solution, on rock heating temperature [8].

Joint Effect of High Temperature and Pressure on the Strength Indices of Rocks

This problem is of practical interest in working minerals at great depths, during the drilling of deep holes, and in other cases in which a different combination of pressures and temperatures is encountered (hydrostatic pressure varies from 0 to 2000 to 3000 kg/cm^2 and temperature from room temperature to 200-500°C). Geologists and geophysicists are also devoting much attention to this matter [9].

Special apparatus is used in testing rocks under the joint influence of high temperatures and pressures. One of them (Figure 7) described by D. Griggs [10], makes it possible to develop a pressure up to 5000 kg/cm^2 with a temperature change up to 800°C. A rock sample is placed within a high pressure chamber filled with nitrogen, argon or carbon dioxide which are used in imparting different pressures to the sample during simultaneous internal heating of the latter. /15

Studies have shown that heating at a constant hydrostatic pressure exerts a different effect on different types of rocks.

Most rocks exhibit a decrease in tensile strength with a temperature increase; some of them are also characterized by a plasticity increase.

Figure 8 illustrates the dependence of the strength and deformation characteristics of rocks on temperatures at hydrostatic pressure (about 1000 kg/cm^2); these curves were constructed using data given in [11].

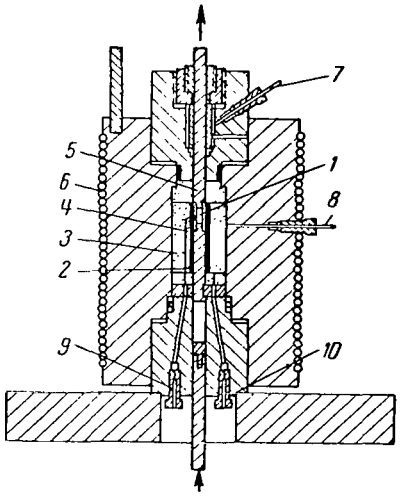

Figure 7. Apparatus for testing rocks at hydrostatic pressure up to 5000 kg/cm^2 and temperatures up to 800°C: 1- rock sample; 2- heating coil; 3- pyrophyllite lining; 4- thermocouple; 5- punch; 6- cooling coil; 7- inlet for compacting pressure; 8- inlet for working pressure; 9- electric lead-in for thermocouple; 10- electric lead-in for heating coil.

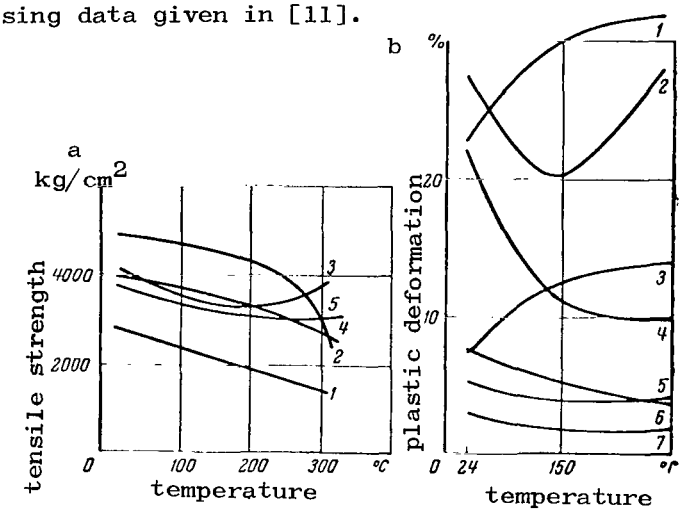

Figure 8. Curves for the dependence of tensile strength (a) and plastic deformation (b) of rocks on temperature for hydrostatic pressure of 1000 kg/cm^2: 1- Yul'skiy marble; 2- limestone; 3- anhydrite; 4- aleurolite; 5- dolomite; 6- clay shale; 7- sandstone.

At a constant heating temperature the boundary between brittle and plastic behavior of rocks varies as a function of the applied pressure and the type of deformation (compression or dilatation). For example, investigations on limestones at a constant temperature and with different hydrostatic pressures [12] /16 revealed that during dilatation plastic flow occurs at a higher hydrostatic pressure than during compression. The transition from brittle fracturing to plastic deformation occurs at lesser hydrostatic pressures when the temperature is increased.

2. Elastic Properties of Rocks

Rock elasticity is characterized by: the elastic modulus (Young's modulus) E, representing the proportionality factor between the effective longitudinal stress and the corresponding relative strain; the shear modulus G, relating shearing stress and shear deformation; the modulus of hydrostatic pressure K, which is a proportionality factor between hydrostatic pressure and the relative decrease in volume; the Poisson coefficient μ, which is proportional to relative longitudinal extension and lateral contraction of the sample.

The indices of rock elasticity for rocks are related to one another by the following expressions:

$$K = \frac{E}{3(1-2\mu)}; \qquad (I.4)$$

$$G = \frac{E}{2(1+\mu)}. \qquad (I.5)$$

Rock elasticity is dependent for the most part on elasticity of the component minerals, density, porosity and other factors.

Rock elasticity exerts a great influence on rock destructibility, which under thermal or electrophysical influences is determined by the intensity of developing thermoelastic stresses. These stresses at any point of the volume to be destroyed are dependent on temperature distribution, body configuration and physical constants: elastic modulus E, coefficient of linear expansion β, and Poisson coefficient μ. In addition to heat conductivity, the elastic modulus and coefficient of linear expansion are of the greatest interest.

When computing thermoelastic stresses it is usually assumed that the physical properties of the rocks are not dependent on temperature. In actuality,

this assumption can be considered correct only in a relatively small range of temperature change and then not for all rocks. For this reason study of the elastic properties of rocks at high temperatures (and particularly in their temperature dynamics) is of great practical and theoretical importance.

Acoustic and ultrasonic research methods have been used extensively recently in studying the elastic properties of rocks as a function of temperature. Under stipulated test conditions these are the only ones employable for measuring unrelaxed elastic parameters of rocks. /17

Despite its timeliness, the study of the effect of temperature on the elastic properties of rocks has not been given adequate attention.

Investigations of this problem have found practical application in solving problems in geophysics and geology [13, 14].

Methods for Determining the Elastic Properties of Rocks at High Temperatures

Static and dynamic methods can be used for investigating the elastic properties of rocks in a temperature field.

In the static test method the measurement problem reduces to determining the change in the size of rock samples under the influence of the applied stresses.

The static elastic moduli are determined during compression or dilatation of the samples exposed to uniform heating. The elasticity parameters are computed with a low accuracy. The principal shortcoming of the static method is that the elasticity parameters are always relaxed, that is, superposed on purely elastic deformation there are deformations caused by creep and elastic lag. As a result, errors in computing the elasticity parameters increase with a temperature increase.

In addition, the elasticity indices determined by static methods are dependent on the duration of the tests and the nature of the loads. For this reason static methods are almost never used in studying elasticity indices in a high-temperature field.

In studies of rocks at high temperature increasing use is being made of dynamic test methods and especially acoustic and ultrasonic methods.

Dynamic test methods are based on the physical phenomenon of propagation of elastic oscillations in rocks.

Dynamic research methods have the following advantages:

absence of any destructive effects on the tested sample (the intensity of the used oscillations is tenths and hundredths W/cm^2);

possibility of an unlimited repetition of tests, thereby increasing the accuracy of these indices;

rapidity of the tests and the virtually "instantaneous" availability of the results;

possibility of investigating the elastic and other properties in their temperature dynamics.

A distinguishing characteristic of dynamic methods is that the test results are obtained in the form of indirect indices (velocity or time of propagation of elastic waves, characteristic frequency of sample oscillations, etc.). /18

Resonance and ultrasonic pulse methods are the most widely used test methods.

Longitudinal oscillations and flexural vibrations. In this case the elasticity modulus is determined using the formulas [15]:

for longitudinal oscillations

$$E = 4\rho l^2 f_{sam}^2; \tag{I.6}$$

for flexural vibrations

$$E = 1{,}639 \cdot 10^{-8} \left(\frac{l}{d}\right)^2 \frac{m}{l} f_{sam}^2, \tag{I.7}$$

where

l, d, m are the length, diameter and mass of the sample;

f_{sam} is the resonance frequency of sample oscillation, Hz;

ρ is rock density, g/cm^3.

The experimental apparatus used for each type of oscillations varies in design [16].

The apparatus schematically represented in Figure 9 has come into broad use when using the longitudinal oscillations of a sample which is heated.

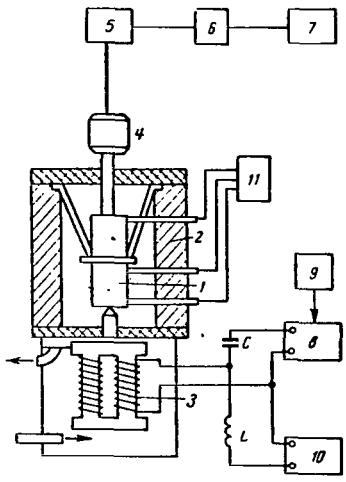

Figure 9. Block diagram of resonance method for measuring the elastic modulus for longitudinal oscillations:
1- sample; 2- furnace for heating; 3- magnetostriction vibrator; 4- piezoelectric transducer; 5- amplifier; 6- oscillograph; 7- quartz heterodyne; 8- power amplifier; 10- source of dc current; 11- potentiometer for measuring emf.

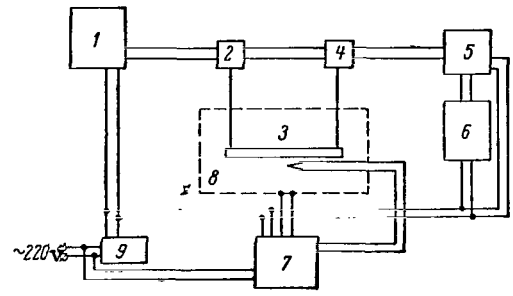

Figure 10. Block diagram of resonance method for measuring elastic modulus for flexural vibrations:
1- audio frequency oscillator; 2- emitter; 3- sample; 4- receiver; 5- amplifier; 6- oscillograph; 7- thermal insulation; 8- heating furnace; 9- voltage stabilizer.

The sample, 1, arranged vertically in the furnace, 2, is connected to the magnetostriction oscillator, 3, placed in a tank through which water flows. For registering the resonance the sample oscillations are transmitted to the piezoelectric transducer, 4, and then through the amplifier, 5, to the oscillograph, 6. The frequency of the oscillations which can be created by the oscillator in this case is 15 to 50 kc/sec. /19

Figure 10 is a block diagram of the apparatus for measuring the elastic modulus by the resonance method. It is based on measurement of the resonance frequency of flexural vibrations of a rod fabricated from rock [14]. The sample is placed by means of suspensions of thin Nichrome wire in the heating space of a demountable electric furnace with a heat regulator. At the same time the

suspension members perform the role of a coupling between the oscillation exciter, rock sample and oscillation receiver. The oscillation converters are outside the electric furnace. In addition, they are protected against the heat flux by special screens in which water circulates. The accuracy in determining the elastic modulus by this method at high temperatures is 3 to 8%.

Resonance methods make possible a rather simple creation of uniform heating conditions. However, experiments have shown that well-processed samples with identical geometric parameters must be selected for the tests. We should also mention the difficulty in taking into account the errors arising due to a decrease in the quality of the mechanical oscillatory system.

Pulsed ultrasonic research methods have come into the widest use for these purposes; they make it possible to carry out measurements more simply and with a high accuracy.

The methods for determining ultrasonic velocity for determining elasticity parameters remain the same as at room temperatures.

The velocities of propagation of elastic waves excited by sonic or ultrasonic oscillations are dependent on the elastic properties of the medium. Accordingly, the elastic properties of a homogeneous isotropic medium can be simply determined if some two velocities of elastic wave propagation are known. Rocks have elasticity of volume and elasticity of configuration and therefore they are capable of transmitting several different types of waves, the most important of which are longitudinal, transverse and surface waves.

The type of wave propagating in the rock sample is determined by the nature of the excited oscillations, configuration of the investigated sample, and its size in comparison with the wavelength.

The velocities of propagation of elastic waves are determined using the following formulas:

velocity of a longitudinal wave in an unbounded medium (wavelength less than the transverse dimensions of the body)

$$c_L = \sqrt{\frac{E}{\rho} \cdot \frac{1-\mu}{(1+\mu)(1-2\mu)}}, \text{ m/sec;} \qquad \text{(I.8)}$$

longitudinal wave velocity in a thin rod (wavelength is greater than the /20

transverse dimensions of the body)

$$C_D = \sqrt{\frac{E}{\rho}}, \quad \text{m/sec;} \tag{I.9}$$

velocity of the transverse wave

$$c_T = \sqrt{\frac{G}{\rho}}, \quad \text{m/sec;} \tag{I.10}$$

velocity of the surface wave

$$c_R = \frac{0{,}87 + 1{,}12\mu}{1 + \mu} \sqrt{\frac{G}{\rho}}, \quad \text{m/sec,} \tag{I.11}$$

where

E is the elastic modulus, kg/cm^2;

G is the shear modulus, kg/cm^2;

μ is the Poisson coefficient;

ρ is rock density, kg/cm^3.

The relationship between the velocities of propagation of the longitudinal c_L, transverse c_T and surface waves c_R is as follows

$$c_L > c_T > c_R. \tag{I.12}$$

"Pure" longitudinal and transverse waves are propagated only in very large bodies.

If the wavelength is commensurable with the diameter of a sample having the configuration of a rod, sound dispersion occurs. This can be attributed, in particular, to the difference in longitudinal wave velocities in an unbounded medium and in a thin rod. Usually the difference between the velocities of longitudinal waves in the rock mass and in a rod for rocks averages 8 to 15%.

Among ultrasonic research methods it is the pulse method which has come into the widest use; it makes it possible to determine the propagation velocities for waves of different types. Despite the electronic instrumentation which is more complex than in resonance methods, measurements can be made in a wide frequency range. The measurement method is simple and requires little time. The measurement accuracy is very high.

The essence of the ultrasonic pulse method for measuring the velocities of propagation of elastic waves in rock samples is as follows. Ultrasonic pulses are continuously fed into the investigated sample. They are received, amplified and fed to an indicator which measures the pulse propagation time. The time for propagation of an ultrasonic pulse through the sample when the distance between the piezoelectric transducers is known is used in judging the velocity of elastic wave propagation in the sample.

The great diversity of apparatus systems employed in the ultrasonic pulse method is attributable to the need for creating uniform or nonuniform heating of samples in the furnace. However, the main reason for creating different measurement methods is the need for ensuring insulation of ultrasonic emitters and detectors from thermal effects. /21

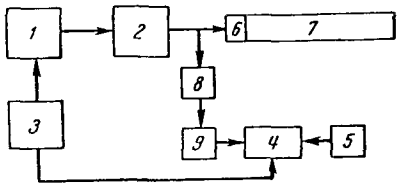

Figure 11. Block diagram of ultrasonic pulse echo method:
1- master oscillator;
2- high-frequency pulse generator; 3- synchronizer;
4- electronic oscillograph;
5- time mark generator;
6- piezocrystal; 7- sample;
8- attenuator; 9- amplifier.

In actual research the following variants of this method have come into use:

a system for through propagation of ultrasonic pulses with nonuniform heating of the sample [17];

a system based on the echo method with samples of complex configuration [16] in which heating is uniform;

a system with through propagation of ultrasonic pulses with uniform heating of the sample [18].

In the case of nonuniform heating the ends of the sample emerge from the furnace and are cooled to a temperature close to room temperature. The dependence of the elasticity indices on temperature is investigated from the nature of temperature distribution along the sample and from the velocity of elastic wave propagation. Graphs of temperature distributions are constructed and the mean time of propagation of oscillation along the sample is measured for finding the ultrasound velocity for each temperature segment.

The principal shortcomings of this system are a need for using long samples

and the complexity of measurement computations; this is quite unsuitable for anisotropic and inhomogeneous rocks.

The echo method employed extensively in sounding (Figure 11) is used in measuring samples which have been uniformly heated. The essence of the method is as follows: ultrasonic pulses emitted by a piezoelectric transmitter (quartz) pass through the sample, are reflected from its opposite end, and are again returned to the piezoelectric transducer. When the sample length is known it is easy to determine the ultrasound velocity.

If one of the sample ends has a steplike configuration, by measuring the time interval between two pulses reflected from the beginning and end of the step, assuming that its length is known, it is possible to determine the velocity of the ultrasonic wave in the heated sample segment.

Despite its simplicity and originality, this system is not very promising for studying the dependence of the elastic properties of rocks on temperature.

The rock physics laboratory at the Moscow Mining Institute has developed an ultrasound system with uniform sample heating and on the basis of the ultrasonic pulse method has created an apparatus for investigating the elastic modulus E in a great temperature range (0 to 900°C).

Figure 12 is a block diagram of an apparatus for determining the elastic /22
modulus of rocks during heating.

The sample to be tested is placed in the middle of an electric furnace and is connected by means of specially inserted mechanical holders with piezoelectric transducers placed on opposite sides of the axis. The holders, which are fused quartz rods, are up to 10-12 cm long. Between 1.5 and 2 cm of the rod is inside the heating furnace.

This makes it possible to place the piezoelectric transducers outside the furnace and avoid heating of the piezoelements above the Curie point because the material of the holders has a very slight heat conductivity. The diameter of the quartz rods corresponds to the transverse dimension of the sample.

The furnace is supplied current from a LATR-1 laboratory autotransformer with an automatic temperature increase.

The sample heating temperature is measured with an electronic chart-recording potentiometer which is connected to thermocouples situated directly in the furnace on the sample.

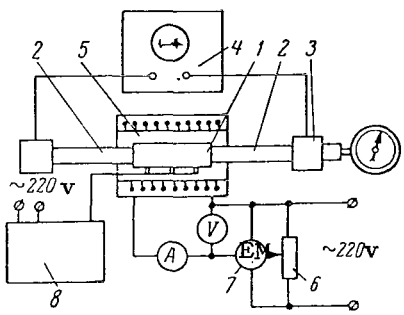

Figure 12. Block diagram of experimental apparatus for determining elastic modulus during heating: 1- sample; 2- quartz rods; 3- ultrasonic piezoelectric transducers; 4- ultrasonic pulse instrument; 5- electric furnace; 6- autotransformer (LATR-1); 7- electric micromotor; 8- fixed potentiometer.

The quartz rods and the sample to be tested, held between the piezoelectric transducers, form an acoustic node through which the ultrasonic wave is propagated. The acoustic contact between the rods and the sample is created as a result of strong compression of springs situated on the same axis behind the transducers.

The distinguishing characteristic of this apparatus is the introduction of fused quartz rods as mechanical checks on ultrasound propagation. These make possible observations with uniform heating of the sample in a broad temperature range.

Fused quartz is capable of slightly changing its elasticity parameters during heating and expands after repeated annealing and cooling. Experiments have shown that with heating of fused quartz rods to a temperature of 500°C the time for ultrasound to propagate 1 cm of length changes by less than 0.1 μsec in comparison with room temperatures.

When part (2-3 cm) of the length of the fused quartz rods is in the furnace, the change in the time of ultrasound propagation is 0.2 - 0.3 μsec; this is approximately equal to the accuracy in measurement by the employed ultrasonic pulse instruments. Accordingly, the change in the elastic modulus in quartz rods can be neglected and the change in the velocity of elastic wave propagation /23 in a rock sample during heating can also be directly registered.

The length of the tested sample is selected in such a way as to create uniform heating in its length. Therefore, the sample is 1.2 - 1.5 times less

than the width of the furnace heating element, selected in such a way that the change in velocity of ultrasound propagation in the sample is determined with an accuracy not less than 1 to 3%. Accordingly, samples 4 to 6 cm in length were used in the experiments.

Sample diameter was selected in such a way that there would be rapid heating with a temperature increase.

In addition, the diameter of the samples must be several times less than their length and less than the length of the ultrasonic wave. It was established experimentally in [19] that in order to register an ultrasonic wave propagating in a sample at the velocity c_D it is necessary to use such samples for which the ratio of the diameter to the wavelength d/λ does not exceed 0.1 to 0.2. Table 3 gives the transverse dimension d of a sample for determining longitudinal wave velocity.

TABLE 3. DETERMINING LONGITUDINAL WAVE VELOCITY IN A ROD

Longitudinal wave velocity, m/sec	Transverse dimension of sample (cm) with frequency of ultrasonic oscillations, kHz			
	50	100	200	300
3000	1.2	0.6	0.3	0.20
4000	1.6	0.8	0.4	0.27
5000	2.0	1.0	0.5	0.33
6000	2.4	1.2	0.6	0.40

The frequency of ultrasonic oscillations in the experiments therefore attained 150 to 200 kHz when the sample diameter was 0.6 to 1.2 cm.

Ultrasonic pulse instruments are used in generating and receiving ultrasonic oscillations.

The principal requirements imposed on these instruments are accuracy in measuring the propagation time for an elastic pulse and the possibility of creating reliable indication and reading of the received signal.

The ultrasonic pulse instrument developed in the rock physics laboratory in collaboration with the All-Union Scientific Research Institute on Reinforced

Concrete, the MIRGEN-1-U, meets the requirements and is used extensively in high temperature experiments [20].

The ultrasonic pulse instrument is designed on the basis of the cable and line tester (IKL-6) standard produced by the Soviet electronics industry.

The operating principle for the MIRGEM-1-U instrument is similar to the operation of other ultrasonic pulse instruments. /24

The MIRGEM-1-U instrument has the following technical specifications:

1) reading method: measuring the distance between the sounding and received signals at the time scale;

2) range of measured time of ultrasound propagation: from 0.2 to 2500 μsec;

3) accuracy in measuring ultrasound propagation time: 1% (from 20 to 2500 μsec);

4) sounding pulse repetition rate: 50 and 25 Hz;

5) the instrument has three operating ranges differing in screen scanning time, scanning hold (maximum measured time), calibration time mark scale, reading accuracy and signal shape observed on a cathode-ray tube screen;

6) scale of calibration marks: in the first and second ranges 2, 10 and 50 μ sec, in the third range 10 and 50 μsec;

7) wide-band amplifier with an amplification factor not less than 10^5;

8) current from an ac network frequency 50 Hz, voltage 220 V.

The instrument ensures a high measurement accuracy due to the introduction of a discrete electric delay line.

The operating principle for the delay line is a uniform-stepped delay with an accuracy of 0.2 μsec of the leading edge of the received signal to its matching with the closest time mark on the cathode-ray tube screen.

For working with short samples the instrument is supplied with a normalizing device ensuring the most precise registry of the leading edge of the ultrasonic pulse. In this case the leading edge of the ultrasonic pulse with an unclear onset is artificially reduced to a shape with a steep leading edge.

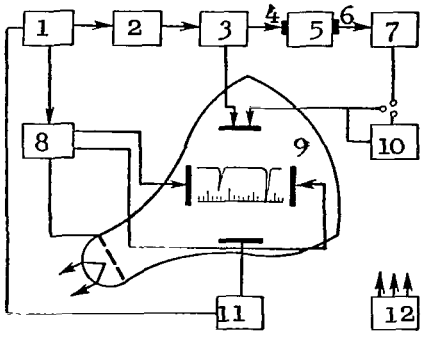

Figure 13. Block diagram of MIRGEM-1-U instrument: 1- unit for generating master pulses; 2- electric delay line; 3- generator of sounding pulses; 4- emitter; 5- sample; 6- receiver; 7- pulse amplifier; 8- scanning unit; 9- cathode-ray tube; 10- normalizer; 11- time mark unit; 12- current source.

Figure 13 shows a generalized block diagram of the MIRGEM-1-U ultrasonic pulse instrument.

The pulse generator, being an integral part of the ultrasonic instrument, creates and sends a pulse to a transducer where it is converted into ultrasonic oscillations. The pulse emitted by this transducer excites ultrasonic oscillations in the rod system present in the furnace (quartz rods - rock sample). These oscillations propagating along the system, reach the piezoelectric receiver. Then the elastic oscillations are converted into electric oscillations. The oscillations are amplified in the ultrasonic instrument and are fed to the cathode-ray tube. The sounding (emitted) and received (propagated through the sample) signals are registered on its screen. The time of propagation of the ultrasonic wave in the rod system is measured using the electronic time scale on the indicator tube screen. /25

Piezoelectric plates made from lead zirconate-titanate ceramic were used in this apparatus as the source and receiver of ultrasonic oscillations. These plates have a Curie point above 500°C. Other piezoelectric materials (quartz, Rochelle salt, barium titanate, and others) can also be used. However, this requires some complications of the design of transducer housings.

Table 4 gives the characteristics of piezoelectric materials used in transducers in ultrasonic investigations.

Despite the small value of the Curie point for some piezomaterials, the use of mechanical holders of fused quartz rods makes it possible to work with high temperatures.

TABLE 4. CHARACTERISTICS OF PIEZOELECTRIC MATERIALS

Piezoelectric crystal	Specific wave resistance $\rho c \cdot 10^6$ kg/m^2. sec	Dielectric constant ϵ	Electro-mechanical coupling coefficient K, %	Piezo-electric constant e, N/V·m
Quartz	15.4	4.5	10	$e_{11} = 0.17$
Rochelle salt (45° section)	4.3	9.4	29	$e_{36/25} =$ 0.11/0.08
Barium titanate ceramic	31.2	1000 to 1200	50	$e_{33} = 16.7$
Lead zirconate-titanate	35.0	1200	50	$e_{33} = 16.7$

The method for determining the indices of rock elasticity as a function of temperature is essentially as follows:

the time t_0 of propagation of elastic waves through the acoustic node present in the furnace (quartz rod - sample - quartz rod) is determined on the cathode-ray tube screen in the ultrasonic instrument;

the time for propagation of elastic waves in the investigated sample during heating is determined using the expression /26

$$t_i = t_0 - t_{rod}, \ \mu sec \qquad (I.13)$$

where

t_{rod} is the time of wave propagation through quartz rods;

the velocity of propagation of an ultrasonic pulse for a known length l of the sample at a stipulated heating temperature is computed using the formula

$$c_D = l/t_i, \ m/sec \qquad (I.14)$$

The desired elastic modulus is computed using Eq. (I.9) for determining the velocity of elastic waves as a function of medium density.

A small improvement in design of the pickup made it possible to create an apparatus for simultaneous determination of the elastic modulus and the coefficient of linear expansion of rocks at high temperatures [21].

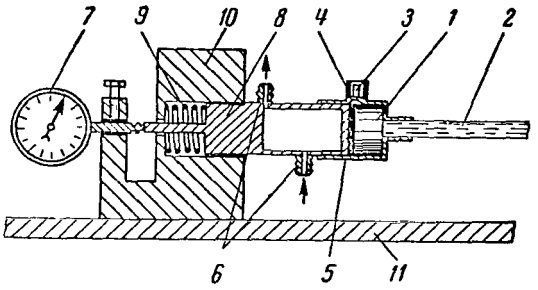

Figure 14. Instrument for determining the elastic modulus and coefficient of linear thermal expansion for rocks.

The apparatus shown in Figure 14 makes it possible, using a single sample, to register simultaneously its linear expansion during heating and to pick up the ultrasonic pulse propagating through the sample; the signal is converted in a piezoelectric pickup into an electric current. The apparatus consists of a piezoelectric pickup, 1, a quartz rod, 2, jack, 3, for the high-frequency cable to the ultrasonic instrument, a positive electric contact, 4, to the piezoelectric pickup, an insulating plate, 5, connecting pieces, 6, for connecting a water hose, mechanical strain gauge indicator, 7, moving rod, 8, spring, 9, supports, 10, and base plate, 11.

The device for cooling the moving rod is for preventing its heating.

In this case the quartz rods prevent heating of the piezoelectric elements of the ultrasonic converters and ensure direct measurement of the coefficient of linear expansion of the investigated rock sample. The sample, expanding during heating, imparts these changes to the quartz rod; its displacement relative to the initial position is used in determining linear expansion.

The coefficient of linear expansion for fused quartz changes insignificantly /27 at high temperatures. Accordingly, when part of the length (2-4 cm) of a fused quartz rod is present in the furnace (total length 20 cm or more) the change in rod length can be neglected in computations of the coefficient of linear rock expansion.

The coefficient of linear expansion for the investigated rock sample as a function of the strain gauge indicator readings is determined using the formula

$$\beta = \frac{l_i - l_0}{l_0 (T_i - T_0)}, \quad 1/\text{degree} \qquad (I.15)$$

where

l_i is sample length at the desired temperature T_i;

l_0 is sample length at room temperature T_0.

Repeated tests of the described apparatuses when using a large number of rock samples revealed that they operate reliably and give a good agreement of results with the earlier measured values of the coefficient of linear expansion and the elastic modulus for these rocks determined by conventional methods.

The accuracy in determining the elastic modulus E with heating by this method is dependent on:

accuracy in measuring the propagation time for ultrasonic waves using a pulsed ultrasound instrument;

effect of the thermal expansion of a rock sample on its density and size;

accuracy in thermocouple calibration.

The principal factor in this case is accuracy in measuring the propagation time for the ultrasonic pulse in the heated rod.

When using the MIRGEM-1-U pulsed instrument, the accuracy in time measurement is ±0.2 μsec. If the travel time for an ultrasonic pulse through a sample is greater than 10 μsec, the admissible relative error is

$$\frac{\Delta t}{t} \leqslant \frac{0.2}{10} = 0.02 \quad \text{or } 2\%.$$

Accordingly, the error in measuring time (and velocity) of elastic wave propagation in a sample in this case is less than 2%.

The influence of thermal expansion on density of the tested rock can be determined from the expression

$$\frac{\rho_T}{\rho_0} = \frac{1}{1 - \frac{\Delta V}{V}}, \qquad (I.16)$$

where

ρ_T and ρ_0 are the densities during heating and at room temperature;

ΔV is the specimen volume increment during heating;

V is the initial volume of the specimen.

The change in rock density during heating, determined using this formula, /28 is 0.01-0.5% of the initial density; this exerts no influence on the accuracy in computing the elastic modulus E. Accordingly, no correction for this change need be introduced into the computations.

Determination of the elastic modulus E by this method using the described instruments makes it possible to reduce the measurement error to 2 to 5%, which is entirely admissible.

3. Pattern of Change in Elastic Properties of Rocks at High Temperatures

Experimental investigations for studying the effect of temperature on the elastic properties of rocks made it possible to draw the following conclusions:

the change in elastic properties for different rocks is different;

the heating regime exerts an influence on the change in elastic properties.

The results of experiments for determining the elastic modulus of rocks in their temperature dynamics are given in Table 5.

The curves for the dependence of the elastic modulus on temperature (Figure 15) show that the elastic modulus changes differently for different rocks. For some rock types (granites, pegmatites) there is an appreciable decrease in the dependence of the elastic modulus E on temperature with a small deviation from a linear dependence; for others the elastic modulus decreases insignificantly with a temperature increase (gabbro, peridotites, and others); for still others (monomineral rocks of the quartzite type) the dependence of the elastic modulus on temperature up to temperatures of polymorphic transformation (T_{trans} = 575°C) drops off linearly.

Thus, on the basis of curves for the dependence of E on temperature it can be concluded that a decrease in the elastic modulus in a definite range of temperature change (from 0 to 500°C) is linear for some rocks, whereas for others it deviates from linearity.

Each experimental point in the table and on the graph was obtained by the averaging of measurements for two to four samples of each rock type. The agree- /29 ment of measurement data obtained for several samples of the same rock is indicative of measurement accuracy.

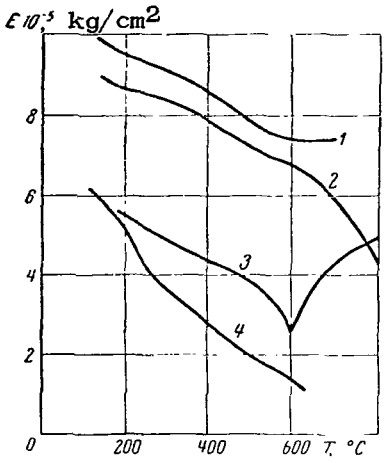

Figure 15. Curves showing dependence of the elastic modulus on temperature: 1- peridotite (Zhdanovskoye deposit); 2- gabbro (Zhdanovskoye deposit); 3- ore-free quartzite (Bakal'skoye deposit) 4- gray granite (Rovnenskoye deposit).

Appendix 1 gives the geological and petrographic characteristics of the investigated rocks.

Reason for Change in the Elastic Modulus During Heating

It was found that the change in the elastic properties of solid polycrystalline bodies is related to relaxation phenomena within the body [22, 23]. It is assumed that the change in the elastic properties of polycrystalline bodies, especially the elastic modulus E, is influenced by:

change in the elasticity of the crystals making up the body themselves;

relaxation processes at the crystal interfaces.

Theoretical investigations show that in a polycrystalline body in the absence of any relaxation phenomena and other processes on the boundaries between the crystals and in the crystals themselves the change in the elastic modulus will have a linear nature with a temperature increase. Such a change in the elastic modulus is assumed to govern up to the melting point.

Accordingly, it can be assumed that the linear dependence of change in the elastic modulus of each rock mineral with an increase in temperature should also cause a linear change in the elastic modulus for the entire rock.

The linear decrease in the elastic modulus of a mineral during heating can be attributed to the thermal energy manifested through the oscillatory motion of particles within the mineral and thermal expansion of the mineral.

In this case the adiabatic elastic modulus can be expressed as follows

$$E = E_0 + A + B. \qquad (I.17)$$

In this formula the first term E_0 represents the elastic modulus in the absence of any oscillatory energy. The second term A characterizes change in the modulus caused by thermal expansion. The third term B represents the direct influence of thermal energy.

The linear nature of the dependence of the elastic modulus on temperature for rock-forming minerals is experimentally confirmed.

Table 6 gives data on change in the elastic modulus for quartz (vein) and microcline in the temperature range from 20 to 500°C.

However, these indices cannot be used in analyzing the dependence of the elastic modulus of rocks on temperature because rocks of one type (quartzite) are characterized by a linear change in the elastic modulus in the temperature range up to the phase transformation, whereas the corresponding temperature curves for other rock types exhibit a deviation from linearity. This change is evidently attributable to inelastic relaxation phenomena on the boundaries of the minerals making up the rock or in the minerals themselves. /34

Figure 16 is a graph of the dependence of the relative change in the elastic modulus for a polymineral rock (granite) and quartz on temperature. The graph shows that the onset of relaxation phenomena in rocks occurs at a definite heating temperature. In the experiments the temperature of onset of relaxation phenomena for most rocks was 200-300°C.

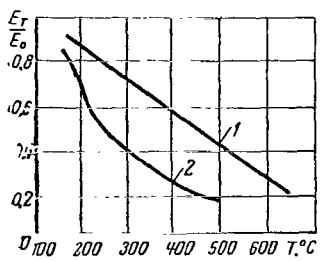

Figure 16. Graph of the dependence of relative change in the elastic modulus on temperature: 1- quartz; 2- granite.

The effect of high temperature on the elastic properties of different rocks is manifested differently. This can be attributed to a different manifestation of relaxation phenomena on the boundaries between minerals, and in some cases in the minerals themselves.

One of the factors responsible for the appearance of relaxation

TABLE 5. DEPENDENCE OF ULTRASOUND PROPAGATION c_D, ELASTIC MODULUS E AND COEFFICIENT OF RELATIVE CHANGE IN ELASTIC MODULUS φ DURING HEATING ON TEMPERATURE T

Rock	Index	Heating temperature, degrees							
		20	100	200	300	400	500	575	600
Oxidized ferruginous quartzite (Mikhaylovskiy quarry, Kursk Magnetic Anomaly) $\rho = 3.51$ g/cm^3	c, m/sec	4060	4040	3920	3860	3770	3510	3360	3240
	$E \cdot 10^{-5}$, kg/cm^2	5,5	5,5	5,25	5,25	4,8	4,5	3,8	3,75
	φ	—	—	0,05	0,05	0,11	0,18	0,31	0,33
Semi-oxidized ferruginous quartzite (Mikhaylovskiy quarry, Kursk Magnetic Anomaly) $\rho = 3.59$ g/cm^3	c, m/sec	4660	4810	4680	4490	4210	3970	3660	3480
	$E \cdot 10^{-5}$, kg/cm^2	7,75	7,95	7,8	7,25	6,35	5,7	4,75	5,3
	φ	—	—0,03	—0,01	0,07	0,22	0,26	0,39	0,32
Gray granite (Rovnenskoye deposit) $\rho = 2.73$ g/cm^3	c m/sec	5010	4880	4260	3630	3070	2520	2170	2010
	$E \cdot 10^{-5}$, kg/cm^2	6,8	6,5	5,2	3,6	2,55	1,7	1,28	1,69
	φ	—	0,04	0,24	0,47	0,62	0,74	0,81	0,84
Siderite (Bakal'skoye deposit) $\rho = 2.7$ g/cm^3	c, m/sec	5800	5550	5200	4860	4610	4170	3350	2620
	$E \cdot 10^{-5}$, kg/cm^2	11.8	10,8	9,7	8,5	7,4	6,2	5,0	2.4
	φ	—	0,09	0,18	0,28	0,37	0,48	0,57	0.68
Dolomite (Bakal'skoye deposit) $\rho = 2.6$ g/cm^3	c, m/sec	4050	3730	3320	3060	2940	3040	—	—
	$E \cdot 10^{-5}$, kg/cm^2	4,15	3,55	2,9	2,3	2,05	2,35	—	—
	φ	—	0,08	0,18	0,24	0,27	0,25	—	—
Shale (Bakal'skoye deposit) $\rho = 2.61$ g/cm^3	c, m/sec	4080	4040	3990	3970	3910	3880	3840	3820
	$E \cdot 10^{-5}$, kg/cm^2	4,2	4,13	4,05	4,0	3,95	3,9	3,85	3,85
	φ	—	0,02	0,04	0,05	0,06	0,07	0,08	0,08

Commas represent decimal points.

TABLE 5 continued

Rock	Index	Heating temperature, degrees							
Diabase (Bakal'skoye deposit) ρ = 2.88 g/cm^3	c, m/sec	4900	4780	4690	4560	4470	4360	4260	4230
	$E \cdot 10^{-5}$, kg/cm^2	6,9	6,6	6,3	6,05	5,7	5,4	5,2	5,15
	φ	—	0,04	0,09	0,12	0,17	0,22	0,25	0,26
Limestone (Bakal'skoye deposit) ρ = 2.44 g/cm^3	c, m/sec	4200	4090	4010	3990	3970	3950	3930	3910
	$E \cdot 10^{-5}$, kg/cm^2	4,3	4,05	3,9	3,85	3,8	3,8	3,75	3,7
	φ	—	0,06	0,09	0,10	0,11	0,12	0,13	0,14
Rosy coarse-grained granite (Rovnenskoye deposit) ρ = 2.66 g/cm^3	c, m/sec	5030	4550	4120	3450	3040	2620	1990	1900
	$E \cdot 10^{-5}$, kg/cm^2	6,6	5,5	4,5	3,3	2,55	1,75	1,05	0,9
	φ	—	0,17	0,32	0,49	0,63	0,74	0,84	0,87
Rosy intermediate-grained granite (Rovnenskoye deposit) ρ = 2.69 g/cm^3	c, m/sec	5660	5660	4400	3630	3030	2350	1740	—
	$E \cdot 10^{-5}$, kg/cm^2	8,8	8,75	5,2	3,55	2,45	1,5	0,75	—
	φ	—	—	0,41	0,60	0,72	0,83	0,91	—
Ore-free quartzite, parallel to stratification (Olenegorskoye deposit) ρ = 3.28 g/cm^3	c, m/sec	5350	5100	4460	4020	3870	3790	3260	3110
	$E \cdot 10^{-5}$, kg/cm^2	9,3	8,55	6,5	5,4	4,7	3,95	3,35	3,1
	φ	—	0,08	0,30	0,41	0,49	0,58	0,64	0,67
Ferruginous quartzite (Olenegorskoye deposit) ρ = 3.78 g/cm^3	c, m/sec	4040	3820	3560	3090	2730	2510	2020	2090
	$E \cdot 10^{-5}$, kg/cm^2	6,02	5,45	4,75	3,5	2,85	2,35	1,50	1,65
	φ	—	0,09	0,21	0,42	0,53	0,61	0,75	0,72
Pegmatite (Olenegorskoye deposit ρ = 3.26 g/cm^3	c, m/sec	3790	3720	3630	3340	3040	2780	2520	2410
	$E \cdot 10^{-5}$, kg/cm^2	3,85	3,6	3,45	2,9	2,45	2,05	1,65	1,55
	φ	—	0,06	0,10	0,24	0,36	0,47	0,57	0,60

Commas represent decimal points.

TABLE 5 continued

Rock	Index	Heating temperature, degrees							
		20	100	200	300	400	500	575	600
Gray fine-grained granite (Shartashskoye deposit) ρ = 2.68 g/cm^3	c, m/sec	3880	3880	3650	3300	3120	2740	3210	2240
	$E \cdot 10^{-5}$, kg/cm^2	4,0	4,0	3,6	3,0	2,7	2,1	1,65	1,45
	φ	—	—	0,11	0,26	0,31	0,48	0,59	0,63
Gray coarse-grained granite (Shartashskoye deposit) ρ = 2.65 g/cm^3	c, m/sec	3530	3360	3180	2940	2690	2350	2010	1880
	$E \cdot 10^{-5}$, kg/cm^2	3,25	3,0	2,65	2,3	1,95	1,45	1,0	0,9
	φ	—	0,08	0,18	0,29	0,40	0,55	0,69	0,72
Gneisous granite (Smolinskoye deposit) ρ = 2.62 g/cm^3	c, m/sec	4160	4140	4010	3850	3580	3240	3010	2830
	$E \cdot 10^{-5}$, kg/cm^2	4,5	4,5	4,15	3,8	3,35	2,75	2,3	2,1
	φ	—	0,01	0,08	0,16	0 26	0,39	0,49	0,55
Granodiorite (Smolinskoye deposit) ρ = 2.6 g/cm^3	c, m/sec	3930	3900	3720	3560	3410	3030	2740	2710
	$E \cdot 10^{-5}$, kg/cm^2	3,85	3,75	3,4	3,1	2,8	2,2	1,85	1,7
	φ	—	0,03	0,12	0,19	0,27	0 43	0,52	0,56
Mineralized peridotite (Zhdanovskoye deposit) ρ = 3.12 g/cm^3	c, m/sec	5860	5850	5200	4320	4120	4100	4280	4300
	$E \cdot 10^{-5}$, kg/cm^2	10,8	10,85	8,45	5,75	5,25	5,2	5,75	5,75
	φ	—	0,01	0,22	0,47	0,51	0,52	0,47	0,46
Biotitic gneiss (Olenegorskoye deposit) ρ = 2.86 g/cm^3	c, m/sec	4720	4360	3780	3380	3060	2560	1920	1840
	$E \cdot 10^{-5}$, kg/cm^2	5,85	5,2	4,0	3,4	2,55	1,85	1,1	0,95
	φ	—	0,09	0,30	0,41	0,56	0,68	0,81	0,84

Commas represent decimal points.

TABLE 5 continued

Rock	Index	Heating temperature, degrees						
Bluish-gray quartzite (Pervoural'skoye deposit) ρ = 2.67 g/cm^3	c, m/sec	4990	4970	4770	4540	4330	3980	3690	3420
	$E \cdot 10^{-5}$, kg/cm^2	6,7	6,6	6,1	5,6	5,15	4,0	3,5	3,25
	φ	—	0,01	0,09	0,16	0,23	0,40	0,48	0,51
Porous ferruginized quartzite (Pervoural'skoye deposit) ρ = 2.39 g/cm^3	c, m/sec	3650	3480	3490	3360	3320	3140	2850	2700
	$E \cdot 10^{-5}$, kg/cm^2	3,15	2,75	2,9	2,7	2,6	2,35	2,0	1,6
	φ	—	0,12	0,08	0,14	0,17	0,25	0,36	0,49
Ore-free weathered quartzite (Bakal'skoye deposit) ρ = 2.65 g/cm^3	c, m/sec	3090	3100	3240	3110	3020	2760	2490	2630
	$E \cdot 10^{-5}$, kg/cm^2	2,6	2,6	2,7	2,55	2,4	2,05	1,55	1,7
	φ	—	—	0,04	0,02	0,08	0,21	0,4	0,35
Ore-free quartzite (Bakal'skoye deposit) ρ = 2.68 g/cm^3	c, m/sec	5010	4860	4520	4260	4020	3730	3090	3320
	$E \cdot 10^{-5}$, kg/cm^2	6,62	6,25	5,35	4,8	4,25	3,7	2,5	3,0
	φ	—	0,05	0,19	0,27	0,36	0,44	0,62	0,54
Gabbro (Zhdanovskoye deposit) ρ = 3.08 g/cm^3	c, m/sec	5860	5570	5240	5200	5030	4790	4660	4620
	$E \cdot 10^{-5}$, kg/cm^2	10,4	9,6	8,6	8,45	7,85	7,1	6,75	6,6
	φ	—	0,08	0,17	0,19	0,24	0,32	0,35	0,37
Ore-free peridotite (Zhdanovskoye deposit) ρ = 3.02 g/cm^3	c, m/sec	5920	5630	5560	5470	5300	5030	4950	4930
	$E \cdot 10^{-5}$, kg/cm^2	10,65	9,55	9,35	9,05	8,5	7,65	7,3	7,25
	φ	—	0,11	0,12	0,15	0,201	0,281	0,31	0,31
Ferruginous quartzite No. 4 (YuGOK) ρ = 3.52 g/cm^3	c, m/sec	5040	4980	4890	4810	4540	4150	3290	—
	$E \cdot 10^{-5}$, kg/cm^2	8,85	8,7	8,55	8,05	7,4	6,1	3,8	—
	φ	—	0,02	0,05	8,09	0,16	0,31	0,57	—

Commas represent decimal points.

TABLE 6. DEPENDENCE OF ULTRASOUND VELOCITY AND ELASTIC MODULUS ON TEMPERATURE FOR SOME ROCK FORMING MINERALS

/34

Heating temperature, degrees	Microline, ρ = 2.53 g/cm^3		Quartz, ρ = 2.65 g/cm^3	
	c_D, m/sec	$E \cdot 10^{-5}$, kg/cm^2	c_D, m/sec	$E \cdot 10^{-5}$, kg/cm^2
20	5280	7.18	4920	6.41
200	4670	5.52	4880	6.30
300	4040	4.12	4470	5.30
400	3510	3.15	4030	4.25
500	3120	2.47	3530	3.31

phenomena in rocks can be viscous slip on the boundary between minerals.

The mechanism of this phenomenon can be explained as follows. On the boundaries between minerals in a polycrystalline rock there is a transitional layer in which the arrangement of atoms differs from their arrangement in the two bounding minerals. This makes it possible to regard a rock which is being heated as consisting of two components, one of which has a truly elastic nature, whereas the other behaves as viscous medium. The behavior of the boundaries between minerals can be judged only on the basis of quantitative observations of changes in the elastic modulus and the attenuation of ultrasound with a temperature increase.

/35

Viscous slip on the boundaries between minerals at increased temperatures leads to a decrease in the elastic modulus E to some E_T value. During the cooling of samples of many rocks this value changes insignificantly and usually does not return to the initial level. The value of the elastic modulus E_T frequently does not change during subsequent heating; this is evidence of a shift in the position of the boundaries between minerals during viscous slip to an equilibrium state.

On the basis of experimental investigations for determining the reasons causing a change in the elastic modulus of rocks during heating it can be concluded that:

the linear dependence of the elastic modulus (mineral, monomineral rocks)

on temperature can be attributed only to changes in temperature within the mineral;

the deviation of this dependence from linear is related to the appearance of relaxation processes on the boundaries between the minerals (polymineral rocks), leading to plastic changes.

Change in Elastic State of Rocks Under the Influence of a High Temperature

Analysis of the results of change in the elastic modulus of rocks in a high-temperature field indicates a different nature of this change.

A comparative analysis of data on the dependence of the elastic modulus on temperature was made for determining the quantitative and qualitative nature of the changes.

In order to clarify the qualitative changes in the elastic modulus the coefficient of relative change in the modulus during heating was introduced

$$\varphi = \frac{E_0 - E_T}{E_0}, \qquad (I.18)$$

where

E_0 is the elastic modulus at room temperature;

E_T is the elastic modulus with heating to the temperature T.

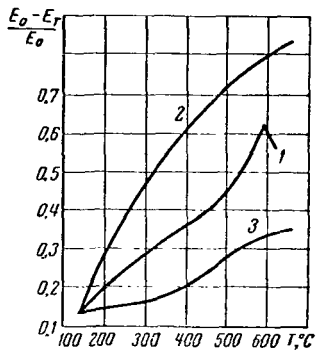

Figure 17. Graph of the dependence of the coefficient of relative change in the elastic modulus on temperature: 1- quartzite (Bakal'skoye deposite); 2- granite; 3- peridotite.

Analysis of the experimental data leads to the conclusion that there are three groups of dependence of the coefficient of relative change in the elastic modulus φ on temperature. Figure 17 shows generalized curves for each group for the coefficient φ. Curve 1, representing the linear dependence of the coefficient φ on temperature, is characteristic for the principal rock-forming minerals, monomineral (quartzite, siderite and others)

and polymineral (gneiss) rocks. This dependence indicates the retention of "pure" elasticity in these rocks in a quite broad temperature range. /36

Curve 2, expressing the dependence of the coefficient φ on temperature for most polymineral rocks of the granite, pegmatite, granodiorite (and others) type is characterized by a small deviation from a linear dependence. As was demonstrated above, this deviation can be attributed to plastic phenomena on the boundaries between minerals.

Curve 3, reflecting the dependence of the coefficient φ on temperature for rocks of the gabbro, peridotite and diabase type, has a marked deviation from a linear dependence which can be attributed to plastic phenomena within the investigated sample during heating. These curves can be described by three types of equations.

If the change in elastic properties of rocks is regarded in its temperature dynamics in the range from 200 to 500°C, all types of investigated rocks (and therefore, by analogy with these types, other rocks as well) can be classified on the basis of elasticity into three groups:

thermally elastic;
thermally elastico-plastic;
thermally plastic.

Table 7 gives a classification of the investigated rocks on the basis of elasticity.

When explaining the mechanism of destruction of rocks under the effect of high temperatures, the condition of the elastic state, which is characteristic of this or that type of rock, must be taken into consideration.

TABLE 7. CLASSIFICATION OF ROCKS BY ELASTICITY DURING HEATING

Group of rocks by elasticity during heating	Rocks	Equation for dependence of relative change in elastic modulus φ on temperature
First - thermally elastic	Ore- free quartzite, biotitic gneiss unoxidized ferruginous quartzites	$\varphi_1 = a_1 T + b_1$
Second - thermally elastico-plastic	Granites, gneissous granites, granodiorite, pegmatite, poorly oxidated ferruginous quartzites	$\varphi_2 = a_2 T^{b_2} + c$
Third - thermally plastic	Peridotites, gabbro-diabases, oxidized ferruginous quartzites	$\varphi_3 = [1/(a_3 + b_3 T)]T$

Here: a_1, a_2, a_3, b_1, b_2, b_3, c are constant coefficients for the particular rock type.

Relationship Between Elastic Modulus in a High-Temperature Field and Other Physical Indices

/37

The dependence of the product of the elastic modulus E and the coefficient of linear expansion, β, which is proportional to the thermal stresses, is of particular interest to researchers concerned with thermoelasticity problems.

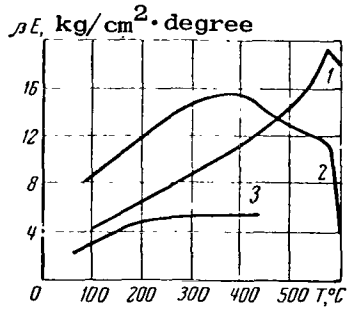

Figure 18. Graph of the dependence of the product βE on temperature: 1- ore-free quartzite; 2-siderite; 3- dolomite.

Table 8 gives the results of joint measurements of the elastic modulus E, coefficient of linear expansion β and their product βE for some rocks.

Figure 18 shows the curves for the dependence of βE on temperature. The curves show a difference in the nature of increase in this parameter and therefore (assuming a small change in the heat conductivity and thermal diffusivity coefficients) the intensities

of the thermal stresses arising in rocks under the influence of heat. For ore-free and ferruginous quartzites there is a constant, almost linear, increase in the thermal stresses proportionality factor βE in the range of temperatures destructive for thermal drilling (400-500°C).

In this temperature range the thermally plastic rocks (diabase, limestone, shale, etc.) are characterized by an almost constant value of the βE product. This means that the thermal stresses do not increase with a temperature increase.

The quantitative relationship between the elastic and thermal properties in their temperature dynamics, represented by the expression $\beta E/c$, where c is the volume heat capacity of the rock, is of practical interest.

Table 9 gives the results of experiments for determining the dependence of the expression $\beta E/c$ on temperature for six types of rocks.

The deviation of the complex index from the mean value for a temperature change 200-450°C for rocks is up to 15-20%. Thus, change in the $\beta E/c$ index in its temperature dynamics is insignificant and it can be neglected.

The absolute values of the complex index for different rocks are different. However, numerous experiments make it possible to trace some tendency in the value of the $\beta E/c$ index for different rocks. For example, this index has its /39
maximum value for rocks of the quartzite type ($\beta E/c > 9$), whereas for rocks of the diabase and dolomite (and others) type this index has a value less than 8. This classification of rocks on the basis of the $\beta E/c$ index corresponds to the rock classification proposed earlier on the basis of elasticity in a high-temperature field.

TABLE 8. DEPENDENCE OF JOINTLY DETERMINED ELASTIC MODULUS E, COEFFICIENT OF LINEAR EXPANSION β AND THEIR PRODUCT βE

Rock	Physical index	Heating temperatures, degrees							
		20	100	200	300	400	500	575	600
Quartzite (Bakal'skoye deposit)	$E \cdot 10^{-5}$, kg/cm^2	7,1	6,5	6,15	5,2	4,3	3,5	2,5	4,5
	$\beta \cdot 10^{5}$, 1/degree	—	—	1,35	1,9	2,2	3,05	8,5	3,0
	βE, kg/cm^2·degree	—	—	8,3	9,9	9,5	11,0	21,2	19,5
Siderite (Bakal'skoye deposit)	$E \cdot 10^{-5}$, kg/cm^2	11,8	10,8	9,7	8,5	7,4	6,2	5,0	3,8
	$\beta \cdot 10^{5}$, 1/degree	—	0,8	1,25	1,75	2,1	2,05	2,3	1,05
	βE, kg/cm^2·degree	—	8,6	12,2	14,8	15,5	12,7	11,5	4,0
Dolomite (Bakal'skoye deposit)	$E \cdot 10^{-5}$, kg/cm^2	4,15	3,65	2,9	2,3	1,95	—	—	—
	$\beta \cdot 10^{5}$, 1/degree	—	—	1,7	2,3	2,7	—	—	—
	βE, kg/cm^2·degree	—	—	4,93	5,3	5,3	—	—	—
Shale (Bakal'skoye deposit)	$E \cdot 10^{-5}$, kg/cm^2	4,2	4,17	4,15	4,11	4,05	3,95	3,85	3,8
	$\beta \cdot 10^{5}$, 1/degree	—	—	0,9	1,05	1,15	1,25	1,35	1,4
	βE, kg/cm^2·degree	—	—	3,74	4,32	4,66	4,94	5,2	5,32
Diabase (Bakal'skoye deposit)	$E \cdot 10^{-5}$, kg/cm^2	4,45	4,4	4,15	4,0	3,8	3,6	3,45	3,3
	$\beta \cdot 10^{5}$, 1/degree	—	—	0,95	1,1	1,2	1,45	1,55	1,6
	βE, kg/cm^2·degree	—	—	3,94	4,4	4,56	5,24	15,35	15,3
Limestone (Bakal'skoye deposit)	$E \cdot 10^{-5}$, kg/cm^2	4,3	4,05	3,9	3,85	3,82	3,8	3,75	3,7
	$\beta \cdot 10^{5}$, 1/degree	—	0,65	0,9	1,0	1,05	2,15	2,95	2,8
	βE, kg/cm^2·degree	—	2,65	3,5	3,85	4,0	8,15	11,1	10,4
Quartzite No. 4 (YuGOK)	$E \cdot 10^{-5}$ kg/cm^2	8,85	8,7	8,55	8,05	7,4	6,1	3,8	—
	$\beta \cdot 10^{5}$, 1/degree	—	0,8	1,2	1,55	2,2	3,65	6,65	4,8
	βE, kg/cm^2·degree	—	6,96	1,03	12,5	18,4	22,3	25,3	—

Commas represent decimal points.

TABLE 9. DEPENDENCE OF βE/c PARAMETER ON TEMPERATURE

Rock	Temperature, °C					
	200	250	300	350	400	450
Microquartzite (Bakal'skoye deposit)	14.3	16.2	15.4	15.2	13.9	14.4
Dolomite (Bakal'skoye deposit)	7.36	7.26	7.32	7.26	6.96	6.5
Diabase (Bakal'skoye deposit)	6.7	6.85	6.96	6.92	6.93	7.64
Ore-free quartzite (Olenegorskoye deposit)	9.3	9.2	9.65	8.9	10.0	9.75
Coarse-grained granite (Rovnenskoye deposit)	7.65	8.05	7.85	7.62	6.0	8.0
Pegmatite (Olenegorskoye deposit)	7.1	7.2	6.9	6.55	6.35	6.3

4. Examples of the Use of the Dependence of the Strength and Elastic Properties of Rocks on Temperature

A detailed study of changes in the strength and elasticity of rocks makes possible a clear differentiation of the field of specific applicability of the electrophysical (high and industrial frequency currents, dielectric breakdown, and other methods) and thermomechanical methods for destroying rocks. Such investigations make it possible to classify all rocks with respect to effectiveness of destruction.

Investigations of the behavior of rocks under the influence of a high-temperature jet stream revealed that the effectiveness of rock destruction with an increase in temperature is determined to a large extent by the nature of the change in rock elasticity.

Comparison of the classification of rocks with the practical indices of the effectiveness of thermal drilling confirms the relationship between thermally elastico-plastic rocks and rocks with average thermal drillability and between thermally plastic rocks and rocks with poor thermal drillability [24].

The relative coefficient of thermal plasticity k_{pl} has been proposed for a comparative evaluation of the change in the thermo-elastic state in different rocks. With an increase in rock heating temperature this coefficient does not remain constant and therefore it should be computed for some definite temperature

range for which this type of destruction is characteristic. In particular, the range 200-400°C has been experimentally established for destruction of rocks during thermal drilling [25]. /40

For these purposes it is desirable to determine the mean relative coefficient of thermal plasticity k_{pl} for the temperature range 200-400°C.

The relative coefficient k_{pl} is determined from the expression

$$k_{pl} = \tan(\alpha_i - \alpha_0), \qquad (I.19)$$

where

α_0 is the slope of the curve representing the dependence of the relative coefficient of change in the elastic modulus φ on temperature for a standard thermally elastic rock, degrees;

α_i is the slope of the curve representing the dependence of the coefficient for the investigated rock on temperature relative to the dependence of the coefficient for the standard rock on temperature, degrees.

A monomineral rock of the type of ore-free quartzite from the Bakal'skoye deposit was selected as the standard thermally elastic rock; the latter gives the best thermal drilling indices.

The results of determination of the coefficient of relative thermal plasticity k_{pl} applicable to thermal drilling problems are given in Table 10.

TABLE 10. VALUES OF THE COEFFICIENT OF RELATIVE THERMAL PLASTICITY AT A TEMPERATURE 200-400°C

Rock	Coefficient k_{pl}	Volumetric rate v of thermal drilling, cm^3/min
Quartzite (Bakal'skoye deposit)	0	400
Ore-free quartzite (Olenegorskoye deposit)	0.02	390
Biotitic gneiss (Olenegorskoye deposit)	0.04	350
Gray fine-grained granite (Shartashskoye deposit)	0.07	380
Ferruginous quartzite (Olenegorskoye deposit)	0.08	330
Pegmatite (Olenegorskoye deposit)	0.14	350
Semi-oxidized ferruginous quartzite (Kursk Magnetic Anomaly)	0.16	240 - 270
Granodiorite (Smolinskoye deposit)	0.17	270
Gray granite, intermediate- and coarse-grained (Shartashskoye deposit)	0.19	230
Rosy, intermediate-grained granite (Rovnenskoye deposit)	0.20	250
Rosy, coarse-grained granite (Rovnenskoye deposit)	0.23	240
Gray granite (Rovnenskoye deposit)	0.28	220
Oxidized ferruginous quartzite (Kursk Magnetic Anomaly)	0.31	30 - 180
Mineralized peridotite (Zhdanovskoye deposit)	0.34	Fuses
Gabbro (Zhdanovskoye deposit)	0.40	Fuses
Ore-free peridotite (Zhdanovskoye deposit)	0.42	Fuses

The data in Table 10 show that the coefficient k_{pl} is different for different /41 rocks. Theoretically, it can vary from 1 to 0. For practical purposes the range in change of the k_{pl} coefficient is from 0 to 0.5.

Those rocks having a coefficient of relative thermal plasticity in the temperature range 200-400°C of 0.35 - 0.5 include thermally plastic rocks of the gabbro and peridotite (and others) type. Rocks whose k_{pl} coefficient is less than 0.1 can be classified as thermally elastic rocks.

Rocks having a k_{pl} coefficient of 0.1 - 0.35 must be classified as thermally

elastico-plastic. It should be noted that at this stage in the investigations this classification is tentative.

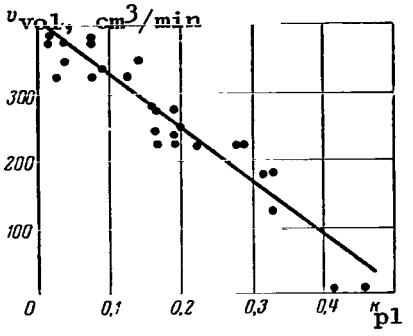

Figure 19. Graph of the dependence of the relative coefficient of thermal plasticity on volumetric rate of thermal drilling.

The coefficient of relative thermal plasticity k_{pl} in the temperature range 200-400°C correlates well with such a fundamental working index of thermal drillability of rocks as the volumetric drilling rate; the graphic relationship between this latter index and k_{pl} is shown in Figure 19.

The values of the volumetric rate of thermal drilling were determined experimentally in an investigation of the same types of rocks as were used in these experiments. The technical specifications were held constant during the entire course of the experiment. The tests were made using an oxygen torch with a diameter of the critical cross section of the nozzle 4.7 mm; chamber pressure was 6 atm; the distance from the nozzle section to the rock surface was 60 mm.

Processing of the experimental data using the methods of mathematical statistics made it possible to find an expression for the dependence of the volumetric drilling rate on the thermal plasticity coefficient:

$$v_{vol} = 387.5 - 727\ k_{pl},\ cm^3/min \qquad (I.20)$$

where

k_{pl} is the coefficient of relative thermal plasticity at a temperature 200-400°C.

The correlation coefficient for processing of experimental data was 0.93.

A close correlation is also discovered between the coefficient of relative thermal plasticity and the specific energy expenditures on thermal drilling.

Thus, the nature of the change in the elastic properties of rocks in their temperature dynamics can be one of the principal criteria for evaluating their drillability by the thermal method.

Practical use of the patterns of change in the strength and elastic properties of rocks at high temperatures are not limited to their use for the prognosis of thermal drilling.

The utilization of the results of change in the strength and elasticity of rocks with heating allows the process of the interaction of the operating element of the machine with rock during cutting and drilling to be more completely studied. These questions also demand study that is applicable to problems of drilling superdeep boreholes.

In addition to this, study of the influence of high temperature on the strength and elastic properties of rocks is of interest when calculating rock pressures in deep mines and pits, and also when determining the resistance of the containing rocks to underground leaching and to the fusion of mineral resources (copper, antimony, sulfur, schist, and others) and the gasification of coal.

Chapter II

THERMAL PROPERTIES OF ROCKS AS A FUNCTION OF TEMPERATURE

1. General Information on the Thermal Properties of Rocks /43

Concept of Thermal Processes

Various thermal effects can appear in rocks, depending on their natural state (porosity, moisture content, structure and texture) and mineralogical composition under the influence of heat; these effects favor the appearance or development of deformations and stress relaxation, causing a change in the phase state of the rocks.

Among these effects are thermal expansion, hydration and dehydration phenomena, polymorphic transformations, isomorphism (replacement of chemical elements in the crystal lattice), dissociation (decomposition into the gaseous phase with a solid residue), boundary processes (plastic flow), density increase (congealing, thermal hardening), and fusion.

Depending on the thermal effect parameters and rock properties, these phenomena may lead to weakening, brittle fracture, fusion, evaporation, strengthening, or dissolving in natural and artificial media, and other rock changes.

In mining, increasing use is being made of thermal processes for solving engineering problems involved in the production of minerals. For example, methods of thermal destruction of rocks (drilling of blast holes and boreholes, nonexplosive fracturing of boulders and large pieces of rock, breaking pieces of rock off from large masses, production and working of rock blocks) are based on the phenomena of thermal expansion, polymorphism, and others.

The possibility of thermal weakening of rocks, obviously being a result of the development of boundary processes (breaking of bonds between minerals, thermal expansion, dehydration and dissociation of minerals), made it possible to develop methods for the combined (thermomechanical) drilling of rocks (heat generators of different types in combination with a cutter or pneumatic hammer).

The rock fusion effect is the basis for methods for their electrothermal /44
destruction (electric arc heating when fracturing pieces of rock; low frequency

destruction method in which the melt plays the role of the working medium), and also shaftless methods of mineral exploitation (sulfur extraction).

Some methods for mining in weak rocks having an increased moisture content are based on the hardening of these rocks (freezing and thermal hardening).

These examples do not exhaust the full list of engineering problems based on the use of thermal processes in rocks. Suffice it to mention the need for solving such important problems as heat exchange in mine workings when exploiting deep levels, the use of natural deep heat (geothermal engineering), etc.

It is obvious that every engineering task must be based on very definite laws of the transpiring of a thermal process. These laws are in turn directly related to different thermal effects manifested in the particular process.

Determination of the conditions for the appearance and transpiring of thermal effects can serve as a basis for controlling thermodynamic processes in rocks.

The appearance of different thermal effects and accordingly the change in the state of rocks are dependent primarily on the mineralogical composition of the rock, the intensity and nature of the thermal effect (field parameters), and at every moment of interaction between the heat and the rock the latter will be characterized by some complex of physical properties (parameters of state).

It should be noted that very little study has yet been made of the problem of heat conductivity for analyzing and controlling the processes of thermal effects on rocks, particularly at high temperatures.

In solving problems involved in determining temperature fields, duration and nature of the heating of rocks during their thermal destruction, heat losses in the surrounding rock complex during the underground extraction of sulfur, subterranean reduction of coal to gas, ventilation of deep workings, etc., it is most important to know the thermal properties of the rocks and the nature of their change with heating.

Indices of Thermal Properties of Rocks

Among the principal indices of the thermal properties of rocks are the following: heat conductivity, thermal diffusivity, linear thermal expansion,

heat capacity, thermal effect, and heat of transformation.

The heat conductivity coefficient λ (cal/m·hour·degree) is the numerical characteristic of the capacity of rock for transfer of the heat of conduction. /45

The thermal diffusivity coefficient a (m^2/hour) characterizes the rate of change in rock temperature as a result of heat absorption or release.

Heat capacity c (cal/kg·degree) is a quantitative characteristic of rock capacity for absorbing thermal energy.

These parameters are related to one another by the equation

$$a = \lambda/c\rho, \tag{II.1}$$

where

ρ is rock density.

The coefficient of linear thermal expansion β (degrees^{-1}) characterizes the capacity of a rock to change its linear dimensions with a change in temperature.

The thermal effect T_{eff} characterizes the temperature at which physicochemical transformations occur in the rock.

The heat of transformation Q (cal/kg) characterizes the quantity of heat which is released or absorbed in the course of the physicochemical transformation.

One can distinguish the mean and true values of the thermal parameters for a definite temperature range; these are related to one another by the following dependence:

$$A_{T_1;\ T_2} = \frac{\int_{T_1}^{T_2} A_T\, dT}{T_2 - T_1}, \tag{II.2}$$

where

$A_{T_1;\ T_2}$ is the mean value of the thermal parameter for the temperature range from T_1 to T_2;

A_T is the true value of the thermal parameter or the value of the thermal parameter at the temperature T.

The heat conductivity of rocks has not yet been adequately studied. Some

aspects of the heat conductivity of coals and rocks were discussed relatively recently in [26].

Now we will examine some of the basic definitions. The heat conductivity value characterizes the capacity of a rock or mineral to transfer thermal energy from one point to another if for any reason a temperature difference appears between them.

The heat in minerals can be transferred by conduction electrons and also by thermal oscillations of the crystal lattice.

In native and pure metals (gold, silver, copper, tin, platinum, etc.) the main role in heat transfer is played by conduction electrons. The motion of electrons does not conform to the laws of classical mechanics and therefore the laws of wave mechanics are used in a theoretical description of heat conductivity of metals. /46

The heat conductivity of rocks can be determined from the following expression [30]:

$$\lambda = \frac{Nl\bar{u}k}{2}, \qquad \text{(II.3)}$$

where

N is the number of atoms in a unit volume;

l is the length of the electron path from one collision with an atomic ion to another (equal to approximately 100 interatomic distances), cm;

$\bar{u}$ is electron motion velocity, cm/sec;

k is the Boltzmann constant, eV/degree.

This formula takes into account only the electron part of heat conductivity.

In the absence of electron conduction in minerals, the heat is transferred by the elastic oscillations of the spatial crystal lattice.

It is known that particles forming a mineral are in constant, perpetual motion. The energy of this motion arises due to the heat absorbed by the mineral as a result of thermal interaction with the surrounding medium. The basis for the heat conductivity of nonconducting minerals is the process of motion of the particles forming the mineral and their interaction, accompanied by an exchange of energy. These complex molecular-kinetic processes constitute

the essence of the heat conductivity phenomenon.

It can be assumed with some approximation that the heat conductivity of a rock consists of the heat conductivity of its component minerals. Accordingly, heat can be transferred in rocks both as a result of electron motion and due to the elastic oscillations of particles.

However, rocks are inhomogeneous and in some cases are multiphase systems. Accordingly, the heat conductivity of rocks is arbitrary: it is equal to the heat conductivity of some homogeneous body through which, assuming identical geometric configuration, size and temperatures at the boundaries of the body, the same quantity of heat passes as through the inhomogeneous body in question.

In such a homogeneous body we will visualize two parallel sections at the distance l, on each of which we take the area S as the sector. If the temperature in one sector is T_1 and in the other is T_2, $T_1 > T_2$, the heat moves from the sector with the temperature T_1 to the sector with the temperature T_2. Obviously, during the time t the greater will be the quantity Q of heat transmitted the closer the sectors are spaced, the greater the area S, the greater the temperature difference $T_1 - T_2$, and the greater the time interval t during which the temperature difference $T_1 - T_2$ is maintained in the selected sectors.

This dependence is expressed by the formula

/47

$$Q = \lambda S \frac{T_1 - T_2}{l} t, \qquad \text{(II.4)}$$

where

λ is the proportionality factor which characterizes the capacity of a rock to transfer heat from one point to another in the presence of a temperature difference.

Thus, λ is a physical index dependent on the rock properties.

The value of the heat conductivity coefficient for a rock is determined by the heat conductivity of the matrix, λ_{sk}, porosity P, and moisture content W. In addition, heat conductivity is a function of temperature T and pressure σ of the system.

Thus

$$\lambda = f(\lambda_{sk}; P; W; T; \sigma). \qquad (II.5)$$

It must be remembered that rock porosity can exert a substantial effect on heat transfer; it can nullify the influence of other factors [26].

Heat transfer through the volume of pores at increased temperatures occurs not only by heat conductivity, but also by convection and radiation. The degree of the influence of convection is determined by the size of the pores and their arrangement (vertical or horizontal). The effect of radiation is dependent to a considerable degree on the absolute temperature of the pore walls. The total quantity Q of heat transferred in a unit time through an air layer with the thickness δ is

$$Q = (k_c + \alpha_r) F (T_{p1} - T_{p2}), \text{ cal/hour} \qquad (II.6)$$

where

k_c is the coefficient of heat transfer by contiguity, cal/m^{2}hour·degree;

α_r is the coefficient of heat transfer by radiation, cal/m^{2}hour·degree;

F is the area of the pore walls, m^2;

T_{p1} and T_{p2} are the wall temperatures, °C.

It is very difficult to compute the precise k_c value. If the pores are small and air (gas) convection is absent, the quantity of imparted heat is fully determined by heat conductivity of the medium, that is

$$Q = k_c F (T_{p1} - T_{p2}) = \frac{\lambda}{\delta} F (T_{p1} - T_{p2}), \qquad (II.7)$$

where

$$k_c = \lambda/\delta. \qquad (II.8)$$

As a simplification the heat exchange process is regarded as the elementary phenomenon of heat transfer only by heat conductivity, introducing the concept of the equivalent heat conductivity coefficient λ_{equiv}. In this case, the quantity Q_c of heat transferred by contiguity is determined from the expression [26]

$$Q_c = k_c F(T_{p1} - T_{p2}) = \frac{\lambda_{equiv}}{\delta} F(T_{p1} - T_{p2}). \qquad (II.9)$$

Then Eq. (II.6) can be written in the form

$$Q = [(\lambda_{equiv}/\delta) + \alpha_r] (T_{p1} - T_{p2}). \quad (II.10)$$

In studying the effect of pores (intercalations) on heat conductivity it is customary to determine the ratio of the equivalent heat conductivity coefficient λ_{equiv} to the heat conductivity coefficient for the mass of solid matter itself λ_{sol}:

$$\varepsilon_{con} = \lambda_{equiv}/\lambda_{sol}. \quad (II.11)$$

This ratio is called the convection coefficient.

Its numerical value characterizes the effect of convection in the heat transfer from the hot to the cold walls of pores.

The heat exchange phenomenon in pores is completely determined by the laws of free movement [27].

Since circulation is governed by the difference in densities of heated and cold particles and is determined using the criterion

$$Nu = f(Gr \cdot Pr), \quad (II.12)$$

ε_{con} must also be a function of this same argument, that is

$$\varepsilon_{con} = f_1(Gr \cdot Pr),$$

where

Nu, Gr, Pr are the Nusselt, Grashof, and Prandtl numbers, respectively.

The presence of pores in a rock leads to an increase in the radiant heat exchange between the surfaces of the pores through the air (gas) cells separating them.

The effect of convection on the heat conductivity coefficient for rock will be the greater the larger the cells. This is graphically illustrated in Table 11, giving the values of the air heat conductivity coefficient for pores of different sizes [26].

TABLE 11. VALUES OF THE HEAT CONDUCTIVITY COEFFICIENT

Mean temperature, °C	λ, cal/m·hour·degree for a pore diameter (mm)			
	0	0,5	1	5
0	0,020	0,022	0,024	0,038
300	0,037	0,053	0,069	0,198
500	0,046	0,086	0,126	0,414

Commas represent decimal points.

The heat conductivity of a rock in a general case is in cubic dependence on porosity P (in fractions of unity) [28]:

$$\lambda = \lambda_0 (1 - P)^3, \qquad (II.13)$$

where

λ_0 is the rock heat conductivity coefficient in the absence of porosity.

If ΔQ of heat is imparted to a rock with the mass m and the rock temperature is thereby increased from T to T + ΔT degrees, it can be assumed that /49

$$\Delta Q = C\,\Delta T, \qquad (II.14)$$

where

C is a proportionality factor, called rock heat capacity, cal/m^3·degree;

$$C = c\gamma$$

c is the specific heat capacity of the rock, cal/kg·degree;

γ is rock specific gravity, kg/m^3.

Rock heat capacity is a function of mineralogical composition and can be computed using the mixture formula [29]

$$C = c_1 x_1 + c_2 x_2 + \ldots = \sum_{i=1}^{n} c_i x_i, \qquad (II.15)$$

where

c_i is the specific heat capacity of the minerals making up the rock;

x_i is the content of corresponding minerals in fractions of unity of the total rock weight.

The mixture formula can be used in computing the heat capacity of a moist rock in a case when its moisture content by weight does not exceed 15-20%.

The dependence of rock heat capacity on temperature was introduced only

for a simplified model of a crystalline state [26].

As is well known, the mean heat capacity C_m of a rock in the temperature range T_1 and T_2 is

$$C_m = \frac{q}{T_2 - T_1}, \tag{II.16}$$

where

q is the quantity of heat required for increasing the rock temperature from T_1 to T_2 degrees.

The true heat capacity at the temperature T is

$$C_m = \frac{dq}{dT}, \tag{II.17}$$

where

dq is the quantity of heat required for increasing the rock temperature from T to T + dT degrees.

If the quantity q of heat required for heating the rock from the temperature T_1 to the temperature T_2 is proportional to the temperature difference $T_2 - T_1$, C is a constant value which does not change with an increase in temperature and is equal to C_m.

In most cases q changes by a different law and the dependence of C_m on temperature can be represented by the following empirical formula:

$$C_m = \frac{q'}{T} = a + bT - cT^{-2}, \tag{II.18}$$

where

a and b are constants.

It is known that under weak external effects rocks exhibit elastic resistance to dilatation and compression. /50

Figure 20 shows a schematic representation of the dependence of the forces between particles on the distance between them; the K_2 curve corresponds to repulsion and K_1 to attraction [30].

The resultant forces are expressed by the curve $K_1 = -K_2$; its shape is similar to the K_2 curve since with an increase in the distance between particles the forces of repulsion change to a greater degree than the forces of attraction. When $K_1 - K_2 = 0$ (intersection of the curve with the X-axis at the distance ρ_0) there is an equilibrium of particles and ρ_0 corresponds to the distance between

them. The potential energy of two contiguous particles is

$$\varphi = -\frac{a}{\rho^m} + \frac{b}{\rho^n}, \tag{II.19}$$

where

m and n are exponents corresponding to the change in the forces of attraction and repulsion as a function of distance.

Here m is equal to approximately 3, but n for different rocks varies in a wide range. However, in all cases n > m.

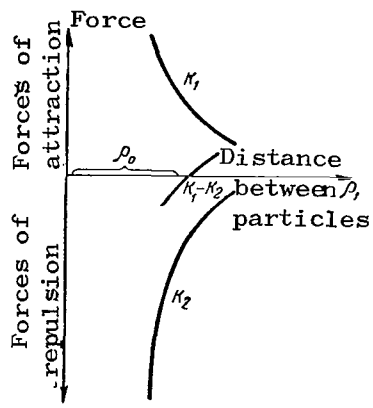

Figure 20. Diagram of interaction of forces among particles.

This inequality means that during heating rocks expand. As is well known, during heating the amplitude of particle oscillation increases. A withdrawal of a particle from a contiguous one will lead to a lesser counteraction of the force of repulsion during approach of particles. As a result, the position of the crystal lattice point changes (this point is the center near which the particle oscillates) and the equilibrium distance ρ_0 increases.

This results in an increase in the lattice constant, that is, thermal expansion occurs. If the $K_1 - K_2$ curve were straight, the amplitude of particle oscillations would increase during heating, but in this case ρ_0 would not change and there would be no thermal expansion.

Under the influence of temperature, various thermal effects can occur in minerals: dissociation, dehydration, disintegration, fusion, etc. Such effects are usually accompanied by heat absorption or release. The quantity of heat Δh which the component (mineral) absorbs with transition from a solid to a liquid state is called the heat of fusion. Fusion is the critical state of a mineral in which as a result of a temperature increase the cohesive force among particles /51 in the spatial crystal lattice is relaxed to such an extent that the mineral melts.

2. Methods for Measuring the Thermal Properties of Rocks as a Function of Temperature

Determination of the Heat Conductivity, Thermal Diffusivity and Heat Capacity of Rocks

The methods for measuring the indices of the thermal properties of rocks are divided into two groups:

1) stationary heat flux methods;

2) nonstationary heat flux methods.

Nonstationary heat flux methods can be classified into regular and irregular heat regime methods.

The stationary heat flux and regular nonstationary heat flux regime methods are unwieldy and at high temperatures do not give the required accuracy. Accordingly, they have little applicability in studying the thermal properties of rocks as a function of temperature.

Among the irregular regime methods the use of a source of constant and instantaneous intensity [31, 32] is of particular interest.

These methods make it possible to determine the heat conductivity coefficient λ and the thermal diffusivity coefficient a of rock in one experiment.

The basis of the source of constant intensity method is the heating of two semibounded rods at whose contact there is a source of constant intensity. The computation formulas for the method are as follows:

$$a = \left[\frac{x}{2\sqrt{\tau}\,\operatorname{arg\,ierfc}\,\frac{\overline{\Delta T_x}}{\Delta T_h \sqrt{\pi}}} \right]^2, \text{ m}^2/\text{hour} \tag{II.20}$$

$$\lambda = \frac{2q\sqrt{a\tau}}{\sqrt{\pi}\,\Delta T_h}, \text{ cal/m·hour·degree} \tag{II.21}$$

where

q is the specific heat flux,

$$q = \frac{0{,}864P}{2F};$$

P is heater power, $P = I^2R$;

I is the current measured from ammeter readings during the experiment, A;

R is heater resistivity, ohms;

F is heater area, m^2;

τ is time, hours;

ΔT_h, ΔT_x are heater temperature and temperature at the distance x from the heater, degrees; /52

ierfc u is the Cramp function derivative.

The volume heat capacity of a rock is determined from the known thermophysical characteristics a and λ determined from one experiment.

$$c = \lambda/a.$$

Figure 21 is a diagram of the experimental apparatus for determining the heat conductivity and thermal diffusivity coefficients.

The tested rock samples were prepared in the form of a parallelepiped measuring 50 x 50 x 20 mm. An electric heater EH, having the configuration of a plate, is fabricated from Nichrome 0.1 mm thick. Temperatures ΔT_h and ΔT_x are measured using two differential copper-constantan thermocouples 2 and 3 with the thermoelectrodes being 0.1 mm in diameter. The hot end of thermocouple 3 is fitted between the heater and the sample; the hot end of thermcouple 2 is at a distance of 5-6 mm from the heater.

The cold ends of the thermocouples fit in the sample at a distance of 45 mm from the heater.

The thermocouples are connected through a resistance box 5 to an automatic potentiometer 4 and are calibrated with it in advance.

Tests at high temperatures are made using a heating furnace in which the samples, heater and thermocouples are placed. Prior to onset of the experiment a conductimeter, consisting of rock samples, a heater, thermocouple and clamp 1, is held in the furnace until the temperature of the samples increases to the furnace temperature and the differential thermocouples do not show a temperature difference between the hot and cold junctions (the instrument hand is set on the zero graduation). The temperature of the samples is registered with a Chromel-Alumel thermocouple, also fitting into the conductimeter. /53

After the samples are heated to a definite temperature the electric heater is switched on. A voltmeter is used in measuring the voltage drop and a wattmeter and ammeter for measuring current parameters.

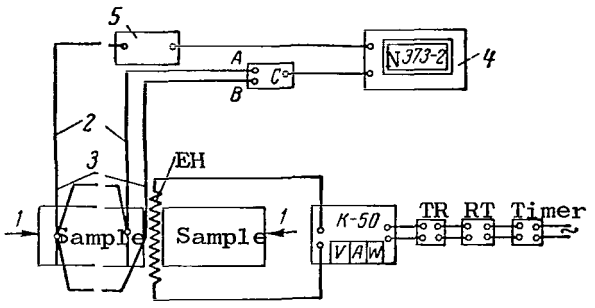

Figure 21. Diagram of the apparatus for complex determination of the heat and thermal conductivity coefficient of rocks.

At the same time a system is activated for registering the time change in ΔT_h and ΔT_x.

The experiment is considered satisfactory if in the coordinates $\Delta T - \sqrt{\tau}$ the change in ΔT_h and ΔT_x is linear; the ΔT_h straight line passes through the origin of coordinates. Deviations are observed in those cases when the thermal contact between the heater and the samples is unsatisfactory.

The basis for the second method is the heating of two semibounded rods with an instantaneous heat source at their contact.

The computation formulas for this method are as follows:

$$a = \frac{x^2}{2\tau_{max}}, \text{ m}^2/\text{hour} \qquad \text{(II.22)}$$

where

x is the distance from the heat source to the temperature gauge, m;

τ_{max} is the time when the temperature maximum is reached at the distance x, hours;

$$\lambda = k \frac{PT}{\tau_{max}\Delta T_{max}}, \text{ cal/m}^2\cdot\text{hour}\cdot\text{degree} \qquad \text{(II.23)}$$

where

$k = \frac{0.24\,x}{1000\,F\sqrt{\pi e}}$, 1/m is a constant;

F is the heater area;

P = UI;

U, I are the voltage and current drop, respectively;

T is the duration of the current impulse;

ΔT_{max} is the maximum excess of temperature over the ambient temperature at the distance x from the heater;

e is the base of natural logarithms.

In order for the error in determining the thermal diffusivity coefficient not to exceed 1% the following condition must be observed

$$T \leqslant 0.01 \frac{x^2}{a}. \qquad \text{(II.24)}$$

The layout of the apparatus is similar to the other (see Figure 21). The difference is that in this apparatus only one thermocouple 2 is used.

A differential thermocouple is connected to a potentiometer and is first calibrated with it. The thermal impulse is imparted by connecting an electric heater to the electric illumination network through a reducing transformer RT, and a time relay TR. The duration of the thermal impulse is checked by an electric timer. /54

The registry of $\Delta T = f(\tau)$ is with a standard automatic potentiometer 4.

A heating furnace is also used in high-temperature tests. A thermal impulse is imparted to the electric heater through the time relay in order to reach a definite furnace temperature. At the same time, the system for registering $\Delta T_x = f(\tau)$ is cut in.

A shortcoming of the method is the small temperature change ΔT_x (several degrees); this results in errors in computing λ and a.

Determining the Coefficient of Linear Thermal Expansion of Rocks

Now we will examine the change in crystal size under the influence of temperature (thermal deformation) at constant pressure. The thermal expansion of most crystals is anisotropic and can be expressed by a diagram of the coefficient of linear expansion, whose value is determined from the expression

$$\beta = \frac{1}{l} \cdot \frac{dl}{dT}, \tag{II.25}$$

where

l is crystal length at the temperature T;

dl is the thermal deformation caused by a temperature change by dT degrees.

The change in crystal size with heating from a temperature T_0 to T_1 is expressed by the exponential dependence

$$l = l_0 \left[\exp \int_{T_0}^{T_1} \beta(T)\, dT \right]. \tag{II.26}$$

If it is assumed that β = const, expression (II.26) is simplified:

$$l = l_0 [\exp \beta (T_1 - T_0)], \tag{II.27}$$

where

l_0 is the initial crystal length.

Since the coefficients of linear expansion of rocks are small and in order of magnitude are $\beta \cdot 10^{-5}$ degree^{-1}, from the latter equation we have the linear expansion law

$$l = l_0 [1 + \beta (T_1 - T_0)], \tag{II.28}$$

hence

$$\beta = \frac{l - l_0}{l_0 (T_1 - T_0)} = \frac{\Delta l}{l_0 \Delta T}.$$

All the quantities on the right-hand side of the equation can be determined on the appparatus (Figure 22) [33].

A rock sample 6 is inserted in the heater 5, which is a tube around which a Nichrome coil is wound; this sample is held between two quartz rods. A fixed rod 7 is attached to a support 8 which is mounted on a baseplate 9. The moving quartz rod 3 is held in the support 1, which has a spring. ∠55

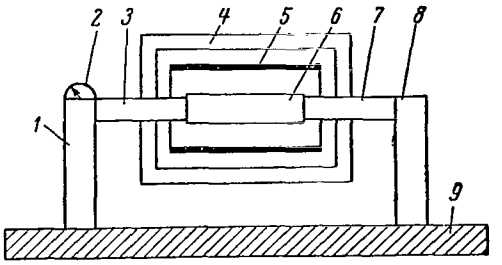

Figure 22. Diagram of apparatus for determining the coefficient of linear thermal expansion of rocks.

Under the influence of temperature the rock sample expands, causing a longitudinal movement of the moving rod; this is registered by a mechanical extensometer 2.

In order to prevent heating of the mechanical part of the apparatus the heater is placed in a cooling housing 4 with circulating water.

The sample temperature is measured by thermocouples on the sample and is registered with an electronic potentiometer.

The coefficient of linear expansion for the investigated rock is computed from the readings of the temperature difference between any two heating points on the specimen and from the relative linear expansion for this temperature range.

Determining the Surface Temperature of Heated Rock During Thermal Destruction

In the theory and practice of drilling in hard rock a determination of the temperature of the irradiated rock surface is of great importance in selecting the optimum heat flux parameters. For example, if the destruction temperature is close to the temperature of energy release of the rock or its components, for this rock there must be a heat flux whose temperature is equal to the destruction temperature. The imparting of heat must be accomplished with a high intensity (with a high heat transfer coefficient).

The described method is based on the fact that during rock heating its resistance changes: with a temperature increase rock resistance usually decreases. Figure 23 shows the regions of the dependence of resistance on temperature.

By constructing a calibration curve of the dependence of rock resistance on temperature and measuring the surface layer resistance during the brittle fracturing process, one can determine the destruction temperature.

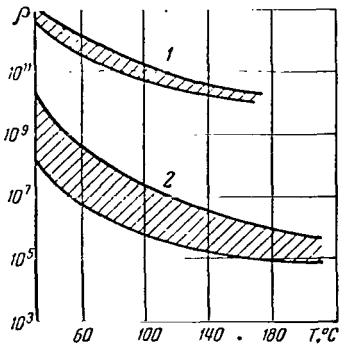

Figure 23. Dependence of resistance of microquartzite 1 and ferruginous quartzite 2 on temperature.

Figure 24 is a diagram of the experimental apparatus for determining the temperature of brittle fracturing of rocks during their exposure to thermal stress. /56

In measuring rock resistance a dc voltage is imparted to the irradiated sector through two point silver electrodes 1. The electrodes are pressed to the rock surface by the springs 2 and are shielded from the heat flux by the heat insulator 3. The current change during heating is registered with an N-700 oscillograph. The rock resistance at the time of destruction is determined from the oscillogram for the current passing through the rock with a constant voltage across the contacts. The rock resistance at any time is determined from the current amplitude.

The oscillogram (Figure 25) shows jumps in current amplitude at the time of particle separation.

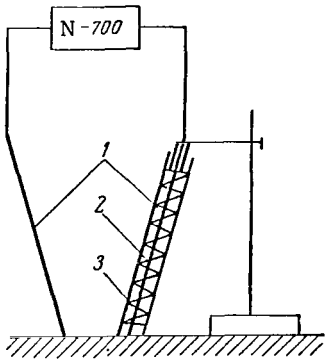

Figure 24. Diagram of apparatus for determining temperature of brittle fracturing of rocks.

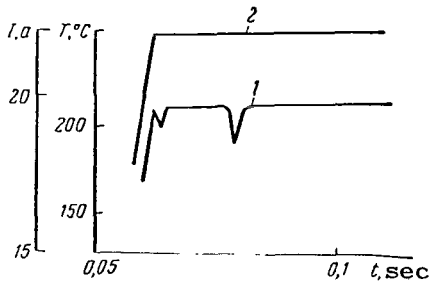

Figure 25. Oscillogram of process of separation of rock particle: 1) change in current strength; 2) rock temperature.

The layer of rock through which the current flows is of some thickness. When measuring resistance the mean temperature of this layer is given. It was established by special investigations that the thickness of the rock layer through which the current flows is not more than 15% of the thickness of the destroyed particle [25].

3. Patterns of Change in Thermal Properties of Rocks at High Temperatures /57

Dependence of Heat Conductivity, Thermal Diffusivity and Heat Capacity on Physical Properties of Rocks

The heat conducitivity and thermal diffusivity of rocks are dependent on their mineralogical composition, density, structure, porosity, moisture content and pressure. Rock salt, sylvite and anhydrite have increased heat conductivity in comparison with other minerals. An increased heat conductivity and thermal diffusivity is also characteristic of rocks whose electron heat conductivity component attains high values; this is because the process of heat transfer by electrons occurs more rapidly than crystal-lattice oscillation heat transfer. These rocks include: graphite, dense ferruginous and polymetallic ores containing hermatite, magnetite, pyrite, etc.

Table 12 gives data characterizing the dependence of the heat conductivity and thermal diffusivity of rocks on the percentage content of ore admixtures. The heat conductivity and thermal diffusivity of rocks are dependent on the granularity of the minerals forming the rock. Coarse-grained rocks have a greater heat conductivity and thermal diffusivity than rocks with fine and intermediate grains because the latter contain many fine mineral particles and accordingly there are many contacts between them which have a reduced heat conductivity.

Table 13 gives data for a number of rocks having a different structure despite identical chemical-mineralogical composition and porosity.

TABLE 12. DEPENDENCE OF INDICES OF THERMAL PROPERTIES OF INVESTIGATED ROCKS ON PERCENTAGE CONTENT OF ORE ADMIXTURES AT A TEMPERATURE 200°C (POROSITY P = 0.7 to 2.3)

Rock	Percentage of ore admixtures	Indices of thermal properties	
		λ, cal/m·hr·degree	$a \cdot 10^{-3}$, m^2/hr
Gabbro (Zhdanovskoye deposit)	1.15	1.689	2.56
Serpentinized peridotite (Zhdanovskoye deposit)	3.38	2.05	2.8
Mineralized serpentinized peridotite (Zhdanovskoye deposit)	12.30	2.6	3.64
Ore-free quartzite, parallel to stratification (Olenegorskoye deposit)	16.32	2.8	3.84
Ferruginous quartzite (Olenegorskoye deposit)	53.58	4.0	5.6
Albitophyre (T = 20°C)* (Degtyarskoye deposit)	1 - 2	1.7	-
Copper pyrite	97	8.5 - 34	-

* Data taken from [40].

TABLE 13. DEPENDENCE OF INDICES OF THERMAL PROPERTIES OF INVESTIGATED ROCKS OF IDENTICAL CHEMICAL-MINERALOGICAL COMPOSITION ON GRAIN SIZE

Rock	Temperature T, °C	Thermal parameters: Fine-grained structure (grain size up to 2 mm)				Thermal parameters: Intermediate and coarse-grained structure (grain size greater than 2 mm)				Data taken from Literature
		λ, cal/m·hour·degree	$a \cdot 10^{-3}$, m^2/hr	$c \cdot 10^3$ cal/m^3·deg	$\beta \cdot 10^{-3}$, deg^{-1}	λ, cal/m·hour·degree	$a \cdot 10^{-3}$, m^2/hr	$c \cdot 10^3$, cal/m^3·deg	$\beta \cdot 10^{-3}$, deg^{-1}	
Granite (Shartashskoye deposit)	200	0,694	1,15	0,602	1,05	0,78	1,3	0,601	0,95	—
Granite (Rovnenskoye deposit) . . .	200	1,69	2,76	0,61	1,35	1,75	2,9	0,604	1,1	—
Granite gneiss (Smolinskoye deposit)	200	1,17	1,8	0,65	1,35	2,6	4,22	0,616	1,02	—
Estonian kucker shale	300	0,105	0,61	0,173	—	0,11	0,72	0,153	—	[26]
Clay shale . . .	17	0,504	—	—	—	1,008	—	—	0,91	[35]
Sandstone (Tkibuli-Shaorskoye deposit)	20	1,73	2,3	0,752	—	2,92	3,73	0,786	—	[42]

Commas represent decimal points.

The data in Table 13 show that the values of the heat conductivity and thermal diffusivity coefficients for a fine-grained structure are smaller than for a coarse-grained structure. /59

Porosity exerts a substantial effect on the thermal properties of rocks. In most cases the heat conductivity and thermal diffusivity of rocks decrease with an increase in porosity (Table 14).

TABLE 14. DEPENDENCE OF INDICES OF THERMAL PROPERTIES OF ROCKS ON POROSITY WITH CONSTANT CHEMICAL-MINERALOGICAL COMPOSITION

Rock	Porosity, %	Temperature T °C	Indices of thermal prop. λ, cal/m·hour·degree	$a \cdot 10^{-3}$, m^2/hour	$c \cdot 10^3$, cal/m·hour·degree	$\beta \cdot 10^{-4}$, deg^{-1}	Data taken from literature
Quartzite (Pervoural'skoye deposit)	0	200	2,14	3,53	0,605	1,35	[41]
Porous quartzite	20	200	1,23	2,56	0,48	1,2	[41]
Coal (Lisichanskoye deposit)	18,7	—	0,18	0,42	—	—	[26]
	37,5	—	0,132	0,4	—	—	[26]
	43,5	—	0,12	0,385	—	—	[26]
Dense limestone	—	100	2,92—1,73	—	—	0,72	[35]
Porous limestone	—	—	1,91—0,95	—	—	—	[35]

Commas represent decimal points.

The lower limit of heat conductivity for highly porous rocks is their heat conductivity and thermal diffusivity. In the direction perpendicular to stratification the heat conductivity coefficient on the average of 10-30% lower than along the stratification; the thermal diffusivity coefficient can be reduced by 100% (Table 15).

The latter fact indicates that along the cleavage planes the particles

entering the crystal lattice interact more intensively and vice versa, molecular motion perpendicular to the cleavage planes is considerably weaker.

Rock structure exerts a substantial effect on heat conductivity. The heat conductivity of rocks in a crystalline state is much higher than in an amorphous state. For example, when a heat flux is propagated parallel to the axis in a quartz crystal the heat conductivity coefficient is 11.7 cal/m·hour·degree, whereas for amorphous quartz glass it is 1.2 cal/m·hour·degree.

As mentioned above, the heat capacity of rocks is dependent on the physical

TABLE 15. INDICES OF THERMAL PROPERTIES OF INVESTIGATED ROCKS RELATIVE TO STRATIFICATION

/60

Rock	Temperature T, °C	Indices of thermal properties for ∥ stratification			Indices of thermal properties for ⊥ stratification			Data taken from literature
		λ, cal/m·hr·deg	$a \cdot 10^{-3}$, m^2/hr	$\beta \cdot 10^{-5}$, deg^{-1}	λ, cal/m·hr·deg	$a \cdot 10^{-3}$, m^2/hr	$\beta \cdot 10^{-5}$, deg^{-1}	
Ore-free quartzite (Olenegorskoye deposit)	200	2.8	3.84	1.31	2.43	3.35	1.2	-
Ferruginous quartzite (Olenegorskoye deposit)	200	4.0	5.6	1.5	3.78	5.28	0.53	-
Granite gneiss (Olenegorskoye deposit)	200	2.28	3.11	1.35	1.9	2.7	0.75	-
Sulfur chlorite shale (Krivoy Rog deposit)	20	2.5	4.9	-	2.25	4.4	-	[34]
Coal	20	0.221	0.69	-	0.204	0.64	-	[26]
	50	0.224	0.71	-	0.211	0.67	-	[26]
Quartzitic sandstone	100	3.82	-	1.02	3.64	-	-	[35]
Marble	100	2.16	-	0.72	2.05	-	-	[35]
Granite gneiss	100	2.38	-	-	1.73	-	-	[35]

TABLE 16. INTERDEPENDENCE OF DENSITY AND HEAT CAPACITY OF CARBON AND SULFUR

Element	Allotropic modification	Specific gravity, g/cm^3	Specific heat capacity, cal/kg·degree
Carbon	Diamond	3.518	0.1128
	Graphite	2.25	0.1604
	Coal (gas coal)	1.285	0.2040
Sulfur	Rhombic	2.06	0.1728
	Monoclinic	1.96	0.1809
	Insoluble amorphous	1.89	0.1902
	Soluble amorphous	1.86	0.2483

properties of the component minerals. It should be noted that the determined experimental heat capacity values agree well with the data obtained using the mixture formula (II.15). The deviations do not exceed ±16%. It was established /61 that with a density increase the specific heat capacity of minerals is reduced (Table 16, Figure 26).

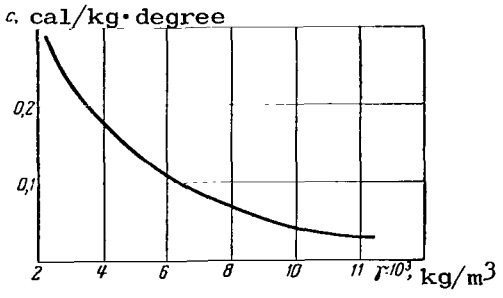

Figure 26. Curve of dependence of specific heat capacity on specific gravity of minerals when T = 200°C.

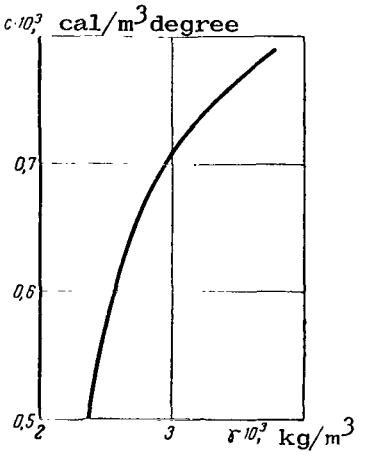

Figure 27. Curve of dependence of volume heat capacity on rock density for T = 200°C.

TABLE 17. DEPENDENCE OF ROCK HEAT CONDUCTIVITY [35] ON WETTING AND PRESSURE

Rock	Density, g/cm³	Porosity, %	λ_0, cal/m·hr·deg	$\frac{\Delta\lambda_W}{\lambda_0}$, %	$\frac{\Delta\lambda_p}{\lambda_0}$, %	$\frac{\Delta\lambda_{Wp}}{\lambda_0}$, %	λ_{con}
Marble	2,67	1,1	2,08	11	13	2	2,38
Limestone	1,55	43	0,76	—	22	—	0,925
Sandstone	2,17	22	1,59	36	40	6	2,26
Shale	2,76	—	1,55	—	4	—	1,62
Gabbro	2,87	—	1,62	—	2	—	1,65
Mica (crystal)	2,83	—	0,6	—	4	—	0,625

λ_0 is the heat conductivity of dry rock not subjected to compression at 45°C;

$\Delta\lambda_W$ is the heat conductivity increase after wetting in water;

$\Delta\lambda_p$ is the increase in the heat conductivity of dry rock after compression to 700 kg/cm²;

$\Delta\lambda_{Wp}$ is the heat conductivity increase for wet rock after compression to 700 kg/cm²;

λ_{con} is the maximum heat conductivity for compressed and wetted rock.

The volume heat capacity values increase with an increase in density (Figure 27). Analysis of the experimental data shows that when all other parameters are equal the heat capacity has a higher value for rocks with a fine-grained structure. The forces of interaction among glass atoms are the same as for the crystalline modification of this substance. Accordingly, heat capacity is not dependent on whether a rock is in the amorphous or crystalline state. For example, the heat capacities of crystalline and fused quartz are identical. /62

With an increase in rock moisture content there is usually an increase in the heat conductivity and thermal diffusivity coefficients, accompanied by an increase in heat capacity. For example, the heat conductivity of moist sandstones is 36% greater than for dry sandstones (Table 17). If the moisture content of coal is increased by 5% (from 1.29 to 6.28%), the heat conductivity and thermal diffusivity coefficients of the coal increase by a factor of about 1.7

and heat capacity increases by a factor of 1.1 (Table 18).

TABLE 18. INFLUENCE OF THE DEGREE OF MOISTENING ON THE INDICES OF COAL PROPERTIES OF THE KUZNETSK BASIN [36]

Coal moisture content W, %	Thermal diffusivity coefficient $a \cdot 10^{-3}$, m^2/hour	Heat conductivity coefficient, λ, cal/m·hour·degree	Heat capacity c, cal/kg·degree
1.29	0.358	0.110	0.370
1.85	0.399	0.124	0.388
3.57	0.487	0.142	0.384
5.05	0.534	0.168	0.424
6.09	0.595	0.181	0.416
6.28	0.625	0.187	0.426
6.80	0.675	0.188	0.409
8.26	0.717	0.210	0.437
9.56	0.730	0.220	0.453

The heat conductivity of rocks increases with increased pressure. For example, at a pressure of 700 kg/cm^2 the heat conductivity of limestones is 22% higher than at normal pressure (see Table 17).

Dependence of Coefficient of Linear Thermal Expansion on Physical Properties of Rocks

The highest absolute value of the coefficient of linear thermal expansion has been registered for quartzite. The value of this coefficient usually decreases with a decrease in the percentage content of quartz in rocks (Table 19).

The coefficient of linear thermal expansion of rocks is considerably affected by porosity; with an increase in porosity the coefficient of linear thermal expansion usually decreases. For example, for ferruginous quartzite in the Pervoural'skiy deposit owned by the Dinasovoy Plant, having a porosity of 20%, the linear thermal expansion coefficient differs by approximately 10% from the linear expansion coefficient for quartzite from this same deposit, in which porosity is absent (see Table 14).

The direction of stratification also exerts an influence on the coefficient of thermal expansion of rocks. The coefficient of linear thermal expansion, measured parallel to the stratification, can be three times greater than the coefficient measured perpendicular to the stratification (see Table 15). /63

TABLE 19. DEPENDENCE OF COEFFICIENT OF LINEAR THERMAL EXPANSION OF ROCKS ON QUARTZ CONTENT

Rock	Temperature, °C	SiO_2, %	$\beta \cdot 10^{-5}$, degree^{-1}	Data from literature
Microquartzite (Bakal'skoye deposit)	225-275	98	1.7	-
Granite (Rovnenskoye deposit)	225-275	28.25	1.5	-
		22.75	1.25	-
Quartzites	20-100	98	1.1	[35]
Sandstone	20-100	95	1.0	[35]
Granite	20-100	25	0.83	[35]
Diorite	20-100	20	0.72	[35]

TABLE 20. VALUE OF COEFFICIENT OF THERMAL LINEAR EXPANSION OF INTERMEDIATE, BASIC, ULTRABASIC AND SEDIMENTARY ROCKS

Rock	Temperature °C	Mean coefficient of linear thermal expansion, degree^{-1}	Data taken from literature
Diabase (Bakal'skoye deposit)	150-300	$1.0 \cdot 10^{-5}$	-
Shale (Bakal'skoye deposit)	200-300	$0.97 \cdot 10^{-5}$	-
Gabbro (Zhdanovskoye deposit)	100-300	$0.62 \cdot 10^{-5}$	-
Peridotite (Zhdanovskoye deposit)	100-300	$0.49 \cdot 10^{-5}$	-
Andesite	20-100	$(7\pm2) \cdot 10^{-6}$	[35]
Basalts, gabbro, diabases	20-100	$(5.4\pm1) \cdot 10^{-6}$	[35]
Sandstone	20-100	$(10\pm2) \cdot 10^{-6}$	[35]
Limestone	20-100	$(8\pm4) \cdot 10^{-6}$	[35]
Marble	20-100	$(7\pm2) \cdot 10^{-6}$	[35]
Shale	20-100	$(9\pm1) \cdot 10^{-6}$	[35]

For intermediate, basic, ultrabasic and sedimentary rocks the coefficient of linear thermal expansion usually does not exceed $1 \cdot 10^{-5}$ degree^{-1} (Table 20). With a further temperature increase there is a smooth increase in the coefficient of linear thermal expansion.

In most cases, assuming an identical chemical-mineralogical composition and porosity, the coefficient of linear thermal expansion of rocks with a fine-grained structure is greater than for those with an intermediate and coarse-grained structure (see Table 13). /64

Dependence of Heat Conductivity and Thermal Diffusivity, Heat Capacity and Coefficient of Linear Thermal Expansion of Rocks on Temperature

The heat conductivity coefficient for pure (native) metals decreases with a temperature increase. Aluminum is an exception. The ratio of the heat conductivity coefficient to the electron conduction coefficient remains approximately constant at different temperatures for "pure" metals (Wiedemann-Franz law) [30]:

$$\lambda/\chi T = \text{const.}$$

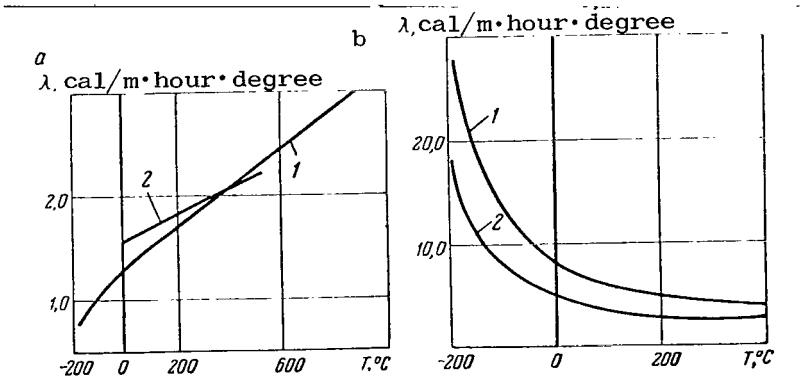

Figure 28. Curves of the dependence of the heat conductivity coefficient of minerals on temperature [35]: a- vitreous structure: 1- fused quartz; 2- obsidian; b- crystalline structure: 1- quartz (⊥ to the optical axis); 2- calcite (⊥ to the optical axis).

If λ is measured in W/cm·degree, absolute temperature in °K, and χ in $ohms^{-1} \cdot cm^{-1}$, for "pure" metals this value varies in the range $2.1 - 2.8 \cdot 10^{-8}$ $V^2/degree^2$. This is evidence of a close physical nature of heat and electric conductivity because both phenomena are caused by the presence of conduction electrons in metals (free electrons).

The heat conductivity coefficient for semiconductor minerals changes differently with a temperature change.

Figure 28 shows curves of the dependence of the heat conductivity of some minerals on temperature.

It was established that for minerals with a vitreous structure (Figure 28, a) the heat conductivity coefficient increases almost linearly with a temperature increase; for minerals with a crystalline structure (Figure 28, b) the heat conductivity coefficient decreases with a temperature increase. The nature of the decrease in the heat conductivity coefficient has a well-expressed nature in the temperature range up to +200°C, after which the change in this coefficient is usually linear. Accordingly, in rocks in which a crystalline structure prevails one should expect a decrease in heat conductivity with an increase in temperature. /65

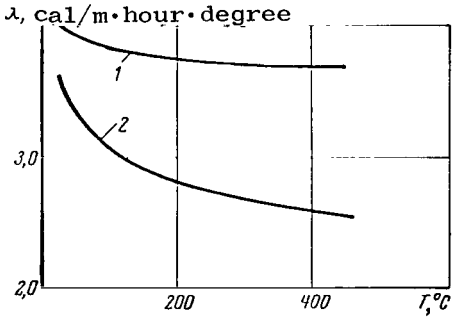

Figure 29. Dependence of rock heat conductivity coefficient on temperature: 1- ferruginous quartzite (Olenegorskoye deposit); 2- dolomite (Bakal'skoye deposit).

In rocks characterized by a dense crystalline structure (quartzites, granite gneiss, etc.) the heat conductivity coefficient decreases with a temperature increase (Figure 29 and Table 21).

In most cases the heat conductivity coefficient for rocks of this type changes sharply in the temperature range 200-250°C. At higher temperatures the change in this coefficient is linear

$$\lambda = \lambda_{200^\circ}[1 + b(T - 200^\circ)], \qquad (II.29)$$

where

T is temperature, °C;

b is the heat conductivity temperature coefficient.

The value b is negative since heat conductivity is decreased with heating. It has been experimentally established that for quartzites and granitoid $b = 2.8 \cdot 10^{-4}$ and for shales and dolomite $b = 4.2 \cdot 10^{-4}$.

The transfer of thermal energy in porous and permeable multiphase rocks which have maximum or partial water saturation (water-, gas- and petroleum-

saturated sands, sandstones, siltstones, limestones, coals) occurs for the most part through heat conductivity and convection of the pore space filler.

The filler behaves differently, depending on temperature (Table 22).

The heat conductivity of rocks with open pores differs from the heat conductivity of rocks with closed pores.

In open pores the air (gas) moves and more favorable heat exchange conditions are created than in a case when these pores are filled with a solid mass, even with a greater heat conductivity than for air.

For example, the presence of pores (P = 20%) exerts an influence on the nature of the temperature dependence of porous ferruginous quartzite. Accordingly, the λ value remains virtually constant in a wide temperature range, since in this case energy transfer by radiation does not exceed heat transfer by heat conductivity. /66

TABLE 21. VALUES OF HEAT CONDUCTIVITY COEFFICIENT FOR ROCKS [35]

Rock	Temperature, °C	Heat conductivity coefficient cal/m·hr·deg	Heat capacity, cal/kg·deg
Granite	0	3,02	0,192
	50	2,81	—
	100	2,59	—
	200	2,34	0,228
	300	2,12	—
	400	—	0,258
Syenite	50	1,89	0,17
	100	1,84	0,21
	200	1,79	0,237
Dunite	0	4,46	—
	50	3,78	—
	100	3,4	—
	200	2,92	—
Dolomitized limestone	130	1,41	—
	181	1,37	—
	268	1,29	—
	377	1,15	—
Marble	118	1,44	0,21
	196	1,29	0,24
	245	1,19	—
	360	0,95	0,271
Quartzitic sandstone	0	4,9	—
	100	3,82	0,26
	200	3,24	—
Shale	0	1,65	0,17
	100	1,51	—
	120	1,33	—
	188	1,41	0,24
	304	1,26	0,245

Commas represent decimal points.

With a temperature increase to 200°C the thermal diffusivity coefficient for dense rocks usually decreases sharply. With a temperature increase to 450°C this coefficient changes more smoothly (Figure 30). A decrease in the thermal diffusivity coefficient with a temperature increase to 200°C is accompanied by a marked decrease in the heat conductivity coefficient and an increase in the heat capacity coefficient (in the ratio $a = \lambda/c\rho$ there is a simultaneous decrease in the numerator and an increase in the denominator).

As mentioned above, the dependence of the heat capacity of rocks on temperature is a function of their mineralogical composition.

TABLE 22. DEPENDENCE OF THERMAL PROPERTIES OF FILLER ON TEMPERATURE

/67

Filler	Indices	Index of thermal properties of filler at a temperature, °C							
		−73	−23	0	27	127	227	427	627
Ice	$a \cdot 10^{-4}$	—	—	4,71	5,15	6,15	6,05	—	—
Water	λ	2,7	2,1	0,475	0,51	0,59	0,561	—	—
	c	0,38	0,47	1,0	0,998	1,015	1,1	—	—
Air	a	0,037	0,047	0,064	0,08	0,135	0,2	0,35	0,51
	λ	0,015	0,019	0,02	0,022	0,029	0,035	0,045	0,054
	c	0,24	0,24	0,24	0,24	0,242	0,246	0,257	0,268

a, m^2/hour; λ, cal/m·hour·degree; c, cal/kg·degree

Commas represent decimal points.

Table 23 gives the dependence of heat capacity of the principal rock-forming minerals on temperature and the constants of Eq. (II.18).

With an increase in temperature the heat capacity of the minerals is increased. A particularly sharp heat capacity increase is observed in the temperature range from -200 to +200°C.

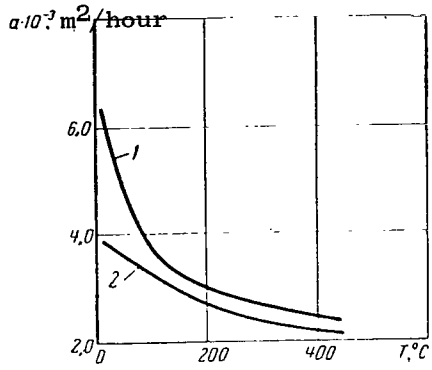

Figure 30. Dependence of thermal diffusivity coefficient of rocks on temperature: 1- granite (Rovnenskoye deposit); 2- peridotite (Zhdanovskoye deposit).

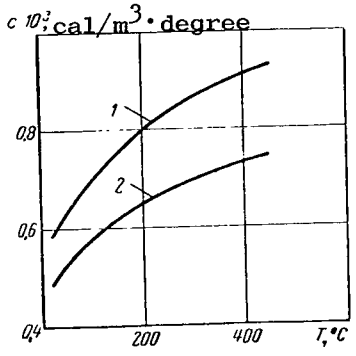

Figure 31. Dependence of volume heat capacity of rocks on temperature: 1- amphibolitic-magnetitic ferruginous unoxidized quartzite (Lebedinskoye deposit); 2- granodiorite (Smolinskoye deposit).

With an increase in temperature the heat capacity of rocks also increases. Figure 31 illustrates the characteristic changes in heat capacity of some rocks as a function of temperature. A particularly sharp increase in heat capacity is observed at a temperature up to 200°C. With a further temperature increase, the heat capacity increases insignificantly. /70

Table 24 gives the constants of Eq. (II.18), selected from experimental results, for some rocks.

Figure 32 gives the change in heat capacity of coal as a function of temperature.

TABLE 23. HEAT CAPACITIES OF PRINCIPAL ROCK-FORMING MINERALS

Mineral	Compound	c_p = (cal/kg·degree), at temperature °C						Constants for eq. $c_p = 0.239 (a + bT - cT^{-2})$. cal/kg·degree		
		−200	0	200	400	800	1200	a	$10^3 b$	$10^{-5} c$
Kaolinite	$Al_8Si_3O_{18}$	—	0,222	0,244	—	—	—	0,806	0,463	0,0
Barite	$BaSO_4$	0,047	0,1076	0,12	0,1315	0,1555	—	0,383	0,253	0
Fluorite	CaF_2	0,0525	0,203	0,213	0,222	0,24	0,263	0,798	0,204	0
Dolomite	$CaMgCO_3$	—	0,222 at 60°C	—	—	—	—	—	—	—
Chalcopyrite	$CuFeS_2$	—	0,129 at 50°C	—	—	—	—	—	—	—
Arsenopyrite	FeAsS	—	0,103 at 55°C	—	—	—	—	—	—	—
Siderite	$FeCO_3$	0,056	0,163	—	—	—	—	—	—	—
Hematite	Fe_2O_3	—	0,146	0,189	0,215	0,258	—	0,640	0,420	0,111
Magnetite	Fe_3O_4	—	0,1435	0,1985	0,2222	—	—	0,744	0,340	0,177
Pyrite	FeS_2	0,0179	0,1195	0,142	0,165	—	—	0,373	0,466	0
Ice	H_2O	0,156	0,492	—	—	—	—	—	—	—
Microcline	$KAlSi_3O_8$	—	0,163	0,227	0,248	0,342	—	0,988	0,166	0,263
Orthoclase	—	—	0,146	0,226	0,251	0,347	—	0,043	0,124	0,351
Garnet	$Mg_3Al_2Si_3O_{12}$	—	0,177 at 58°C	—	—	—	—	—	—	—

Commas represent decimal points.

TABLE 23 continued

Mineral	Compound	c_p = (kcal/kg·degree), at temperature °C						Constants for Eq. $c_p = 0.239 (a+bT-cT^{-2})$, cal/kg·degree		
		-200	0	200	400	800	1200			
Magnesite	$MgCO_3$	0,0385	0,207	—	—	—	—	—	—	—
Pyroxene	$MgSiO_3$	—	0,18	0,246	0,275	—	—	0,973	0,336	0,233
Amphibole		—	0,177	0,246	0,27	0,296	—	1 067	1,183	0,281
Olivine	$Mg_2Fe_2SiO_4$	—	0,189 at 36°C	—	—	—	—	—	—	—
Talc	$Mg_3H_2Si_4O_{12}$	—	0,208 at 59°C	—	—	—	—	—	—	—
Albite	$NaAlSi_3O_8$	—	0,1695	0,236	0,26	0,286	—	1,018	0,187	0,268
Galena	PbS	0,034	0,0496	0,0528	0,0562	—	—	0,188	0,007	0
α-quartz	SiO_2	0,0414	0,167	0,232	0,2695	—	—	0,7574	0,607	0,168
β-quartz	SiO_2	—	—	—	—	0,28	0,3165	0,763	0,383	0
Cassiterite	SnO_2	—	0,0814	0,103	0,115	0,132	—	0,387	0,157	0,007
Zircon	$ZrSiO_4$	—	0,146 at 60°C	—	—	—	—	—	—	—
Labradorite	2Ab·3An	—	0,196 at 60°C	—	—	—	—	—	—	—
Oligoclase	2Ab·1An	—	0,2035 at 60°C	—	—	—	—	—	—	—
β-graphite	C	—	0,152	0,282	0,348	0,45	—	0,932	0,913	0,4077
Diamond	C	—	0,104	0,253	0,328	0,445	—	0,754	1,067	0,454
Apatite	—	—	0,24	—	—	—	—	—	—	—
Serpentine	—	—	0,227	—	—	—	—	—	—	—
Mica (monocrystal)	—	—	0,208	—	—	—	—	—	—	—
Asbestos	—	—	0,195	—	—	—	—	—	—	—

Commas represent decimal points.

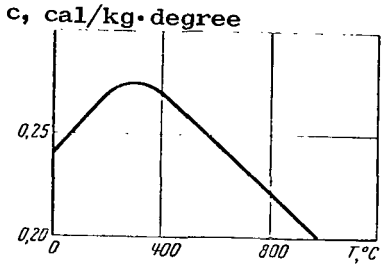

Figure 32. Dependence of mean specific heat capacity of thick coals on temperature [1].

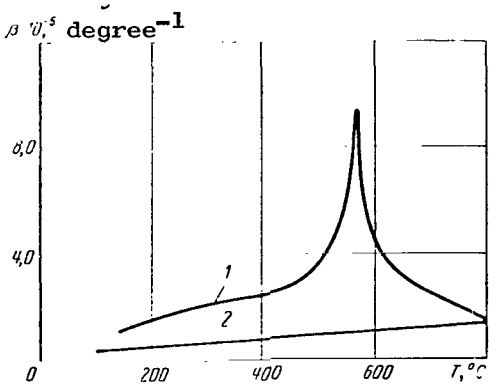

Figure 33. Dependence of coefficient of linear thermal expansion of rocks on temperature:
1- microquartzite (Bakal'skoye deposit);
2- gabbro (Zhdanovskoye deposit).

TABLE 24. HEAT CAPACITIES OF INVESTIGATED ROCKS

Rock	Constants for Eq. $c_p = 0.239 (a+bT - cT^{-2})$ cal/kg·degree			Error in temperature range 18-450°C, %
	a	10^3b	10^{-5}c	
Granite (Shartashskoye deposit)	0.964	0.252	0.294	±13
Granodiorite (Smolinskoye deposit)	0.955	0.29	0.233	±12
Diabase (Bakal'skoye deposit)	0.68	0.5	0.075	±17
Gabbro (Zhdanovskoye deposit)	0.94	0.28	0.23	±14
Quartzite (Bakal'skoye and Pervoural'skoye deposit)	0.75	0.6	0.17	±8
Shale (Bakal'skoye deposit	1.07	0.15	0.3	±12
Marble (mean of six samples)	0.823	0.497	0.129	±9

TABLE 24 continued

Rock	Constants for Eq. $c_p = 0.239 (a + bT - cT^{-2})$ cal/kg·degree			Error in temperature range 18-450°C, %
	a	$10^3 b$	$10^{-5} c$	
Porcelain clay, kaolin	0.607	0.707	0	±8
Diorite (andesite 50%, amphibole 40%, orthoclase 9%	1.024	0.187	0.273	±11

In the temperature range up to 300°C the heat capacity of coal increases and attains a maximum at 270-350°C; with a further increase in temperature the heat capacity of coal decreases, at 1,000°C approaching the heat capacity of graphite. /71

Now we will examine the patterns of change in mineral parameters with their heating. Table 25 gives data on the expansion of crystals as a function of temperature with respect to size with heating from 20°C.

Table 25 shows that with an increase in temperature the linear and volume thermal expansion of minerals increases. The rock dimensions also increase with heating.

The coefficient of linear thermal expansion of rocks usually increases with a temperature increase (Figure 33). In the case of quartz, the coefficient of linear expansion has a maximum value in the temperature range 570-650°C. This effect is obviously caused by the polymorphic transformation of α-quartz into β-quartz. Table 26 gives the values for the thermal expansion of quartz at different temperatures.

TABLE 25. RATIO OF THERMAL EXPANSION OF CRYSTALS TO SIZE OF CRYSTALS WITH HEATING FROM 20°C [35]

Crystal	Orientation relative to crystal axes	Expansion of crystals % relative to size with heating to a temperature, °C					
		100	200	400	600	800	1000
Ag		0,15	0,35	0,78	1.26	1,8	—
As		0,04	—	—	—	—	—
Au		0,11	0,26	0,57	0,90	1,26	—
Bi	∥ st.	0,15	—	—	—	—	—
	⊥ st.	0,11	—	—	—	—	—
	V.T.E.*	0,37	—	—	—	—	—
C (Diamond)		0,2	0,05	0,11	0,19	—	—
Cu		0,13	0,29	0,64	1,02	1,44	—
Fe (pure)		0,12	0,25	0,55	0,90	1,19	—
S		0,65	—	—	—	—	—
Zn	∥ st.	0,57	1,16	—	—	—	—
	⊥ st.	0,14	0,39	—	—	—	—
	V.T.E.*	0,85	1,94	—	—	—	—
Compounds with haloids							
CaF_2 (fluorite)		0,16	—	—	—	—	—
KCl (sylvite)		0,27	0,63	1,50	2,54	—	—
NaCl (halite)		0,32	0,74	1,71	2,82	—	—

* Volume thermal expansion

TABLE 25 continued

Crystal	Orientation relative to crystal axes	Expansion of crystals % relative to size with heating to a temperature, °C					
		100	200	400	600	800	1000
Sulfides							
Ag_3SbS_3 (Pyrargyrite)	∥ st.	0,02	—	—	—	—	—
	⊥ st.	0,16	—	—	—	—	—
	V.T.E.*	0,34	—	—	—	—	—
$CuFeS_2$ (Chalcopyrite)		0,14	—	—	—	—	—
FeS_2 (Pyrite)		0,07	—	—	—	—	—
$Fe_{10}S_{11}$ (Pyrrhotite)	∥ st.	0,03	—	—	—	—	—
	⊥ st.	0,25	—	—	—	—	—
	V.T.E.*	0,53	—	—	—	—	—
PbS (Galena)		0,15	—	—	—	—	—
ZnS (Sphalerite)		0,06	—	—	—	—	—
HgS (Cinnabar)	∥ st.	0,17	—	—	—	—	—
	⊥ st.	0,14	—	—	—	—	—
	V.T.E.*	0,45	—	—	—	—	—
Oxides							
Al_2O_3 (Corundum)	∥ st.	0,06	0,13	0,30	0,49	0,69	0,89
	⊥ st.	0,04	0,11	0,28	0,46	0,63	0,82
	V.T.E.*	0,14	0,35	0,86	1,41	1,95	2,53
Fe_2O_3 (Hematite)	∥ st.	0,06	—	—	—	—	—
	⊥ st.	0,06	—	—	—	—	—
	V.T.E.*	0,19	—	—	—	—	—
Fe_3O_4 (Magnetite)		0,07	—	—	—	—	—
SnO (Cassiterite)	∥ st.	0,03	—	—	—	—	—
	⊥ st.	0,03	—	—	—	—	—
	V.T.E.*	0,09	—	—	—	—	—
$FeOCr_2O_3$ (Chromite)		0,05	0,12	0,29	0,46	0,65	0,80
Carbonates							
$CaCO_3$ (Aragonite)	∥ *a*	0,05	0,13	0,33	Is transformed into calcite		
	∥ *b*	0,11	0,29	0,74			
	∥ *c*	0,20	0,58	1,39	—	—	—
	V.T.E.*	0,36	1,00	2,48	—	—	—
$CaCO_3$ (Calcite)	∥ st.	0,17	0,45	1,07	1,80	—	—
	V.T.E.*	0,08	0,21	0,60	1,14	—	—
$CaCO_3$ (pure)	∥ st.	0,207	0,494	—	—	—	—
	V.T.E.*	0,131	0,322	—	—	—	—
Sulfates							
$CaSO_4 \cdot 2H_2O$ (Gypsum)	∥ *b*	0,34	—	—	—	—	—
	V.T.E.*	0,58	—	—	—	—	—

* Volume thermal expansion

TABLE 25 continued

Crystal	Orientation relative to crystal axes	Expansion of crystals % relative to size with heating to a temperature, °C					
		100	200	400	600	800	1000
Silicates							
Augite	⊥ 100	0,03	0,06	0,16	0,29	0,44	0,63
	∥ *b*	0,08	0,19	0,44	0,72	1,03	1,37
	∥ *c*	0,04	0,10	0,23	0,36	0,51	0,67
	V.T.E.*	0,15	0,35	0,83	1,37	1,98	2,67
Beryl	∥ st.	0,007	0,011	—	—	—	—
	⊥ st.	0,027	0,034	—	—	—	—
	V.T.E.*	0,061	0,079	—	—	—	—
Olivine	∥ *a*	0,04	0,10	0,26	0,43	0,58	0,76
	∥ *b*	0,08	0,18	0,43	0,74	1,04	1,36
	∥ *c*	0,07	0,18	0,42	0,68	0,92	1,20
	V.T.E.*	0,19	0,46	1,11	1,85	2,54	3,32
Orthoclase	∥ *a*	0,12	0,32	0,69	1,08	1,48	1,80
	∥ *b*	0,06	—	—	—	—	—
	V.T.E.*	0,20	—	—	—	—	—
Zircon	∥ st.	0,03	0,08	0,20	0,34	0,48	—
	⊥ st.	0,02	0,05	0,11	0,19	0,28	—
	V.T.E.*	0,07	0,17	0,42	0,73	1,05	—
Muscovite (aggregate)		0,03	0,15	0,37	0,66	1,30	1,55
Tourmaline	∥ st.	0,08	—	—	—	—	—
	⊥ st.	0,06	—	—	—	—	—
	V.T.E.*	0,20	—	—	—	—	—

*Volume thermal expansion

Commas represent decimal points.

TABLE 26. THERMAL EXPANSION OF QUARTZ (IN COMPARISON WITH QUARTZ DIMENSIONS AT 20°C)

Temperature °C	Change in length of quartz crystal, % in direction		Volume change %	Temperature, °C	Change in length of quartz crystal, % in direction		Volume change %
	∥ to c axis	⊥ to c axis			∥ to c axis	⊥ to c axis	
50	0,03	0,07	0,17	570	0,84	1,46	3,76
100	0,08	0,14	0,36	580	1,03	1,76	4,55
150	0,12	0,22	0,56	600	1,02	1,76	4,54
200	0,18	0,30	0,78	650	1,02	1,76	4,54
250	0,23	0,40	1,03	700	1,01	1,75	4,51
300	0,29	0,49	1,27	750	1,00	1,74	4,48
350	0,36	0,60	1,56	800	0,97	1,73	4,43
400	0,43	0,72	1,87	850	0,94	1,72	4,38
450	0 51	0,87	2,25	900	0,92	1,71	4,34
500	0,62	1,04	2,70	1000	0,88	1,69	4,26
550	0,75	1,29	3,33				

Commas represent decimal points.

The coefficient of linear thermal expansion of minerals and rocks in a liquid state (at high temperatures) is several times greater than this same coefficient for rocks in a crystalline state. For example, the coefficient of linear thermal expansion of fused diabase is four times greater than this same coefficient at a temperature of 150° and 2.5 times greater at a temperature of 600°C (Table 27). /74

TABLE 27. THERMAL EXPANSION OF MINERALS AND ROCKS IN A LIQUID STATE [35]

Mineral rock	Temperature, °C	Thermal expansion $\beta \cdot 10^{-5}$, degree^{-1}
Akermanite	1458	5.6
Diabase	1200	3.8
Basalt	1250	8.2
Diorite	1250	14.0
Plagioclase	1480	5.6
Copper	1083	14.3
Pure iron	1535	14.4
Common salt	804	36.7
Sylvite	776	40.2
Diopside	1391	6.4

Physicochemical Transformation in Rocks Under Thermal Stress

Rocks as multicomponent heterogeneous systems are complex chemical formations. With a change in the state of the system under the influence of external stresses a number of phenomena can occur in the rocks. For example, during heating conditions can be created for a transformation of the rock material from one phase to another or the formation of a new phase.

These phase transitions include a number of physical and chemical phenomena: evaporation, condensation, fusion, hardening, the allotropy and polymorphism phenomena, ferroelectric and antiferroelectric, ferromagnetic and antiferromagnetic transformations, and transformation of rock from a normal to a superconducting state and vice versa. For example, at definite heating temperatures processes occur within a rock which cause a change in the internal nature of the minerals forming the rock and in many cases profound structural changes.

These changes may be of a purely physical nature.

If the rock includes oxides, in addition to the redox process and the formation of complex compounds, it is most common to observe polymorphic trans-

formations associated with a transition of one crystalline form into another with a change in thermodynamic conditions. The chemical nature of the compounds remains unmodified. /75

Polymorphic transformations can be of two types: reversible (enantiotropic) for which stability at definite temperatures and pressures of each of the polymorphic modifications is possible, and irreversible (monotropic), in which one modification during the entire time of its existence up to fusion is more stable than the other.

All quartz transformations are reversible.

Table 28 lists minerals with different modifications [42].

TABLE 28. TEMPERATURE OF TRANSFORMATION FROM ONE MODIFICATION TO ANOTHER

Mineral	Modification	Transition temperature, °C	Mineral	Modification	Transition temperature, °C
Corundum	$\alpha \rightarrow \beta$	1500-1800	Chalcosite	$\alpha \rightarrow \beta$	91
Diamond → graphite	-	3000	Iron	$\alpha \rightarrow \gamma$	910
Calcite → aragonite	-	400 (pressure 10,000 atm)	Quartz	$\alpha \rightarrow \beta$	573
Pyrrhotite	$\alpha \rightarrow \beta$	138			
Sulfur	$\alpha \rightarrow \beta$	95.5			

In other cases there is a change in the chemical nature of the minerals forming the rock. In such cases they break down into simpler chemical compounds or entering into chemical reactions with one another form new, more complex substances (minerals).

If a rock contains salts, such as carbonates or sulfates and other compounds, the most important reactions which can occur are combination, decomposition (particularly dissociation, dehydration), reduction and oxidation.

Thermochemical processes can also be classified as reversible and irreversible. For example, if thermal dissociation occurs with the release of the

gaseous phase, the process is irreversible, that is, it transpires in one direction during rock heating and does not recur during its cooling.

Investigations make it possible to obtain the most varied, precise and quite exhaustive information concerning the intracrystalline processes transpiring during transformation. These methods include: methods based on the Mossbauer effect, electron-diffraction, neutron-diffraction and roentgenographic methods and thermography.

A thermal curve in the form of a standard thermogram makes it possible to diagnose minerals and rocks, study their structure, and on this basis determine the engineering process for extracting a mineral. /76

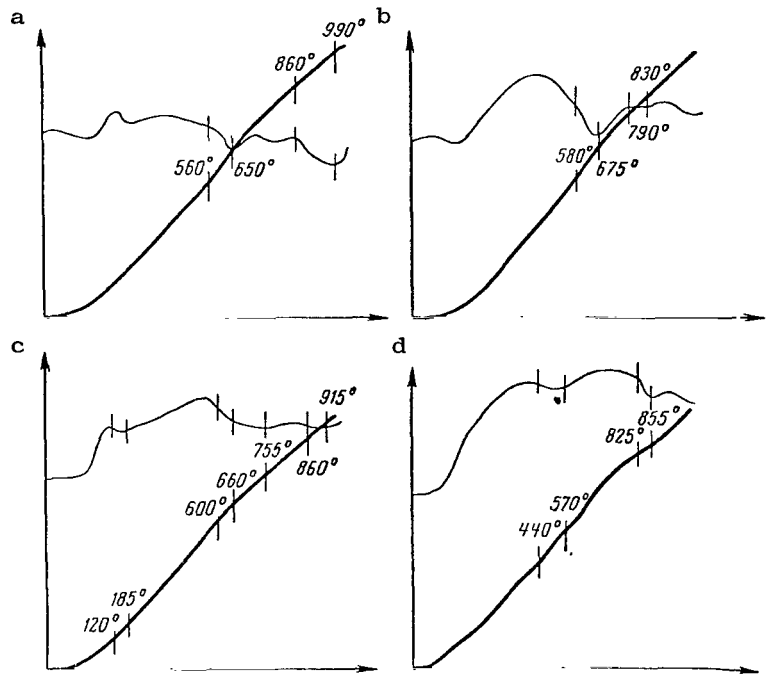

Figure 34. Thermograms of rocks from the Altyn-Topkanskoye deposit. a) shale; b) sandstone; c) granodiorite; d) skarn.

Figure 34, a, b, and c shows thermograms for shale, sandstone and granodiorite. On the thermograms one can trace an endothermic effect at a temperature of about 650°C (it begins from approximately 560°C). The effect characterizes the transformation of α-quartz into β-quartz and the decomposition of

feldspars (release of constitution water). The endothermic effect of a polymorphic transformation of SiO_2 is detectable above 900°C.

An increase in rock volume at 573° leads to an increase in thermal stresses which immediately are leveled out due to the decomposition of clayey components.

Figure 34 d shows a thermogram for skarn; there is a clearly detectable endothermic effect at 570°C (transformation of α-quartz into β-quartz) and an endothermic effect at 855°C, probably associated with the decomposition of garnets and pyroxenes.

Accordingly, at a temperature of 570°C an increase in the volume of quartz /77
grains by +2.7% will favor an increase in thermal stresses.

In the process of producing a mineral the matter of controlling phase transitions assumes great importance; these transitions can radically change the picture of thermal stresses. Phase transitions sometimes lead to a decrease in the initial thermal stresses. In some cases, as a result of an increase in the rock volume and elastic properties these stresses increase sharply, as occurs, for example, in quartz transformations. In most cases qualitative transformations of matter associated with the absorption of thermal energy cause an increase in thermal stresses. The processes of disintegration and destruction of crystal lattices are associated with heat release. These changes decrease the thermal stresses.

Any physicochemical transformation is characterized by a definite temperature and a definite kinetics of the process, that is, by a certain rock heating rate.

During prolonged rock heating definite conditions prevail for their physicochemical transformations.

During heating, whose duration is fractions of a second (the process of brittle thermal fracturing of rocks by intensive heat fluxes), the role of phase transformations is inadequately clear.

Below we will give some results from a study of physicochemical transformations of rocks containing quartz and the products of their decomposition obtained during thermal drilling.

Chemical analysis of rocks and the products of their thermal destruction. A study was made of pure quartzites from the Bakal'skoye iron ore deposit containing up to 92% SiO_2 and ferruginous quartzites from the Krivoy Rog and Olenegorskoye deposits with a content of 40 to 50% iron and 50 to 60% SiO_2.

In addition to the initial rocks, a study was made of the destruction products (so-called "exfoliation") obtained during the thermal drilling of these rocks.

In order to avoid a thermal effect on the exfoliated material from the emanating hot gases, during the thermal drilling process a plasma beam was used which removed a layer from the rock surface with a thickness of one "exfoliation." Destruction was accomplished in such a way as to preclude a temperature effect on the exfoliated layers after their separation.

The inalterability of the phases characteristic for the initial rocks as a result of energy release was confirmed by roentgenographic methods.

Thermographic studies of rocks. Thermographic analysis was with a Kurnakov chart-recording pyrometer under conditions of uniform heating approximately to a temperature of 1,000°C with a heating rate of 10 to 12 degrees/min. Some heating or cooling curves, for increasing sensitivity in the differential thermocouple circuit, were registered with R_{dif} = 50 ohms. /78

Figure 35 shows a heating curve for a sample of quartzite from the Bakal'skoye deposit, representing almost pure quartz.

The curve reveals an endothermic effect with a minimum at a temperature of 588°C corresponding to a polymorphic transformation of α-quartz into β-quartz (which according to data in the literature is observed at 573°C) and an exothermic effect with a maximum at a temperature of 778°C.

The nature of this effect has not yet been clarified.

A cooling curve for this sample was also registered; it shows an exothermic effect at a temperature of 560°C, corresponding to the endothermic effect on the heating curve (as is known from data in the literature, all polymorphic transformations of quartz are reversible).

On the cooling curves one can observe only exothermic effects, because

according to the second law of thermodynamics, unless there is a compensating process there can be no imparting of heat from the cooler to the heater. The exothermic effect on the cooling curve is registered as an endothermic effect on the heating curve.

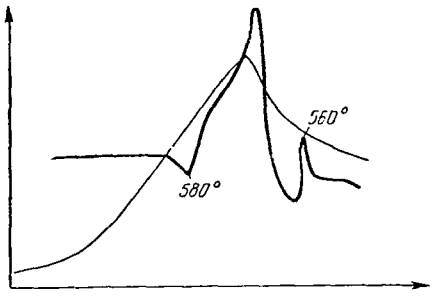

Figure 35. Thermogram of the heating and cooling of quartzite (Bakal'skoye deposit).

Some difference in the temperature of the polymorphic transformation on the heating and cooling curves can be attributed to the fact that during cooling the temperature of the transformation is reduced as a result of a lag in the process. Accordingly, on the heating curves, the temperature of the polymorphic transformation is somewhat higher than the equilibrium temperature, whereas on the cooling curve it is lower. The heating and cooling curves for quartz were registered as a comparison (Figure 36). On this curve there is an endothermic effect approximately in this temperature region (about 555°C).

Figure 37 is a thermogram for ferruginous quartz from the Krivoy Rog deposit. The quartzite samples contain 60 to 65% quartz and 34 to 36% ferruginous minerals in the form of oxides (magnetite, hematite).

The heating curve shows two thermal effects: one at a temperature of 600°C, corresponding to a polymorphic transformation of quartz (it must be assumed that the temperature shift is related to the high quartz content in the initial sample), and a second at a temperature of 790°C, associated with a change in the crystal lattice of hematite.

A thermogram of a sample (Figure 38) was also registered after the thermal drilling of ferruginous quartzite in the Krivoy Rog deposit (exfoliated material). /79
The heating curve shows a double endothermic effect at 580 to 620 and 750°C. The thermal effect at 540 to 600°C is duplicated on the cooling curve; this is associated with the polymorphism of quartz. The thermal effect at a temperature of 750°C corresponds to a polymorphic transformation of iron oxides.

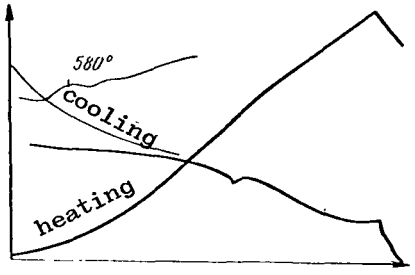

Figure 36. Thermogram for the heating and cooling of quartz.

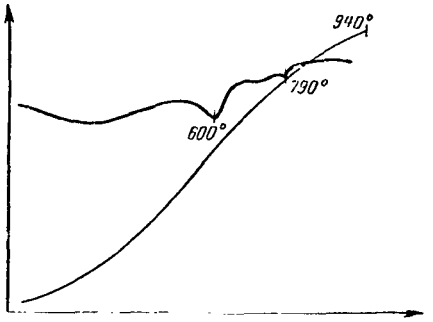

Figure 37. Thermogram for ferruginous quartzite (Krivoy Rog deposit).

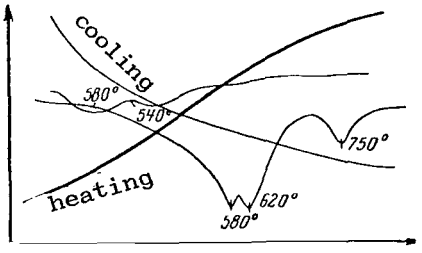

Figure 38. Thermogram for the heating and cooling of "exfoliated" ferruginous quartzite.

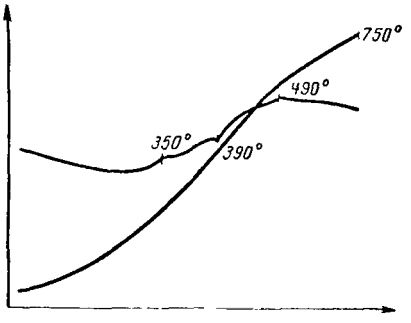

Figure 39. Thermogram of quartzite from the Olenegorskoye deposit.

The corresponding thermogram for ferruginous quartzite from the Olenegorskoye deposit (see Table 30) is shown in Figure 39. The curve was registered with a resistivity of 50 ohms in the differential thermocouple circuit.

The heating curve shows three thermal effects, two of which are exothermic at temperatures of 350 and 750°C, whereas one is endothermic at a temperature of 570°C; it is noted for all the studied samples. /80

The thermal effect at a temperature of 350°C probably corresponds to a crystalline process observed in oxide ores containing iron in this temperature region, whereas at 750°C it corresponds to polymorphism in the Fe_2O_3 crystal

lattice.

A study of the physicochemical transformations of rocks in the Bakal'skoye, Krivoy Rog and Olenegorskoye iron ore deposits makes it possible to draw the following conclusions.

The chemical composition of the principal components of the investigated rocks and the products of their thermal destruction remains constant; this is confirmed by chemical and x-ray investigations.

The heating and cooling curves reveal thermal effects corresponding to the polymorphic transformations of quartz and iron oxides.

Investigation of the Thermal Properties of Sulfur Ores and Country Rock in the Rozdol'skoye Deposit

The development of new geoengineering methods for producing sulfur requires a careful study of the physical properties of sulfur ores. At the present time the only geoengineering method for the extraction of sulfur is its melting-out by various heat carriers and therefore the thermal parameters of ores must be known for improving the sulfur extraction method.

The sulfur ores of the Rozdol'skoye deposit can be classified as calcareous and clayey, depending on the country rock.

The limestones in which sulfur is found are usually massive, fissured and cavernous. The caverns are filled with calcite. The sulfur content is rather stable and falls in the range 20 to 30%. A fine-grained type of sulfur (grain size 0.005 to 0.025 mm) predominates in the deposit and accounts for about 60% of the total quantity.

Another variety of sulfur which occurs in the deposit is coarse-crystalled, represented by well-delimited crystals of a considerable size (up to 5-7 mm). Coarse-crystalled sulfur forms pockets, seams and intercalations. Cryptocrystalline sulfur, constituting about 8% of all the sulfur in the deposit, forms inclusions of different configuration and size which have a dense appearance.

The country rocks are represented by limestones, gypsoanhydrites and anhydrites which contain no sulfur.

The heat capacity of the sulfur increases linearly with a temperature

increase to 105°C [39]. In the temperature range 105 to 115°C there is a change in heat capacity associated with the fusion of all sulfur. With further heating a slower increase in heat capacity occurs.

The specific heat conductivity of sulfur decreases uniformly to a temperature of 95°C (Figure 40); then it drops off sharply (in the temperature range 95 to 115°C).

A slight increase in the heat conductivity of liquid sulfur is observed at higher temperatures. /81

The heat conductivity and heat capacity of sulfur ores are usually greater than the heat conductivity and heat capacity of sulfur and calcite. This can be attributed to the presence of moisture.

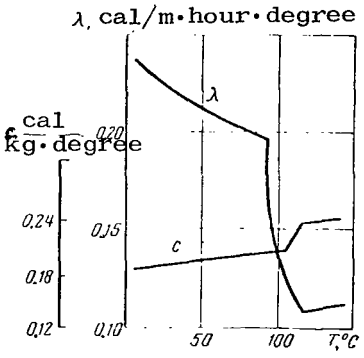

Figure 40. Dependence of heat capacity and heat conductivity coefficient of sulfur on temperature.

The coefficient of linear thermal expansion of sulfur increases with a temperature increase. The value of this coefficient for sulfur ores is smaller than for pure sulfur.

The thermal properties of calcite remain virtually unchanged in the considered range. Temperature exerts a substantial effect on the thermal properties of sulfur ores and country rock.

Analysis of the experimental data reveals that for most sulfur ores there is a decrease in heat conductivity approximately to a temperature of +70°C (Figure 41 a). In the temperature region 80 to 90°C, a maximum heat conductivity value is observed, after which there is a sharp dropoff [43].

Thus, the change in heat conductivity of sulfur ores with an increase in temperature differs from the heat conductivity of pure sulfur. At a temperature of 90°C rhombic sulfur may undergo a transition into monoclinic sulfur and therefore the presence of a maximum point on the heat conductivity curve may be attributable to this polymorphic transition.

The decrease in heat conductivity to the minimum point is obviously caused by drying-out of the rock samples, whereas its sharp decrease with a temperature increase above 90° is caused by the fusion of sulfur.

The dependence of the heat capacity of most sulfur ores on temperature also differs to a considerable degree from the corresponding dependence for pure sulfur (Figure 41 b).

The curves of the dependence of heat capacity on temperature for sulfur ores consist of three segments. Up to a temperature of 70°C the heat capacity exhibits a smooth decrease. In the temperature region 80 to 90°C there is an increase and then a decrease in heat capacity. The first segment is obviously related to the drying-out of the ore, whereas the maximum point corresponds to a polymorphic transformation of sulfur.

The dependence of the thermal diffusivity of sulfur ores on temperature in most cases is characterized by a minimum value of 90°C and a maximum at the melting point, after which there is a decrease in the thermal diffusivity coefficient (Figure 41 c).

The coefficient of linear thermal expansion of sulfur ores increases with a temperature increase. This coefficient has two maxima which can be traced for /83 almost all the ore samples (Figure 41 d). The first maximum falls in the region 60 to 70°C and the second in the region 90 to 110°C; the second maximum is greater than the first.

The heat conductivity and thermal diffusivity of the country rock are higher than the heat conductivity and thermal diffusivity of the sulfur ores.

The temperature curves for the country rocks, in contrast to those for the ores, do not have any anomalous points. In most cases the heat conductivity, thermal diffusivity and heat capacity coefficients decrease linearly with a temperature increase (Figure 42 a, b, c). The coefficient of linear thermal expansion for the country rock increases smoothly (Figure 42 d).

Investigations of the thermal properties of sulfur ores and country rock for the Rozdol'skoye deposit make it possible to determine the optimum parameters for the subterranean melting-out of sulfur, compute the heat accumulation zones, and control the technical operations in production.

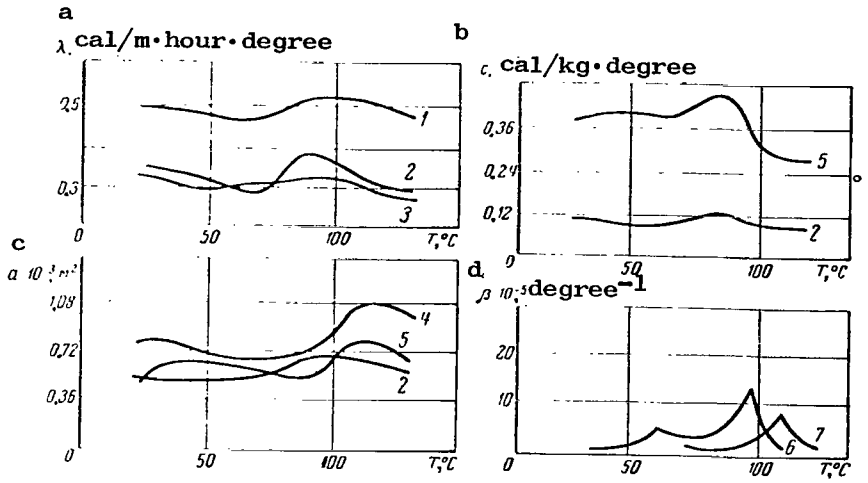

Figure 41. Curves of the dependence of heat conductivity, heat capacity, thermal diffusivity and coefficient of linear thermal expansion of sulfur ores on temperature: 1) gray limestone, streaky-impregnated sulfurization, crystalline sulfur; 2) gray limestone, finely impregnated sulfurization, clayey intercalations present; 3) gray limestone with a banded structure, thickness of limestone layers up to 1.2 cm, thickness of calcite and sulfur layers 2 to 5 mm; 4) unconsolidated limestone, found at depth of 56.3 m; 5) dense limestone, streaky impregnated sulfur, at depth of 54.5 m; 6) fissured limestone, finely impregnated sulfurization; 7) strong limestone, finely impregnated sulfurization, clayey material is observed.

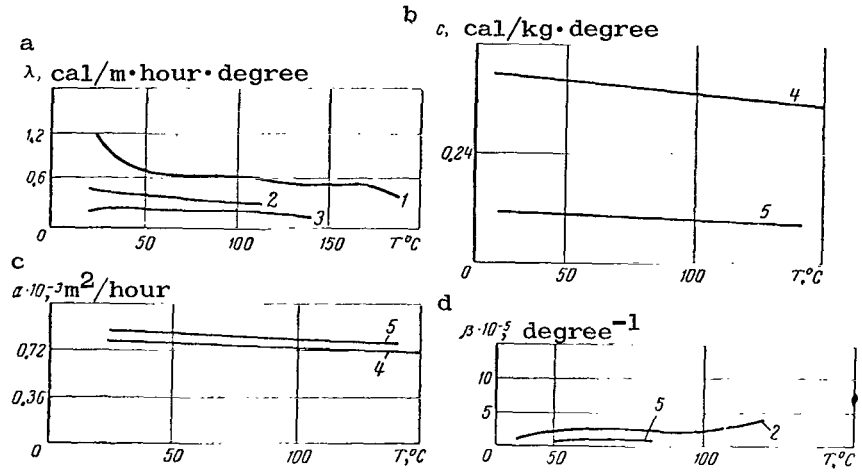

Figure 42. Curves of dependence of heat conductivity (a) heat capacity, (b) thermal diffusivity, (c) and coefficient of linear thermal expansion (d) for country rock on temperature: 1) fine-grained limestone without sulfur, with clayey intercalations, depth 41.6 m; 2) fine-grained limestone, depth 56.7 m; 3) finely impregnated limestone; 4) clayey limestone without sulfurization; 5) gray limestone, streaky-impregnated sulfurization, crystalline sulfur.

4. Examples of the Use of Thermal Properties of Rocks

/83

Change in the thermal properties of rocks is used extensively in solving various problems: in the thermal destruction of rocks and determining the parameters of the heat exchange process in the underground melting-out of sulfur.

As is well known, thermal destruction methods are used in drilling shot holes and boreholes in hard rock, in the secondary fracturing of rocks, and in other cases of constructing mine workings.

The possibility and efficiency of applying these methods for the breaking-off of hard rocks are determined primarily by their physical properties.

Below we will examine the problems involved in determining the conditions for the thermal destruction of rocks and evaluating their effectiveness.

Validation of a Rock Drillability Scale When Using Thermal Method

The advantages of thermal drilling of some extremely hard rocks are well known. However, the physical nature of the destruction process has not yet been adequately studied.

Study of the process of rock destruction by a directed heat flux essentially involves solution of the thermoelasticity problem with boundary conditions of the third kind.

As demonstrated by the experience of fire drilling, the size of the separating particles during brittle fracturing of the rocks is much less than the size of the heating spot. Accordingly, it can be assumed without great error that in a semi-infinite rod the heat is propagated along the X-axis (along the normal to the surface of rock heating), that the temperature gradient along the radius of the heating spot $\partial T/\partial z$ is infinitely small in comparison with the gradient $\partial T/\partial x$, and that a source with the constant intensity q is operative at the rock surface (x = 0) at the initial time. Accordingly, one must solve the differential heat conductivity equation /84

$$\frac{\partial T(x, t)}{\partial t} = a \frac{\partial^2 T(x, t)}{\partial x^2}, \qquad \text{(II.30)}$$

with the boundary conditions

$$\frac{\partial T(\infty, t)}{\partial x} = 0; \quad \lambda \frac{\partial T(0, t)}{\partial x} + q = 0, \qquad \text{(II.31)}$$

where

T(x, t) is the body temperature at the time t and at the distance x from the heating plane;

a, λ are the thermal diffusivity and heat conductivity coefficients.

Investigations revealed that with heating of the half-space existing during thermal drilling the following solution of the heat conductivity equation can be used with a sufficient degree of accuracy

$$\theta = 2c\,\mathrm{Ti}\,\mathrm{ierfc}\frac{1}{2\sqrt{\mathrm{Fo}_x}}, \qquad \text{(II.32)}$$

where

Ti is the Tikhonov criterion;

$$\mathrm{Ti} = \mathrm{Bi}_x \sqrt{\mathrm{Fo}_x};$$

Bi_x is the Biot criterion;

$$\mathrm{Bi}_x = \frac{\alpha x}{\lambda};$$

Fo_x is the Fourier criterion;

$$\mathrm{Fo}_x = \frac{at}{x^2};$$

α, λ, a are the heat transfer, heat conductivity and thermal diffusivity coefficients;

θ is a dimensionless parameter;

$$\theta = \frac{\Delta T(x, t)}{\Delta T_{\mathrm{eff}}} = \frac{T(x, t) - T_0}{T_{\mathrm{eff}} - T_0};$$

$T(x, t)$ is rock temperature at the time t and at the distance x from the heating plane;

T_{eff} is the effective (mean) temperature of the jet;

T_0 is the initial rock temperature.

The parameter c determines the nature of heat transfer to the rock by the gas jet:

$$c = 1 - 0.5 \frac{\Delta T_{\mathrm{surf}}}{\Delta T_{\mathrm{eff}}} \qquad \text{(II.33)}$$

where

$\Delta T_{\mathrm{surf}} = T_{\mathrm{surf}} - T_0$;

T_{surf} is the surface temperature of the rock at the time of its destruction.

The appearance of a high temperature field leads to the appearance of thermal stresses and under definite conditions leads to a dynamic effect in the rock. /85

The rock destruction method can be investigated by the method which is employed in computing stresses and strains arising in the welding process [38].

We will visualize that a semi-infinite body consists of an infinite number of longitudinal rock rods which are not connected to one another[2].

---

2. We will examine a quasi-isotropic state of rock. Heating of the rock by a "reactive" torch does not result in melting or any loss in the elastic properties of the rock.

The strains arising in the rod can be determined using the equation

$$\varepsilon = \beta \Delta T (x, t), \tag{II.34}$$

where

β is the coefficient of linear thermal expansion of rock.

The strain curves (see II.34) correspond in shape to the T(x, t) curves, although their true value is expressed by a different scale.

Now we will examine the true strains which can arise in a rock. Some rocks in the half-space are not free and are interconnected. The connection between a fiber and its neighbors restricts the freedom of its movement when its length changes. The true strains ware not equal to the possible strains determined by Eq. (II.34).

The difference between the possible and true strains determines the stressed state of a rock:

$$\sigma_z = E [\beta \Delta T (x, t) - \Delta], \tag{II.35}$$

where

σ_z is the normal stress, kg/cm^2;
E is the elastic modulus, kg/cm^2.

The sign in the brackets indicates the nature of the stress (dilatational or compressive).

We will seek the form of the function Δ in the solution of a differential equation in the form $\Delta'' - k^2\Delta = 0$, which for our conditions has the form

$$\Delta = A \exp(-kx), \tag{II.36}$$

where

A and k are some constant values.

During thermal drilling the rock is free of external bonds and therefore the sum of all internal forces and the sum of their moments relative to any point must be equal to zero, that is

$$\int_0^\infty \sigma_z dx = 0; \qquad \int_0^\infty x\sigma_z dx = 0.$$

Investigations show that solution of Eq. (II.36) assumes the form /86

$$\Delta = c\beta \Delta T_{\text{eff}} \text{Ti} \exp\left(-\frac{1}{\sqrt{\text{Fo}_x}}\right). \tag{II.37}$$

Substituting the determined values $\beta\Delta T(x, t)$ and Δ into the expression for normal stresses, we will have

$$\sigma_z = c\beta E \Delta T_{\text{eff}} \text{Ti}\left[\exp\left(-\frac{1}{\text{Fo}_x}\right) - 2\text{ierfc}\frac{1}{2\sqrt{\text{Fo}_x}}\right]. \tag{II.38}$$

Analysis of Eq. (II.38) shows that normal stresses (compression) have a maximum value at the heating surface and are compressive. With increasing distance from the surface the compressive stresses decrease and are transformed into dilatational stresses (they attain a maximum) and when $x \to \infty$ are transformed into zero.

Now we will examine the extremal σ_z values:

$$\sigma_{\text{com}}^{\max} = 0.128 c\beta E \Delta T_{\text{eff}} \text{Ti}. \tag{II.39}$$

The abscissa of the point at which the maximum dilatational stresses occur can be found by taking the derivative of the function of form (II.38) and equating it to zero:

$$x = 2.45\sqrt{at}. \tag{II.40}$$

Then

$$\sigma_{\text{dil}}^{\max} = 0.0386 c\beta E \Delta T_{\text{eff}} \text{Ti}. \tag{II.41}$$

We will find the ratio of the extremal values

$$\frac{\sigma_{\text{com}}^{\max}}{\sigma_{\text{dil}}^{\max}} = 3.32.$$

For most rocks the compression strength is more than 3.32 times greater than the tensile strength $[\sigma]_{\text{com}}/[\sigma]_{\text{dil}} \geqslant 3.32$ and therefore in thermal drilling the dilatational stresses more rapidly attain the breaking point than do the

compressive stresses.

However, under definite conditions destruction of the rock surface can occur by breaking-off as a result of the action of the maximum shearing stresses caused by compression.

Investigations show that the analytical expression for shearing stresses has the form

$$\tau = c\beta G \Delta T_{\text{eff}} \frac{a}{\lambda} B \left[\operatorname{erfc} \frac{1}{2\sqrt{\text{Fo}_x}} - \exp\left(- \frac{1}{\sqrt{\text{Fo}_x}} \right) \right], \qquad \text{(II.42)}$$

where

B is some constant value determining the distance from the center of the irradiated area to the particular point;

G is the elastic modulus of the second kind, kg/cm^2.

The surface shearing stresses are equal to zero. With increasing distance from the surface in the region of compressive stresses these stresses attain a maximum, then change sign, again increase to a maximum, and tend to zero when $x \to \infty$. In absolute value the first maximum is much greater than the second and therefore the distance from the surface where the destruction probability is greater is determined using the expression /87

$$x = 0.66\sqrt{at}. \qquad \text{(II.43)}$$

Investigations show that in this place the temperature of the exposed surface is considerable. It must be expected that as the working face advances it will increase until a thermal effect occurs (fusion, dissociation, dehydration) in the rock or in its individual components.

As a result, it can be assumed that the effect of shearing stresses alone has a negative effect on the efficiency of the thermal drilling process.

In the case of destruction from breaking stresses, the newly formed surface will be exposed to the very same conditions to which the destroyed surface had been subjected (its temperature is equal to the initial temperature of the rock, stress from the surface disappears). In the case of continuous imparting of heat (when working with a single-nozzle torch) the process is repeated and thus

the face moves forward.

Its rate of advance is obviously

$$v = \frac{h}{t_{sep}}, \tag{II.44}$$

where

h is the thickness of the separated particle ("exfoliated material")

t_{sep} is the time of its separation from the face.

Expressing h and t_{sep} through the indices of the physical properties of the rock and the jet parameters, we obtain

$$t_{sep} = \frac{670}{ac^2}\left(\frac{\sigma_{sep}\lambda}{\beta E\alpha\Delta T_{eff}}\right)^2; \tag{II.45}$$

$$h = \frac{63\sigma_{sep}\lambda}{c\beta E\alpha\Delta T_{eff}}. \tag{II.46}$$

The rate of rock destruction is

$$v = 0.0936c\,\frac{\beta E}{\sigma_{sep}c'v}\,\alpha\Delta T_{eff}, \tag{II.47}$$

where

c' is the rock volume heat capacity.

The plasticity index v was introduced into expression (II.47) for taking into account the rock properties; this index characterizes the ratio of the work of destruction to the work of elastic deformation.

Expression (II.47) is approximate because it was derived from a simplified model for computing temperatures and stresses. However, it is applicable for a qualitative evaluation of the process.

TABLE 29. DRILLABILITY SCALE FOR ROCKS WHEN USING THERMAL METHOD

Rock	Drillability criterion D, cm^3/cal	Thermal drilling category φ	Rock group	Specific energy expenditures, cal/cm^3
Bakal'skoye micro-quartzite	0.191	20		2.1-2.53
Pervoural'skiy quartzite	0.165	17		2.1-2.53
Ore-free Olenegorskiy quartzite (∥ stratif.)	0.159	16		2.34-2.93
Olenegorskiy pegmatite	0.147	15		2.95-3.3
Ore-free Olenegorskiy quartzite (⊥ strat.)	0.145	14		3.0-3.65
Olenegorskiy ferruginous quartzite (∥ strat.)	0.125	13	Easily drilled	3.24-3.65
Olenegorskiy gneiss (∥ stratification)	0.115	12		3.28-4.02
Smolinskiy gneissose granite	0.111	11		3.74-4.0
Fine-grained Shartashskiy granite	0.104	10		4.2-4.35
Olenegorskiy ferruginous quartzite (⊥ strat.)	0.102	10		4.42-4.92
Olenegorskiy gneiss (⊥ stratification)	0.101			4.8-5.05
Fine-grained granite (Rovnenskoye deposit)	0.0985	10		4.45-5.94
Coarse-grained granite (Rovnenskoye deposit)	0.096	10		5.4-5.96
Coarse-grained granite (Shartashskoye deposit)	0.0945	9		5.74-6.24
Porous ferruginous quartzite (Pervoural'skoye deposit)	0.094	9	Satisfactorily drilled	5.26-6.3
Gray granite (Rovnenskoye deposit)	0.094	9		5.4-7.25
Dolomite (Bakal'skoye deposit)	0.0755	8		
Granodiorite (Smolinskoye deposit)	0.065	7		5.72-8.7

TABLE 29 continued

Rock	Drillability criterion D, cm^3/cal	Thermal drilling category φ	Rock group	Specific energy expenditures, cal/cm^3
Gabbro (Zhdanovskoye deposit)	0.049	5		
Ore-free peridotite (Zhdanovskoye deposit)	0.048	5		
Diabase (Bakal'skoye deposit)	0.045	5	Drilled with difficulty	
Shale (Bakal'skoye deposit)	0.043	4		
Mineralized peridotite (Zhdanovskoye deposit)	0.0435	4		

The surface temperature at the time of its destruction when x = 0 can be determined by substituting Eq. (II.45) into expression (II.32): /89

$$\Delta T_{surf} = 29.2 \frac{\sigma_{sep} v}{\beta E} . \qquad (II.48)$$

The parameter $D = \beta E/\sigma_{sep} c'v$ is determined by the physical properties of the rock and characterizes its thermal drillability, that is, the capacity for brittle fracturing.

The indices for the thermal properties of the rocks are given in Appendix 2.

The scale for drillability of rocks by the thermal method is given in Table 29. The value of the D criterion was determined taking into account the properties taken with $T_{mean} = \Delta T_{surf}/2$. Table 29 also gives the specific energy expenditures obtained in experimental drilling of rocks with oxygen and air-fire jet thermodrills. The results of experimental drilling of rocks in quarries are given in Table 30.

TABLE 30. INDICES FOR THE EXPERIMENTAL DRILLING OF SHOT HOLES

Rock	Drilling rate, m/hour		Rate of hole formation m/hour	Mean diameter, mm		Specific energy expenditures, cal/cm^3
	maximum	average		pothole widening	shaft	
Microquartzite (Bakal'skoye deposit), φ = 20	10.5	7	3 (single stage excavation)	350	200	1.4
Quartzite (Pervoural'skoye deposit), φ = 17	9	6.6	3	340	200	1.5
Olenegorskiy rock complex, φ = 10-16	6-8	4-9	8	400	200	4.3
Ferruginous quartzite (YuGOK), φ = 9-10	6	4.6	14	480	200	4.7

Thus, a theoretically sound and experimentally confirmed thermal drillability criterion D can be used as a basis in a preliminary evaluation of the effect from thermal destruction of rocks.

Determination of Efficiency of Destruction Process

Using the thermal drillability criterion, one can examine the problem of the thermal efficiency of the brittle fracturing process in the fire drilling of rocks.

Determination of the efficiency of the process of brittle fracturing of a rock is of interest for both the theory and practice of drilling because in this case it is possible to determine the properties of solid bodies which serve to convert thermal into mechanical energy. /90

The thermal efficiency of the process of brittle fracturing can be represented as the ratio of the energy A expended on the destruction of a unit volume of rock to the total energy Q:

$$\eta_T = \frac{A}{Q} 100\%. \qquad (II.49)$$

The quantity of heat imparted to the rock is determined from the expression

$$Q = \eta_{eff}\eta_{hr}\frac{G_{fuel}H}{V_{vol}}, \text{ cal}, \tag{II.50}$$

where

η_{eff} is the effective efficiency of heat transfer from the jet to the rock;

η_{hr} is the coefficient of heat release in the combustion chamber;

G_{fuel} is the quantity of heat spent on destroying the volume V_{vol} of a particular rock, kg/m^3;

H is the heat-generating capacity of the fuel.

The A values can be determined:

from the load on the samples and from its deformations, determined from the diagram of destruction of a sample of a particular rock;

from the number of "exfoliated pieces" in a unit volume, from their newly formed surface, and from the critical deformation;

from the inverse value of the thermal drillability criterion D^{-1}, representing the energy required for destroying a unit volume of a particular rock:

$$A = D^{-1} = \frac{\sigma_{sep}^{cv}}{\beta E}, \text{ cal/cm}^3. \tag{II.51}$$

Determination of A by the first two methods involves some difficulties due to the lack of reliable experimental data. The latter method makes it possible to determine the A parameter from the results of studies of the physical properties of rocks with subsequent checking of drillability data.

Influence of Thermal Effects of Rocks on Their Thermal Destructibility

The stability of the process of brittle fracturing of rocks during thermal drilling, as is well known, is dependent on the constancy of the difference in rock surface temperature at the time of its destruction and the initial temperature. This temperature difference is a function only of the physical properties of the drilled rock:

$$\Delta T = T_{surf} - T_0 = 29.2 \frac{\sigma_{sep} v}{\beta E},$$

where

T_{surf} is the surface temperature;

T_0 is the initial temperature of the rock mass ($T_0 \approx 0 - 20°C$).

The drilling process will be extremely unstable if the surface temperature of the layer to be destroyed exceeds the temperature at which there is a thermal effect of the rock or its individual components. Thus, a study of the physical properties of the rocks and their components is of great importance in formulating a thermal drillability criterion for predicting and expanding the field of applicability of the highly productive method for the fire drilling of shot holes. /91

Investigations have revealed the range of rock surface temperatures for their brittle fracturing on the basis of a study of their physical properties and also on the basis of the experiment described above (Table 31). The characteristics of destruction of these rocks have been given before (see Table 29).

TABLE 31. ROCK SURFACE TEMPERATURE DURING THERMAL DRILLING

Thermo-drillability group	Rock	Experimental surface temperature, °C	Temperature, °C, computed using formula (II.48)
1	Quartz, microquartzite, ferruginous quartzites	Up to 350	Up to 400
2	Granite gneisses	-	400 - 600
3	Gabbro, diabase, shale, peridotites, talc	-	More than 900

A study of the melting points of rocks and minerals was made using the method described above.

The results of these investigations are given in Table 32. There was a satisfactory agreement between the results of these investigations and data in the literature [35-37] (Appendix 3).

We note that rocks having a low temperature of brittle fracturing and a relatively high thermal effect temperature are most effectively destroyed. Rocks of the quartzite class fall into this group.

The destruction temperature for rocks in the granitoid group is close to the temperature of the thermal effects of their component elements. The efficiency of the brittle fracturing of rocks of this group is dependent on the percentage content of minerals with a low thermal effect temperature (for the most part of a dark color). Accordingly, granitoids are very sensitive to thermal energy and the way it is imparted in their destruction.

In rocks of the third group, the surface temperature is close to and sometimes exceeds the temperature of the thermal effects of the minerals forming these rocks. Accordingly, one should not expect a stable directed brittle fracturing in these rocks. The effective destruction of rocks in this group evidently requires an artificial change in the conditions for imparting heat. For example, the preliminary cooling of the surface layer of rock (a decrease in T_0) leads to an increase in its brittleness and accordingly lower surface temperatures. /92

TABLE 32. DECOMPOSITION TEMPERATURE OF INVESTIGATED MINERALS AND ROCKS

Rocks, minerals	Temperature, °C
Garnet	800-850
Talc	800-840
Pyrrhotite	1000-1100
Chlorite	850-920
Epidote	800-900
Muscovite	850-950
Clay shale	900-950
Coal shale	900-950
Dark-colored skarn components (Altyn-Topkan)	900-950
Dark-colored components of gray granite in Rovnenskoye deposit	700-850
Labradoritic porphyrite	650-700
Feldspar	950-1050
Olivinitic gabbro-diabase	More than 1000
Gabbro of Zhdanovskoye deposit	800-900
Orthoclase	1170
Plagioclase	More than 1100
Calcite	950-1050
Galena	1100
Pegmatite from Olenegorskoye deposit	850-900
Syenite	850-950
Apatite (Khibiny)	More than 1100
Serpentine	More than 800
Bakal'skoye diabase	More than 1100

Chapter III

ELECTRIC AND MAGNETIC PROPERTIES OF ROCKS AS A FUNCTION OF TEMPERATURE

1. General Information on the Electric and Magnetic Properties of Rocks

As is well known, minerals constitute ionic compounds in which the ions are /93
bound for the most part by the forces of electrostatic attraction. The strength of the electrostatic field holding ions in the crystal lattice is influenced by an external force. This causes a change in the electric properties of minerals. Thus, by knowing the change in the electric properties of minerals one can make a quantitative determination of the external effect exerted upon them. Accordingly, the change in the electric properties of minerals and rocks in which particular minerals are found can be used in obtaining information on the state of rocks and minerals in the rock mass.

With the electric and magnetic properties of minerals taken into account, methods are created for acting upon them. Investigations have shown that the electromagnetic effect makes it possible to restructure minerals and change their physical properties in the necessary direction, as well as the properties of the rocks in which these minerals are incorporated.

Accordingly, if minerals are held in the crystal lattice by electric forces, the properties of these minerals can be changed by these same forces. The interaction of the electromagnetic field with matter, especially with minerals, is described by the Maxwellian equations. When solving problems on the basis of the Maxwellian equations, it is necessary to know the following indices of the electric and magnetic properties of minerals:

$g(\text{ohm}\cdot\text{cm})^{-1}$ is conductivity [or $\rho(\text{ohm}\cdot\text{cm})$ is resistivity, a parameter the inverse of g];

ε' is the relative dielectric constant (the true part of the complex dielectric constant);

$\varepsilon' = \varepsilon_{abs}/\varepsilon_{rel}$, where ε_{abs} is the absolute dielectric constant, F/m;

μ is relative magnetic permeability (true part), henry/m.

Conductivity g is in fact the proportionality factor between the current I /94
and voltage U in Ohm's law

$$I = gU \frac{S}{t} .$$

The dielectric constant is the proportionality factor between electric displacement $\bar{D}$ and electric field strength $\bar{E}$:

$$\bar{D} = \varepsilon' \varepsilon_0 \bar{E}.$$

The ε' parameter is dimensionless, but the value of the dielectric constant for a vacuum is

$$\varepsilon_0 = 8.885 \cdot 10^{-12}, \text{ F/m}.$$

Magnetic permeability μ is the proportionality factor between magnetic induction $\bar{B}$ and magnetic field strength $\bar{H}$:

$$\bar{B} = \mu\mu_0 \bar{H}.$$

The μ parameter is dimensionless, but the value of the magnetic constant for a vacuum is

$$\mu_0 = 12.57 \cdot 10^{-5}, \text{ henry/m}.$$

Minerals are conductors of the first and second kinds, semiconductors and dielectrics. Conductors of the first kind are electron conductors in which the charge transfer is by electrons without a significant transfer of mass. In conductors of the second kind the charge transfer is primarily by ions with a considerable mass transfer.

Conductors of the second kind have a high conductivity only at high temperatures, whereas at low and medium temperatures these are dielectrics because they are characterized by an extremely low conductivity.

Semiconducting and dielectric minerals have a mixed ion-electron conductivity, that is, the charges in them are transferred by both ions and electrons, but in semiconducting minerals the charges are transferred for the most part by electrons, even at high temperatures. In order to know whether a particular mineral is a dielectric or semiconductor, it is necessary to determine the type of charge carrier (ions or electrons), their mobility and the number in a unit volume (density), as well as the width of the forbidden band.

Rocks consisting only of semiconducting minerals are called semiconductors and rocks consisting only of dielectric minerals are called dielectrics. The electric properties of rocks consisting of dielectric, semiconducting and conducting minerals are inhomogeneous. The latter group of rocks is relatively numerous, but the first is relatively rare. The group of dielectric rocks has an extremely broad distribution.

Dielectric minerals and rocks have a relatively low relative dielectric constant (5-10); semiconducting minerals and rocks have a high relative dielectric constant (more than 10). Inhomogeneous rocks have a higher dielectric constant and its value is dependent on the rock content of conducting and semiconducting minerals. /95

Depending on their magnetic properties, minerals are diamagnetic ($\mu < 1$) and paramagnetic ($\mu > 1$). The magnetic permeability of paramagnetic minerals is approximately equal to unity. These minerals, as well as the rocks consisting of them, almost do not differ in their magnetic properties from a vacuum. The magnetic permeability of ferromagnetic minerals $\mu > 1$ (up to 2), but their number is small. The best known are magnetite, titanomagnetite and pyrrhotite. Rocks which contain ferromagnetic minerals in adequate quantity have a magnetic permeability $\mu > 1$; the μ value is dependent on the content of ferromagnetic material in the rock.

In order to obtain information on the state of the rock with respect to the change in any physical property, the first prerequisite is a study of the nature of the influence of this external effect on the change in this property.

In determining the electromagnetic effect on a rock it is necessary to know how and to what degree any electric or magnetic property may change under the influence of any particular external effect.

Temperature exerts the strongest effect on the electric and magnetic properties of minerals and rocks. By changing the temperature of a rock it is possible to change its electric and magnetic properties to a definite value.

Electric and magnetic properties are used in monitoring the condition of a rock mass, determining the content of a useful component in rock, dividing a rock into components, for imparting electromagnetic energy to a rock, etc. Since

electromagnetic energy is relatively cheap and extremely convenient for practical use, it is obvious that electric methods for studying and influencing rocks will be extensively used and intensively developed. The sections which follow describe the methods used and the results of investigating the electric and magnetic properties of rocks and also give examples of the use of these properties in the engineering methods for mineral extraction.

2. Methods for Investigating the Electric and Magnetic Properties of Minerals and Rocks

The electric and magnetic properties of rocks as a function of temperature are investigated for the most part by using well-known methods with some modifications which take into account the structure and texture of the rock, and standard instruments with specially devised adaptations for the insertion of samples. Now we will examine methods for investigating the electric and magnetic properties of rocks in temperature and force fields. /96

Investigation of the conductivity of minerals and rocks

The conductivity (or resistance) of minerals and rocks at low electromagnetic field frequencies is measured for the most part by the two- and four-electrode methods.

In the four-electrode method the sample is connected to the power supply (Figure 43) by means of current electrodes and the voltage across some part of the sample is measured with probe-type electrodes. In this method the current is measured in the circuit of the current electrodes and the voltage is measured in the circuit of the probe-type electrodes; this precludes any effect from the intermediate resistance of the contacts on the accuracy in measuring sample resistance. The voltage across the probe-type electrodes is measured with a high-resistance voltmeter. The voltmeter input resistance must be two orders of magnitude greater than the resistance of the sample between the probes in order to preclude current leakage through the instrument. When this condition is satisfied the error in measuring resistance can be reduced to 1%. Sample resistivity is computed using the formula

$$\rho = U/I \cdot S/l \ , \qquad \text{(III.1)}$$

where

U is the voltage across the probe-type electrodes, V;

T is the current flowing through the sample, A;

I is the sample cross section, cm^2;

S is the distance between the probe-type electrodes, cm.

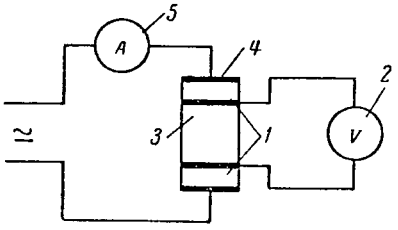

Figure 43. Diagram showing measurement of conductivity by the four-electrode method: 1- probe-type electrodes; 2- high-resistance voltmeter; 3- sample; 4- current electrodes; 5- ammeter.

Thus, sample resistance can be measured to 10^5 - 10^6 ohms. The samples are not homogeneous, the nature of the electric field distribution in them is extremely complex and the measurement result is dependent on the placement of the probe-type electrodes on the sample.

It is difficult to measure resistance by this method; the probe-type electrodes must be fabricated from non-oxidizing conductors whose material will not enter into reaction with the material of the samples; during measurements the contacts with the samples must be stable.

In the two-electrode method for measuring conductivity, the sample is connected to the power supply by means of current electrodes and voltage is directly measured in the sample circuit (Figure 44). The voltmeter input resistance must be two orders of magnitude greater than the sample resistance. A grounded shielding electrode (guard ring) is superposed on the sample in order to preclude surface conductivity. The electrodes are ground down onto the sample or are applied by vacuum spraying. The electrodes must be fabricated from a non-oxidizable material. If the temperature range is low, silver, gold, platinum or copper electrodes are used. Silver cannot be employed when investigating sulfide minerals because it reacts with the sample at high temperatures. /97

The two-electrode method is simpler but less precise than the four-electrode method. The errors caused by the intermediate and space charge resistances in the sample can attain 50% or more. During high-temperature measurements they are reduced and both methods give virtually identical results. When measuring

resistance by the two-electrode method suitable ohmmeters can be employed. Resistivity is computed using the formula

$$\rho = RS/l, \qquad \text{(III.2)}$$

where

R is sample resistance, ohms;

l is sample length, cm.

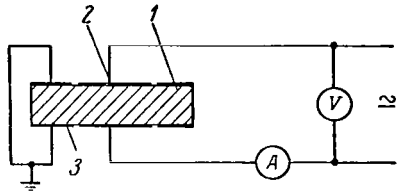

Figure 44. Diagram of measurement of conductivity by the two-electrode method: 1- sample; 2- current electrodes; 3- guard ring.

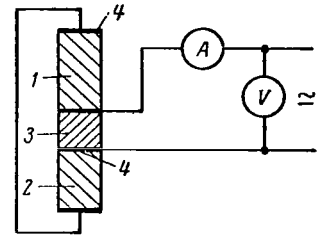

Figure 45. Diagram of measurement of sample resistance without special insulators: 1 and 2- "insulating " samples; 3- sample to be measured; 4- electrodes.

In both cases the sample is held between insulators by a special clamp. At any temperature the insulator resistance must be two orders of magnitude greater than the sample resistance because this eliminates current leakage through the insulator. Mica (muscovite) can be used as an insulator. If no suitable insulator exists for a particular sample, the material of the sample itself can be used as an insulator. In this case the resistance is measured using the system illustrated in Figure 45. If the resistance of the insulating plates is two or three orders of magnitude greater than the sample resistance, in such a case the sample resistance is measured. If these resistances are commensurable, sample resistance is computed using the formula /98

$$R_3 = \frac{(R_1 + R_2) R_{cir}}{R_1 + R_2 - R_{cir}} \qquad \text{(III.3)}$$

where

R_1, R_2 are the resistances of the insulating plates;

R_{cir} is circuit resistance.

In order to determine the dependence of temperature on resistance the sample is placed in a thermostat from which leads extend for transmitting the voltage to the sample; the leads must be carefully insulated from the body of the thermostat. Temperature in the thermostat is measured with thermometers or thermocouples (Figure 46). Thermostat temperature is changed by changing voltage across the heater. The rate of temperature change must be such that the sample will be heated to the same temperature. When these conditions are met the measurement accuracy can be equal to the accuracy of the instruments employed.

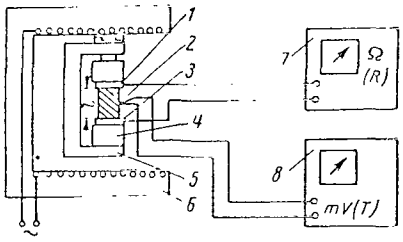

Figure 46. Diagram of apparatus for investigating the dependence of the resistance of minerals and rocks on temperature (two-electrode method): 1- sample; 2- thermocouple; 3- electrode; 4- insulator; 5- clamp; 6- thermostat; 7- ohmmeter; 8- pyrometer.

In the case of samples with a monocrystalline structure the symmetry axis must be taken into account. When preparing rock samples their texture and structure must be taken into account: the sample must contain not less than one structural unit; for example, polymineral samples must include grains of all the minerals making up the rock. The number of grains in all directions must be identical.

The dependence of the conductivity of minerals and rocks on electromagnetic field strength is investigated using the same apparatus and the same measurement methods as when measuring the dependence on temperature. In this case the voltage source must ensure a smoothly changing voltage; this makes it possible to change the field strength in the sample in a broad range.

The two-electrode method is employed in studying the dependence of the

conductivity of samples on their deformation.

The dependence of the conductivity of minerals and rocks on electromagnetic field frequency is investigated jointly with a study of the dependence of the dielectric constant on frequency.

Determination of Type of Current Carriers /99

The current carriers in minerals and rocks can be ions and electrons because minerals for the most part are ionic compounds. The current flowing through a mineral is expressed by the formula

$$I = nqv, \qquad \text{(III.4)}$$

where

n is the number of charges in a unit volume of the mineral (charge density), $1/cm^3$;

q is the charge strength, coulombs;

v is charge velocity, cm/sec;

E is electromagnetic field strength, V/cm.

The current flowing through the rock is determined using the formula

$$I = nqxE, \qquad \text{(III.5)}$$

where

x is charge mobility, $cm^2/V \cdot sec$.

It can be seen from formula (III.4) that the conductivity of a mineral is dependent on the number of charges, density, charge strength and its mobility:

$$g = nqx \qquad \text{(III.6)}$$

Due to the small mass of an electron, electron conduction is not accompanied by any significant mass transfer. Ion conduction, on the other hand, is accompanied by mass transfer in accordance with the Faraday electrolysis law:

$$M = AIt/Fz, \qquad \text{(III.7)}$$

where

F is the Faraday number (F = 96,496 coulomb);

A is atomic weight of an ion, g;

z is ion valency.

The current carriers in minerals can be ions of different elements (ions of the same of opposite signs). In most cases minerals are complex compounds and therefore electrons also participate in charge transfer. Thus, conductivity in rocks and minerals for the most part is by ions and electrons. The Faraday law is used in determining the type of current carrier. If a mineral is a simple compound consisting of two elements, under the influence of the electric field one of the ions, having the lesser ionic radius, usually moves. In this case the nature of the conductivity is determined in the following way: the mineral is divided into three samples, from which a circuit is formed. Prior to the experiment the two outermost samples are weighed together with the electrodes. Then a dc current is passed through this circuit and it is determined what quantity of electricity (in coulombs) has passed through the circuit. Then the samples are weighed together with the electrodes. If the weight of the sample adjacent to the anode has increased, the cargo transfer in the mineral has accordingly /100 been the result of negative ions. In this case the weight of the sample adjacent to the cathode will have decreased by the same amount as the increase for the sample adjacent to the anode. The change in weight indicates what ion has carried the charge and the Faraday law is used in determining the role of the ionic current, that is, the ratio of ion and electron conduction.

If ions of both signs move, thin plates are inserted between the second and third samples and will block movement of a particular ion. In other respects, the method for determining the role of the ionic current is the same, With a change in temperature the nature of the conductivity changes sharply: when the temperature increases both ions begin to move; the quantitative role of the current carried by ions also changes with a temperature change. This means that these measurements must be made with the sample temperature held constant.

Determining Density and Mobility of Current Carriers

The Hall effect is used in determining the density and mobility of current carriers (Figure 47).

As is well known, Hall emf is determined using the expression

$$\bar{\varepsilon}_x = \frac{1}{qn}[\bar{B}\bar{I}], \qquad \text{(III.8)}$$

where

$1/qn = R_x$ is the Hall constant.

In scalar form ε_x the Hall effect is expressed by the formula

$$\varepsilon_x = d/qn\ BI, \qquad \text{(III.9)}$$

where

d is the plate thickness of the investigated mineral.

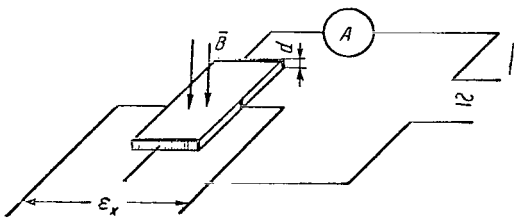

Figure 47. Diagram of measurement of Hall emf: ε_x is Hall emf; d is sample thickness; B is the magnetic induction vector.

The sign of the Hall constant determines the nature of the conductivity: when $R_x > 0$, p-type conductivity (by positive ions) is observed; when $R_x < 0$, conductivity by electrons (n-type conductivity, or conductivity by negative ions) is observed. If conductivity is mixed, the sign of the Hall constant determines the sign of the predominant conductivity. The R_x value makes it possible to determine the density n of the current carriers and then the conductivity can be used in determining the mobility of the current carriers

$$x = gR_x. \qquad \text{(III.10)}$$

The measurements are made in the following way: the current electrodes are arranged over the entire width of the mineral plate and a dc voltage is fed. /101
One Hall electrode is mounted securely to the plate whereas the second moves in such a way that in the absence of a magnetic field there will be no current in the Hall circuit. An electromagnet then is energized and the Hall emf determined. If current leakage in the power net cannot be prevented by this method, the change in Hall emf is determined from the change in magnetic field strength:

$$\Delta\varepsilon_x \quad IR_x d\,(B_2 - B_1) = \varepsilon_{x_2} - \varepsilon_{x_1}. \qquad \text{(III.11)}$$

Then the Hall constant is computed

$$R_x = \frac{\Delta\varepsilon_x}{I\,(B_2 - B_1)\,d}. \qquad \text{(III.12)}$$

In most cases the Hall emf is small and therefore the two currents method

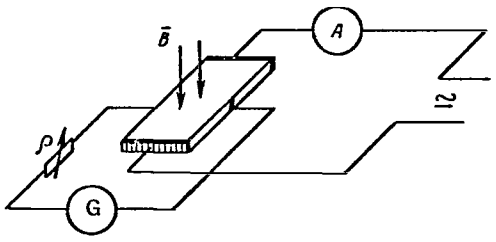

Figure 48. Diagram of measurement of Hall emf by the two currents method: ρ = variable resistance; G = galvanometer.

can be used (Figure 48) [44]. The variable resistance ρ is connected in series with the measuring instrument in the Hall circuit. The Hall emf is measured after measuring the currents I_1 and I_2 with the variable resistances ρ_1 and ρ_2 respectively in the Hall circuit. The Hall emf is computed using the formula

$$\varepsilon_x = \frac{I_1 I_2 (\rho_1 - \rho_2)}{I_1 - I_2}. \qquad \text{(III.13)}$$

The measurements are made with two polarities with a constant voltage in the power circuit. Then the mean Hall emf is computed.

Study of the Dielectric Constant of Minerals and Rocks

The methods for measuring the dielectric constant are dependent on the range of electromagnetic field frequencies. The use of not less than five or six instruments is required for covering a considerable frequency range, such as from 0 to 10^9 Hz. The measurements are made by three or four methods. Since each method gives different errors, in the case of a great frequency range it will be difficult to correlate the results. Now we will examine the most used methods for measuring the dielectric constant in different frequency ranges.

Low frequencies. Bridges of different types, such as the Sotti Bridge (Figure 49), are used for low frequencies (from 0 to 10^3 Hz). The measuring capacitor, in which the mineral or rock to be investigated serves as the dielectric, is connected in one of the bridge arms; the bridge is balanced by the R_1 and R_2 resistors. When in a balanced state the indicator shows that no current is present in the circuit. The capacitance of the measuring capacitor is computed using the formula

/102

$$C_x = C(R_2/R_1), \qquad \text{(III.14)}$$

where

R_1 and R_2 are variable balancing resistors;

C is a standard capacitor.

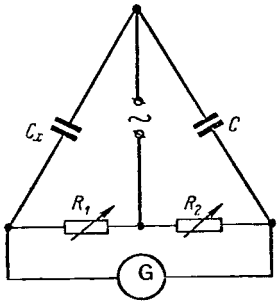

Figure 49. Diagram of bridge for measuring capacitance: C_x is the measured capacitance; R_1 and R_2 are the bridge arm resistors; G is the indicator (galvanometer).

The bridge makes it possible to measure capacitances greater than 20 μμF; with an increase in capacitance the measurement accuracy increases. The measurement error when using a bridge attains 10-15%. In order to achieve a high measurement accuracy the capacitance must have a range of about 10^3 μμF. There are practical difficulties in preparing rock samples for a capacitor with such a capacitance when the rock sample must be homogeneous. If an oscillograph is used as the indicator, the measurement error, even in the case of a small capacitance, can be reduced to 5%.

The dielectric constant for a rock sample is computed using the formula for a plane-parallel capacitor

$$\varepsilon' = C_x d/S\varepsilon_0, \qquad \text{(III.15)}$$

where

ε' is the relative dielectric constant of the investigated sample;

C_x is the capacitance of the measuring capacitor with the sample, F;

d is sample thickness, m;

S is the sample surface, m^2;

ε_0 is the dielectric constant of a vacuum ($\varepsilon_0 = 8.885 \cdot 10^{-12}$ F/m).

When investigating the dependence of the dielectric constant of rocks on temperature the measuring capacitor is placed in a thermostat. The thermostat temperature is varied at such a rate that the sample is uniformly heated. The diagram for this experiment is similar to the diagram shown in Figure 47, where the ohmmeter is replaced by an instrument for measuring capacitance.

Intermediate and high frequencies. Resonance methods for measuring the dielectric constant are used at intermediate and high frequencies (from 10^3 to 10^8 Hz).

The resonance method for measuring capacitance involves the following (Figure 50).

An oscillator circuit is tuned to resonance with the oscillator oscillations by a variable capacitor. Voltage resonance appears in the circuit and is recorded by the reading of a voltmeter connected across the circuit: the instrument hand is deflected by the maximum value at the time of resonance. The capacitance of the variable capacitor C_1 and the instrument readings Q_1 are registered during resonance. Then the capacitor with the investigated sample, which is used here as a dielectric, is connected to the Q-meter circuit in parallel with the variable capacitor. Then the circuit "goes out of resonance." In order to tune the circuit in resonance it is necessary to reduce the capacitance of the variable capacitor by the capacitance of the measuring capacitor. The capacitance of the capacitor C_2 and the instrument readings Q_2 are registered when obtaining resonance. It is obvious that the capacitance of the investigated capacitor is

/103

$$C_x = C_1 - C_2. \qquad \text{(III.16)}$$

The readings of the instrument, Q, in resonance depend on capacitor resistance: the greater the resistance of the capacitor, the greater the Q, and the longer it will hold a charge. Accordingly, the Q value is called the capacitor quality (to be more precise, the quality of the dielectric filling the capacitor). The magnitude $\tan\delta = 1/Q$ determines the loss of electromagnetic energy in the dielectric, that is, $\tan\delta$ is the ratio of quantity of energy absorbed by the dielectric to the quantity of energy passing through the dielectric.

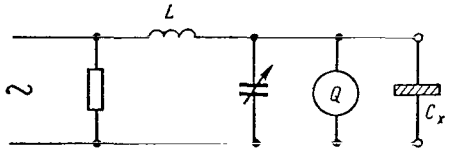

Figure 50. Resonance system for measuring capacitance: L is the changeable inductance; C_x is the measured capacitance.

The tan δ value is determined using the formula

$$\tan\delta = \frac{Q_1 - Q_2}{Q_1 Q_2} \cdot \frac{C_1}{C_1 - C_2}. \qquad \text{(III.17)}$$

The Q-meter voltmeter is graduated in quality units. In making measurements with the Q-meter one must take into account possible errors. Figure 51 is a diagram of the measuring capacitor.

In order to reduce the edge capacitance of the capacitor one must maintain the following relation: $10d^2 \ll S$. In addition, the thickness of the capacitor plate must be much less than the thickness of the investigated sample. A guard ring can be used to eliminate edge capacitance.

The gap capacitance between the investigated sample and the C_2 plate is eliminated by tight fitting of the plate or by vacuum spraying of a metal layer on the sample. In this case $C_2 = 0$. The ohmic resistance of the sample is taken into account when determining tan δ.

The errors associated with the use of connecting leads are computed and taken /104 into account in the measurements. If the leads are short these errors can be neglected. Figure 52 is a diagram of the voltage distribution in the capacitor [45]. With such a voltage distribution the radius of the capacitor plate must not exceed

$$r \leq 3.8 \cdot 10^{-2} \frac{\lambda}{\sqrt{\varepsilon}}, \qquad \text{(III.18)}$$

where

λ is the wavelength, cm;

ε is the dielectric constant of the material investigated.

Usually the accuracy in measuring capacitance with a Q-meter is 5%; the accuracy in measuring tan δ is 10%.

Superhigh frequencies. Cavity resonators of the open type (in the form of a two-wire line) are used in investigating the dielectric constant at high and superhigh frequencies (above 200 MHz/sec). The samples are 0.1-0.3 mm thick (the thinner the sample, the more precise is the measurement). The sample is prepared in the form of a disk 9 mm in diameter with two slots along the diameter for admitting the line leads. The dielectric constant is measured by the I. A. El'tsin method [46]. The investigations revealed that this method involves considerable errors (up to 20%) in determining the dielectric constant; these cannot be eliminated. The method for measuring the dielectric constant with a coaxial line [47] is more precise. LI-3 and LI-4 measuring lines can be used for measuring ε and tan δ. The LI-3 line makes it possible to measure a dielectric constant up to 700 MHz/sec.

The sample is placed at the antinode of an electromagnetic standing wave for determining the dielectric constant. The line is shortcircuited

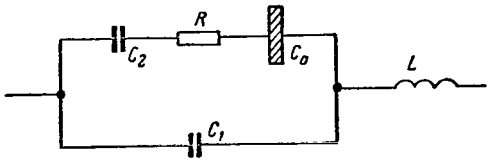

Figure 51. Equivalent circuit of measuring capacitor: C_0-capacitance of investigated capacitor; C_1 - capacitor edge capacitance; L- inductance of connecting leads.

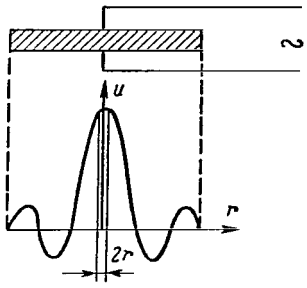

Figure 52. Diagram of voltage distribution in capacitor.

by use of a check tube and a moving short-circuiting plunger which constitutes part of the line outfit. Samples, in the form of disks up to 5 mm thick, are inserted into the coaxial line plug, to which the check tube is then connected. The first node of the standing wave is in the measuring line; measurements are made by the usual method. The measurement accuracy is dependent on wavelength, /105 that is, on the wavelength in the line. At frequencies up to 600 MHz/sec, the measurement errors do not exceed 10%.

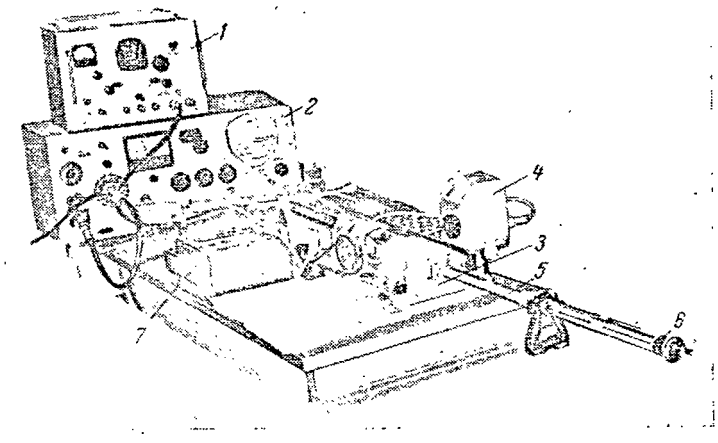

Figure 53. General appearance of apparatus for measuring ε and tan δ at high and superhigh frequencies: 1- superhigh-frequency generator (2000-3000 MHz/sec); 2- high-frequency generator (1000-2000 MHz/sec); 3- LI-3 line; 4- indicator head; 5- coaxial line with sample; 6- screw for moving short-circuiting plunger; 7- microammeter.

A special measuring coaxial line with a groove along the generatrix for a probe had to be fabricated for measuring the dielectric constant for the LI-4 line (Figure 53). This coaxial line is connected to an LI-3 line, from which only the measuring head is used. The line itself is a guide for the measuring head. The LI-4 line makes it possible to measure the dielectric constant at frequencies up to 10^4 MHz/sec with measurement errors up to 10%. The measurement method and the samples are the same as when making measurements with an LI-3 line. The sample dielectric constant is determined using the formula

$$\varepsilon = 1 + \Delta x/d, \qquad \text{(III.19)}$$

where

Δx is the displacement of the first node in a line with and without a sample, cm;

d is sample thickness, cm.

Sample thickness must satisfy the condition $\lambda/d > 30$, where λ is wavelength, cm.

Study of Magnetic Permeability of Minerals and Rocks /106

Relative magnetic permeability is measured relative to the air because the magnetic permeability of air with a high accuracy is equal to the magnetic permeability of a vacuum. Solenoid inductance is

$$L = 4\pi\mu \frac{n^2}{l} S \cdot 10^{-9}, \text{ henry} \qquad \text{(III.20)}$$

where

μ is the magnetic permeability of the medium, henry/m;

n is the number of solenoid turns, 1/m;

l is solenoid length, m;

S is the winding area, m^2.

The number of solenoid windings for a particular instrument is selected in such a way as to ensure the maximum instrument response. The length of the solenoid is selected taking into account that the sample is in a uniform field.

With constant solenoid parameters its inductance is changed if a sample whose magnetic permeability differs from the magnetic permeability of air is placed in the solenoid. Magnetic permeability can be computed from the expression

$$\mu_{samp} = \frac{10^9 L l}{4\pi n^2 S}. \qquad \text{(III.21)}$$

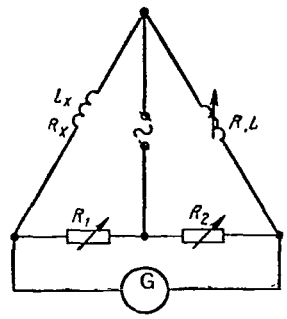

Figure 54. Maxwell bridge for measuring inductance: G- galvanometer; R_1 and R_2- variable resistors; L and R- known (standard) inductance and its resistance; L_x and R_x- measured inductance and its resistance.

For the particular solenoid the relative magnetic permeability is

$$\mu_{rel} = \frac{\mu_{samp}}{\mu_{air}} = \frac{L_{samp}}{L_{air}}, \qquad \text{(III.22)}$$

where

μ_{samp} is sample magnetic permeability;

μ_{air} is the magnetic permeability of air;

L_{samp} is inductance with a sample;

L_{air} is inductance without a sample (with air).

Solenoid inductance is measured using a Maxwell bridge (Figure 54) by means of comparing the known inductance L with the measured inductance L_x. The current can be excluded from the galvanometer circuit by changing the inductance L and the resistances R_1 and R_2. Inductance is computed using the formula

$$L_x = \frac{1}{\omega}\sqrt{\left(\frac{R_1}{R_2}\right)^2 (R^2 + \omega^2 L^2) - R_x^2}, \qquad \text{(III.23)}$$

where

ω is the frequency of the voltage fed to the bridge.

Instruments of the Yel2-1 type, making it possible to measure inductance with an accuracy to 5-10%, operate on the principle of addition of the frequencies of a standard oscillator and the frequency of an oscillator in whose circuit the investigated inductance is incorporated. /107

Magnetic permeability is measured at different temperatures by the following methods:

a) the investigated inductance with a sample is placed in a thermostat so that the sample will be uniformly heated and the inductance of the solenoid with the sample is measured at a stipulated temperature; then the magnetic permeability of the sample is computed at a stipulated temperature. The solenoid wire must be

such that with a temperature change the solenoid inductance changes insignificantly. These changes are then taken into account when determining the dependence of the magnetic permeability of the sample on temperature;

b) the sample is heated in a thermostat and is placed in a measuring solenoid. The magnetic permeability measurements are encumbered by errors caused by a change in sample temperature during measurements. This method can be used with sample temperatures which are low in comparison with the ambient temperature;

c) the heating winding of the thermostat is used as the primary winding for the transformer, whose secondary winding is the measuring inductance and whose core is the investigated sample. The secondary winding is placed on top of the layer of thermal installation and is therefore not heated. The magnetic flux of the primary winding causes the appearance of an induced emf in the secondary winding; this is determined using the formula

$$E_2 = \frac{\partial \Phi}{\partial t}. \tag{III.24}$$

The strength of the magnetic flux is dependent (all other parameters being constant) on the magnetic permeability of the sample, computed from the expression

$$\Phi = 4\pi\mu \frac{n^2}{l} SI, \tag{III.25}$$

where

n is the number of turns in the primary winding, 1/m;

l is solenoid length, m;

I is the current in the primary winding.

Assuming that

$$I = I_0 \sin(\omega t + \delta), \tag{III.26}$$

we obtain

$$\Phi = 4\pi\mu \frac{n^2}{l} SI_0 \sin(\omega t + \delta). \tag{III.27}$$

Differentiating flux with respect to time, we obtain

$$E_2 = 4\pi\mu\omega \frac{n^2}{l} SI_0 \cos(\omega t + \delta). \tag{III.28}$$

Accordingly, if all the parameters of the primary and secondary windings remain constant, the true current also remains constant and the emf in the secondary winding will be dependent on the magnetic permeability of the sample /108

$$\frac{E_t}{E_0} = \frac{\mu_t}{\mu_0} \qquad \text{(III.29)}$$

where

E_t is the induced emf for the corresponding μ_t, which corresponds to the temperature T°;

E and μ_0 are the induced emf and magnetic permeability at the initial temperature.

$$\mu_t \approx \mu_0 E_t / E_0.$$

Thus, the dependence of μ on temperature is determined by measuring the emf in the secondary winding. The same method makes it possible to determine the Curie point for a particular sample: at the Curie point $E_t \to 0$.

Sample magnetization is computed using the formula

$$I = B/\mu. \qquad \text{(III.30)}$$

In this case the magnetic permeability is measured by the methods described above and magnetic induction B is determined by measuring the Hall emf in the particular field.

3. Regularities in the Change of the Electric and Magnetic Properties of Minerals and Rocks with a Temperature Change

The results of measurements of sample resistances at different temperatures are used in constructing graphs of the dependence of conductivity of this mineral on temperature $g = f(T°)$ (Figure 55). The $g = f(T°)$ curves for minerals have the shape of exponential curves; the dependence of conductivity of minerals on temperature in the region of intrinsic conductivity is described by the expression [7]

$$g = A \exp\left(-\frac{Q}{2kT}\right), \qquad \text{(III.31)}$$

where

A is a constant characteristic for the particular mineral $(\text{ohm}\cdot\text{cm})^{-1}$;

Q is the charge activation energy for the mineral, J;[1]

k is the Boltzmann constant, J/degree;

T is absolute temperature, °K.

Intrinsic conductivity of minerals predominates at temperatures higher than 400-500°K. At higher temperatures expression (III.31) can be used without allowance for extrinsic conductivity. In the region of intrinsic conductivity A and Q will be constants characteristic for the particular mineral. /109

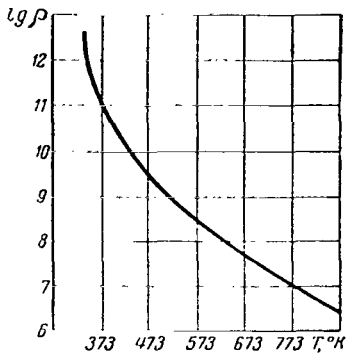

Figure 55. Dependence of resistivity of quartz on temperature.

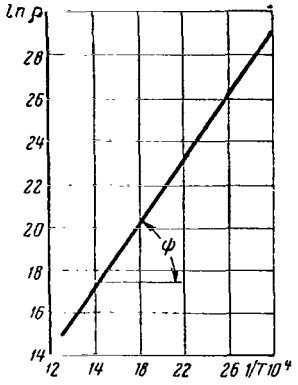

Figure 56. Dependence of ln ρ on 1/T for quartz.

Expression (III.31) describes conductivity as a function of temperature for semiconductors and conductors of the second kind (solid electrolytes).

Minerals, being ionic compounds, have ionic and electronic intrinsic conductivity. Ionic conductivity begins to appear in minerals at a higher temperature. The presence of ionic conductivity and its role in total conductivity can be judged from mass transfer. The prolonged passage of a dc current through mineral samples leads to a change in their conductivity; this is also attributable to ionic conductivity.

The mineral characteristics A and Q can be determined from the $g = f(T°)$ curves. It is more convenient to use resistivity ρ, rather than conductivity, in determining these parameters. As is well known, g and ρ are related to one

1. Q is the energy which must be expended on freeing the charge from the bonds in the crystal lattice, J.

another as $\rho = g^{-1}$; accordingly, the dependence of ρ on temperature is expressed by the equation

$$\rho = A^{-1} \exp\left(\frac{Q}{2kT}\right). \qquad \text{(III.32)}$$

Formula (III.32) is reduced to logarithmic form for determining Q

$$\ln \rho = -\ln A + \frac{Q}{2k} \cdot \frac{1}{T}. \qquad \text{(III.33)}$$

It can be seen from expression (III.33) that the dependence $\ln \rho = \varphi(1/T)$ is linear (Figure 56).

Differentiating (III.33) for 1/T, we obtain

$$\frac{\partial \ln \rho}{\partial 1/T} = \frac{Q}{2k}. \qquad \text{(III.34)}$$

The first derivative is equal to the tangent of the slope of the tangent to the curve at a particular point. In our case

$$\frac{\varphi}{2k} = \operatorname{tg} \psi, \qquad \text{(III.35)}$$

hence

$$Q = 2k \operatorname{tg} \psi, \qquad \text{(III.36)}$$

where the tan ψ value is determined from the $\ln \rho = \varphi(1/T)$ curves.

The constant A can be determined from this same graph: when $1/T = 0$ ($T \to \infty$) it follows from equation (III.33) that $\ln A = \ln \rho$, that is, $\ln A$ is the segment intercepted by the straight line $\ln \rho = \varphi(1/T)$ on the $\ln \rho$ axis; accordingly, A is the resistance of the mineral when $T \to \infty$. /110

In order to exclude any effect from the intermediate resistance, the constant A must be determined by another method. If the contact resistance does not change during the measurement process, that is, the contact plate is not oxidized and does not interact with the sample, the contact resistance ρ_{con}, not dependent on temperature, is added to the true resistance. Accordingly, the measured resistance is

$$\rho = \rho(T) + \rho_{con} \qquad \text{(III.37)}$$

The sample resistance ρ_{con} is measured with a constant error; accordingly, the shape of the $\rho = \psi(T)$ curve does not change, but it is displaced parallel to its initial position by ρ_{con}. On the $\ln \rho = \varphi(1/T)$ graph the straight line shifts but its slope to the 1/T axis remains constant; this means that the error in measuring ρ enters into the constant A. In order to exclude this error we will differentiate Eq. (III.37) for T

$$\frac{\partial \rho}{\partial T} = \frac{\partial \rho(T)}{\partial T} = \tan \theta. \qquad \text{(III.38)}$$

Accordingly, the A value can be determined from the $\rho = \psi(T)$ curve.

We will differentiate ρ in expression (III.32) with respect to T

$$\frac{\partial \rho}{\partial T} = -\frac{Q}{2kT^2} A^{-1} \exp\left(\frac{Q}{2kT}\right) = \tan \theta, \qquad \text{(III.39)}$$

hence

$$A = \frac{Q \exp\left(\frac{Q}{2kT}\right)}{\tan \theta 2kT^2}, \qquad \text{(III.40)}$$

where

$\tan \theta$ is the tangent of the slope of the tangent to the $\rho = \psi(T)$ curve at some point K with the coordinates (ρ_{con}, T_{con}). The point K must be taken with a quite high temperature in order to avoid the influence of extrinsic conductivity. For practical purposes K must fall on the straight line in the $\ln \rho = \varphi(1/T)$ graph (Figure 57).

The A and Q values are given in Table 33.

The literature gives different classifications of minerals by conductivity [48, 49]. We feel that the most complete classification of minerals is based on band theory [8]. According to this theory, all minerals (like any substances) can be classified as conductors (whose activation energy is $Q \ll kT$) semiconductors (whose activation energy is $Q \approx kT$), and dielectrics (whose activation energy is $Q \gg kT$). /111

Native metals and some varieties of graphite are among the conducting minerals. Since the width of the forbidden band for minerals changes smoothly within the range of one order of magnitude, it is impossible to detect a sharp boundary between semiconductors and dielectrics. Such a boundary is also

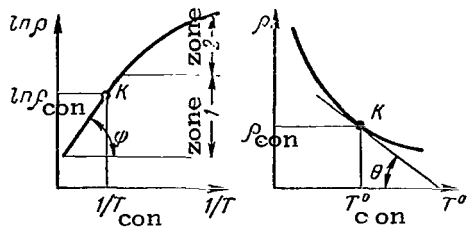

Figure 57. Determination of K point:
1- region of intrinsic conductivity;
2- region of extrinsic conductivity.

TABLE 33. VALUES OF COEFFICIENT A AND CHARGE ACTIVATION ENERGY FOR SOME MINERALS

Mineral	A, ohm/cm	Q	
		$1/2 \cdot 10^{-20}$ J	eV
Quartz	0.93	15.32	1.913
Chalcopyrite	0.1334	2.68	0.334
Halite	0.585	17.94	2.24
Magnetite	0.63	1.518	0.0915
Hematite	0.00324	7.76	0.965
Oligoclase	$4.32 \cdot 10^{3}$	7.87	0.98
Sphalerite	1530	5.35	0.667
Calcite	0.077	17.55	2.19
Labradorite	2600	7.44	0.93
Fluorite	22	12.4	1.55
Apatite	$4.78 \cdot 10^{-3}$	17.6	2.2
Siderite	0.617	11.5	1.44
Microcline	430	12.32	1.54
Nepheline	12.2	8.6	1.13
Chlorite	724	9.62	1.2
Tremolite	199	11.2	1.4
Barite	0.0266	20.3	2.53
Ilmenite	0.0763	3.45	0.43
Diopside	19.7	8.6	1.07

TABLE 33 continued

Mineral	A, ohm/cm	Q	
		$1/2 \cdot 10^{-20}$ J	eV
Anhydrite	988	8.35	1.04
Corundum	$3.4 \cdot 10^{-13}$	4.6	5.74
Coal	$2.5 \cdot 10^{-4}$	21.2	2.65
Muscovite	$3.57 \cdot 10^{-4}$	-	3.5
Diamond	-	-	4.5-5

undetectable for conductivity which changes for minerals at room temperature from 10 to 10^{-14} $(\text{ohm} \cdot \text{cm})^{-1}$. This boundary can be set artificially if one agrees to classify as semiconductors those minerals whose charge activation energy is not greater than 10^{-19}J and whose initial resistance (at room temperature) is not greater than 10^{10} ohm·cm and as dielectrics those minerals with ac- /112
tivation energy greater than 10^{-19} and initial resistance greater than 10^{10}ohm·cm.

Table 33 shows that for the most part the semiconducting minerals are compounds of heavy metals and the dielectrics are compounds of light metals and nonmetals. Semiconductors and dielectrics fall in the same mineralogical category.

Minerals in the carbonate, silicate, sulphate, halide and phosphate categories are for the most part dielectrics, whereas the oxides and sulfides are for the most part semiconductors. Accordingly, the conductivity of minerals is dependent on the properties of the elements included in a particular mineral and on the formed crystal lattice: for example, if a metal (that is, a conductor) and a nonmetal (that is, a dielectric) are combined, a semiconductor is formed from the simple compound consisting of these two elements. Exceptions are compounds of the halide type. In these compounds the valence electrons of the metal, poorly held, pass to the halogen, which holds them tightly. Dielectrics are formed when a semiconducting element is combined with a dielectric element. Complex compounds which include conductors, dielectrics and semiconductors are for the most part dielectric minerals. These regularities are of a qualitative character. In this case quantitative computations are made on the basis of the

Schrödinger equation and are virtually impossible.

Minerals are characterized by the presence of a large number of impurities. Table 34 gives the chemical composition of some minerals. The impurities substantially affect the conductivity of minerals in the region of low and intermediate temperatures: conductivity increases considerably for minerals with an activation energy greater than 0.2 eV. The impurities create donor levels in the forbidden band of minerals; the width of the formed energy gaps is considerably less than the width of the forbidden band of the mineral. Here the term "forbidden band" applies to the energy barrier between the conductivity band and the valence band in the crystal. The term "energy gap" means the energy barrier for the extrinsic ion or for electrons of the extrinsic ion.

The dependence $\ln \rho = \varphi(1/T)$ is nonlinear (see Figure 57, zone 2). This indicates that in the forbidden band several energy gaps of different width are formed at the same time. On the basis of chemical composition and the Debye powder diagram its conductivity can be approximately computed, but this requires more time than direct measurement of electric conductivity. The quantity and quality of the impurities can be judged from the dependence of conductivity on temperature.

The exponential decrease in resistivity of minerals continues up to the melting point. This sector (from the region of predominance of intrinsic conductivity) is described by expression (III.32). At the melting point the resistivity is sharply reduced (by several orders of magnitude in dielectric minerals) to the resistivity of the melt for the particular mineral. /114

This means that the phase change from a solid to a liquid state is accompanied by a considerable decrease in mineral resistance. In a liquid state all the ions become charge carriers; in addition, the number of free electrons increases because the system energy increases. With heating of a melt of minerals their resistivity decreases insignificantly with a relatively large temperature increase. A typical curve of the dependence of mineral (magnetite) resistivity on temperature is shown in Figure 58. Here the segment AB shows an exponential decrease in mineral resistivity to the phase transition; the segment BC shows a decrease in resistivity at the phase transition; the segment CD shows the resistivity of the mineral melt.

TABLE 34. CONTENT OF ELEMENTS IN MINERALS, %

Element	Mineral									
	Gypsum	Labradorite	Oligoclase	Sphalerite	Calcite	Quartz	Anhydrite	Halite	Siderite	Apatite
Be	10^{-4}	Traces	$(2-3)\ 10^{-3}$	—	—	—	—	—	—	—
Sc	—	—	—	—	—	—	—	—	—	—
P	—	—	—	—	—	—	—	—	—	>10
Mn	$(1-3)\ 10^{-3}$	$(1-3)\ 10^{-2}$	10^{-3}	0,1—0,3	0,7—0,9	$(4-6)\ 10^{-4}$	Traces	$3 \cdot 10^{-4}$	1—2	$(4-6)\ 10^{-2}$
Se	—	—	—	0,1—0,3	—	—	—	—	—	—
Zn	—	—	$(1-3)\ 10^{-2}$	>10	—	—	—	—	—	0,001
Sn	—	$(4-6)\ 10^{-3}$	$(7-9)\ 10^{-3}$	—	—	—	—	—	—	—
Ga	—	—	—	—	—	—	—	—	$(4-6)\ 10^{-3}$	—
Ma	—	—	—	—	—	—	—	—	—	—
V	$3 \cdot 10^{-4}$	Traces	$(1-3)\ 10^{3}$	0,01—0,03	Traces	$3 \cdot 10^{-4}$	Traces	10^{-3}	$(1-3)\ 10^{-3}$	$3 \cdot 10^{-4}$
Cu	—	—	Traces	0,4—0,6		—	—	Traces	—	—
Ag	—	1—3	—	—	—	—	0,01	—	—	0,1—0,3
Na	—	—	—	—	—	—	—	>10	—	—
Ti	—	0,1—0,3	Traces	$(1-3)\ 10^{2}$	Traces	Traces	—	—	$(1-3)\ 10^{2}$	—
Co	—	—	—	—	—	—	—	—	—	—
Ni	—	—	—	0,001	—	—	—	—	Traces	Traces
Mg	0,01	1	$(4-6)\ 10^{3}$	0,01	0,4—0,6	$(1-3)\ 10^{-3}$	$(4-6)\ 10^{-3}$	0,01	6—10	0,1—0,3
Si	0,01—0,03	>10	>10	4—6	0,01—0,03	>10	0,04—0,06	$(7-9)\ 10^{-3}$	1—3	0,1
Al	$(4-6)\ 10^{-3}$	>10	>10	—	$(1-3)\ 10^{-3}$	$(1-2)\ 10^{-2}$	$(4-6)\ 10^{-3}$	$(7-9)\ 10^{-3}$	1	0,001
Fe	0,01	0,7—0,9	$(1-3)\ 10^{-2}$	>10	0,4—0,6	$(7-9)\ 10^{-3}$	Traces	$5 \cdot 10^{-4}$	>10	0,04—0,06
Ca	>10	>10	1—3	0,04—0,06	>10	0,03	>10	0,1—0,3	—	>10
Ba	—	0,4—0,6	1	—	0,01—0,03	—	—	0,005	—	—

Note: No other elements were detected.

Commas represent decimal points.

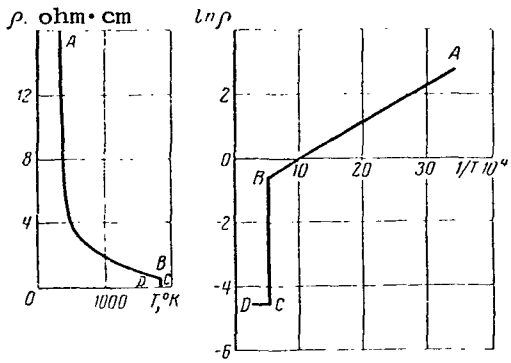

Figure 58. Dependence of magnetite resistivity on temperature.

Rock Conductivity as a Function of Mineralogical Composition and Conductivity of Minerals Forming a Rock

It can be assumed that the conductivity of minerals, their content and arrangement in a rock determine its conductivity (resistance).

We will examine two cases:

1) for a direct current, when the electromagnetic field frequency is low;

2) for a high-frequency electromagnetic field.

We will discriminate two rock structures: crystalline, in which crystals of different minerals are mixed in the rock mass, and stratified, in which the layers consist of different minerals.

In the case of a stratified structure with a direct current the vector of electric field strength is directed parallel to the layers. In this case there will be an in-parallel connection of layer resistances. The resistance of stratified rock is determined in this case by the resistance of the layer with a small (in comparison with the other layers) resistance because for the most part all the current passes through this layer. If the resistances of the other layers are two or more orders of magnitude greater, they can be neglected. /115

If the electric field vector is perpendicular to the layers, the current strength is determined by the resistivity of the layer with the maximum resistance in comparison with the resistance of the other layers. If the resistance of the other layers is two or more orders of magnitude less, they can be neglected.

In this case a circuit of resisting layers is obtained, connected in series. The resistance of the mineral with the greatest resistivity is decisive for the considered case; accordingly, the rock resistance is equal to the resistance of this mineral.

These cases indicate a marked anisotropy of the conductivity of stratified rocks.

In hypocrystalline structures, regardless of the direction of the field strength vector, the rock conductivity is approximately identical, that is, the rock is isotropic in its conductivity. If the grains of semiconducting minerals with a low resistivity (and accordingly with a high conductivity) are separated by intercalations or grains of dielectric minerals with a high resistivity, the rock resistance is equal to the resistance of the dielectric minerals. On the other hand, if the grains of semiconducting minerals are bound together, the rock resistance is determined by the resistivity and size of these grains. The same relationship is characteristic for other cases as well, such as for rocks consisting of dielectric or semiconducting minerals.

The conductivity of each grain of rock mineral is important for the electromagnetic field, for a traveling or standing electromagnetic wave.

The losses of electromagnetic energy in a mineral grain with the volume V_1 and the electric conductivity g_1 and with an electric field strength E are

$$Q_1 = g_1 V_1 E^2, \quad \text{J} \tag{III.41}$$

In other grains characterized by the volumes V_2, ..., V_i and the same conductivity, g_2, ..., g_i, the losses are determined by the same method using the expression (III.41) with the corresponding g_i and V_i values. By adding the losses of electromagnetic energy in all mineral grains in a rock, we obtain the losses in electromagnetic energy in the volume V of a rock:

$$Q = \sum_{i=1}^{n} g_i E^2 V_i. \tag{III.42}$$

The same loss in the volume V can be obtained if its conductivity is G: /116

$$Q = GE^2V. \tag{III.43}$$

By equating expressions (III.42) and (III.43) we obtain the rock conductivity as a function of the conductivity of the minerals forming the rock and their content in the rock:

$$G = \sum_{i=1}^{n} g_i \frac{V_i}{V}, \quad (\text{ohm} \cdot \text{cm})^{-1}. \tag{III.44}$$

By denoting the content of the i^{th} mineral in the rock as

$$c_i = \frac{V_i}{V}, \tag{III.45}$$

we obtain

$$G = \sum_{i=1}^{n} g_i c_i. \tag{III.46}$$

Conductivity is computed using formula (III.46) with a high accuracy if the content of conducting minerals in the rock is not greater than 40-50%. With higher contents of conducting minerals the linear dependence is not confirmed; this can be attributed to the influence of local Lorenz fields. The local field strength is determined from the expression

$$E' = E\left(\frac{\varepsilon' + 2}{3}\right), \tag{III.47}$$

where

E' and E is the electromagnetic field strength with and without allowance for local fields;

ε is the rock dielectric constant.

With a local field taken into account, expression (III.46) assumes the form

$$G = \left(\frac{\varepsilon' + 2}{3}\right)^2 \sum_{i=1}^{n} g_i c_i. \tag{III,48}$$

Expression (III.48) is correct for a rock content of conducting minerals greater than 50-60%.

Expression (III.48) is well confirmed experimentally if the resistance of the conducting minerals differs by two or more orders of magnitude from the conductivity of the remaining minerals present in the rock.

Dependence of Rock Conductivity on Temperature

In investigating the dependence of rock conductivity on temperature, serious attention must be given to the representativeness of the samples, that is, the dimensions of the sample must be far greater than the dimensions of the mineral grains. The sample must include all the minerals in the quantity in which they are present in the rock. In preparing the samples it is also necessary to take into account the rock structure: if the electric field strength vector is perpendicular to the sample stratification, the mineral with a maximum width of the forbidden band is of basic importance in rock conductivity. Thus, in each specific case it is possible to compute rock conductivity by constructing an equivalent electric diagram for it. Such an evaluation will obviously be extremely approximate, since it is difficult to take into account the contact resistances among the mineral layers and grains, as well as the influence of defects (fractures and cavities) and moisture content. /117

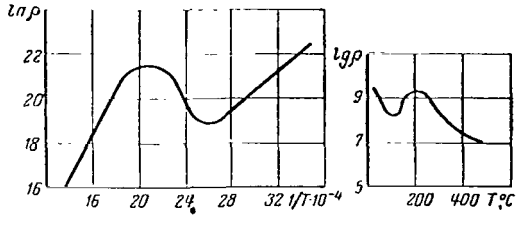

Figure 59. Dependence of granite resistivity on temperature.

The temperature dependence curves for the conductivity of rocks consisting of minerals with different forbidden bands differ from the temperature dependence curves for individual minerals: conductivity first increases to a temperature of 80-200°C and then begins to decrease to a minimum. In many cases, the conductivity at the minimum point is less than the initial value. Further heating again leads to an exponential conductivity increase. In the case of monomineral rocks, or rocks for which the mass of the basic mineral includes impregnations of grains of other minerals, there is an exponential dependence of conductivity (or resistivity) on temperature (Figure 59), customary for the basic mineral. The charge activation energy for such rocks coincides with the corresponding value for the basic mineral. Determination of the activation energy for polymineral rocks revealed that for these rocks it is equal to the activation energy of this mineral, which among the minerals forming this rock has a maximum activation energy. For example, the activation energy in sandstone, granite and quartzite is 1.21, 1.2 and 1.23 eV respectively. The

activation energy in quartz is 1.2 to 1.4 eV. Accordingly, the conductivity of these rocks is determined by the conductivity of quartz. Gabbro has an activation energy equal to the activation energy of plagioclase: 1.67 eV.

Thus, a decrease in conductivity in the temperature range 100-200°C can be attributed to evaporation of the present moisture and blocking of the through conductivity of rock by the mineral with the maximum activation energy. As a result of such blocking a space charge is formed which increases the rock resistance.

The space charge increases until the energy of the charge carriers becomes /118
equal to the activation energy of the blocking mineral. The latter hypothesis is supported by the fact that during the cooling of polymineral rocks this effect is observed in the same temperature range. A model can be constructed for this effect: the conductivity of the minerals making up a series circuit is measured, the activation energy of these minerals being different. These phenomena are observed only in contact measurements. In superhigh-frequency fields heating of rocks occurs exponentially since in an electromagnetic field each mineral is of independent importance. In superhigh-frequency fields only semiconductors and conductors are heated. The phenomenon is also observed in stratified rocks, each of whose layers consists of minerals with different forbidden bands. In the low-temperature region such phenomena are not observed.

Study of Mineral and Rock Conductivity in Low-Temperature Region

The resistance of minerals and rocks in the low-temperature region is investigated by the same method as in the high-temperature region. The samples, first placed in a vise, are paraffined for excluding the influence of the cooling medium and are then placed in a thermostat (Dewar vessel with a coolant). The readings are made after the entire sample assumes the temperature of the coolant; in this case its resistance is set at the value characteristics for the particular temperature. Solutions of salts, dry carbon dioxide (-78.5°C), liquid nitrogen (-196°C), or liquid hydrogen are used as the coolant.

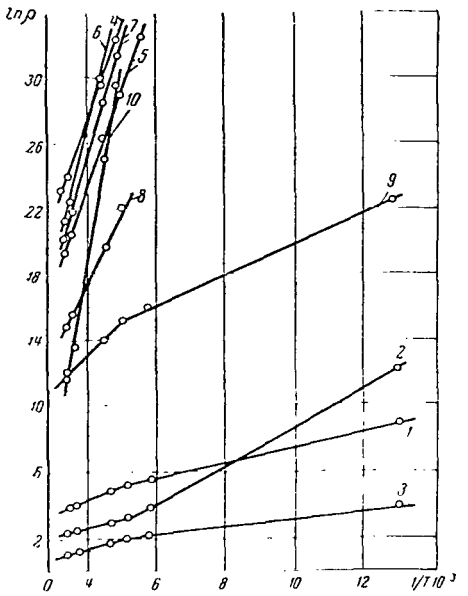

Figure 60. Dependence of ln ρ on 1/T for rocks and minerals at low temperatures: 1- coal; 2- galena; 3- pyrrhotite; 4- corundum; 5- sandstone; 6- halite; 7- granite; 8- ferruginous quartzite; 9- sphalerite; 10- labradorite.

In the case of minerals and rocks /119 having a great width of the forbidden band, the conductivity decreases sharply and at a temperature 170-200°K is not detected by instruments. An exponential dependence does not persist for semiconducting minerals with a low activation energy with a decrease in temperature. This is particularly characteristic for sulfides (Figure 60). Such deviations are evidence of the presence of impurities. Pyrrhotite exhibits a conductivity anomaly: in a wide temperature range (77-1000°K) the conductivity of pyrrhotite changes very little. Pyrrhotite evidently occupies an intermediate position between conductors and semiconductors. Formula (III.36) can be used in computing the activation energy of a mineral or rock at a particular temperature. The activation energies are given in Table 35.

The activation energy of minerals and rocks is considerably less at low temperatures than at high temperatures. This means that conductivity at low temperatures is caused by the presence of impurities.

Some varieties of pyrrhotite (pyrrhotites of the Kola Peninsula) have a very low activation energy and therefore their conductivity is virtually unchanged at both high temperatures and with strong cooling.

The content of a particular element can be determined from the conductivity at a particular temperature and from the valency of extrinsic ions and electron mobility.

TABLE 35. ACTIVATION ENERGIES

Mineral, rock	Activation energy, eV	Temperature of sample at which activation energy was determined, °K
Corundum	0.887	170
Nepheline	0.638	170
Sylvite	1.15	170
Halite	0.908	170
Granite	1.32	170
Sandstone	0.95	170
Labradorite	1.773	170
Ferruginous quartzite	0.716	150
Sphalerite	0.155	77
Galena	0.189-0.0618	77
Coal	0.115	77
Magnetite	0.0507	77
Pyrrhotite	0.0353-0.0021	77

Dependence of Conductivity of Minerals and Rocks on Electric Field Strength /120

It has been established that the electric field strength exerts an effect on the conductivity of minerals and rocks. In the case of dielectric minerals and rocks an increase in strength by more than 20-30 V/m causes the conductivity to begin a smooth increase. Then at a certain strength an electric drop occurs in such rocks (Figure 61). With the electric drop the circuit is short-circuited and the breakdown channel is fused, but no significant sample heating occurs. In semiconducting minerals and rocks conductivity begins to increase when the strength is greater than 10^{-3}-1 V/m; the conductivity increases the greater the initial resistance of the particular mineral. In some minerals (Figure 62) there is a considerable temperature increase for the samples and a thermal drop.

Experimental measurement of the dependence of conductivity on electric field strength at frequencies from 0 to 10^3 Hz is accomplished in the following way:

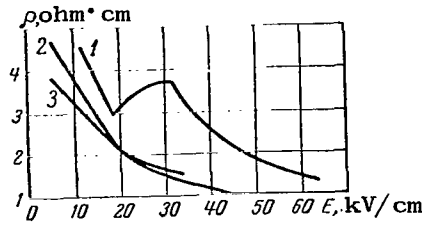

Figure 61. Dependence of resistivity of a dielectric mineral (oligoclase) on electric field strength: 1, 2 and 3- cycles of voltage application.

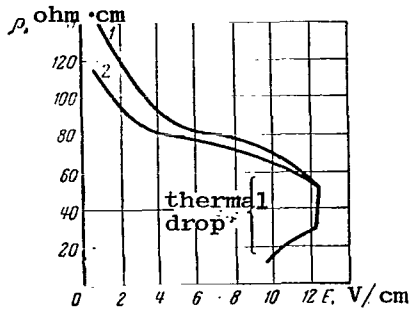

Figure 62. Graph showing the dependence of resistivity of a semiconducting mineral (ilmenite) on electric field strength: 1 and 2- cycles of voltage application.

the sample is clamped between contact rods and is paraffined to prevent atmospheric breakdown. A high voltage is applied to the sample and is smoothly increased. The current and voltage are measured in the circuit. The sample conductivity (or its resistivity) is computed for a particular strength, after which curves are constructed for the dependence of sample conductivity on electric field strength. The choice of sample thickness is dependent on its structure.

The mechanism for increasing conductivity at a high voltage involves a force excitation of the charge carriers. The excitation can be either in the form of a cutoff of the charge carrier by the force F = eE, or a result of impact ionization, caused by the fact that the free charges, accelerating, knock off /121 bound charges, making them free. On the basis of the experimentally constructed graphs it is possible to describe the dependence of resistance on electric field strength by the exponential formula

$$\rho = B \exp\left(\frac{Q}{aeE}\right), \quad \text{ohm·cm}, \tag{III.49}$$

where

Q is the width of the energy gap (activation energy) for the particular mineral or rock, J;

e is the charge, coulomb;

a is the maximum path of the particular charge, cm;

E is electric field strength, V/cm.

Using formula (III.49), employing a method similar to that given above, we compute the energy gap. For this purpose we reduce expression (III.49) to logarithmic form

$$\ln \rho = \ln B + \frac{Q}{ea}\left(\frac{1}{E}\right) \qquad \text{(III.50)}$$

and we will differentiate Eq. (III.50) for 1/E

$$\frac{\partial \ln \rho}{\partial \frac{1}{E}} = \frac{Q}{ea} = \tan \varphi, \qquad \text{(III.51)}$$

hence

$$Q = ea \tan \varphi. \qquad \text{(III.52)}$$

If the charge is assumed to be $e = 1.6 \cdot 10^{-19}$ coulomb, that is, equal to the electron charge, the path would be equal to the maximum distance between the atomic planes in the crystal lattice in the direction of the electric field and the width of the energy gap can be computed. The width of the energy gap for these values is given in Table 36. From a comparison of these values with the energy of thermal ionization it can be seen that in this case the energy of impact ionization is two to seven orders of magnitude less than the energy of thermal ionization. This free charge obviously has a greater path length than the crystal lattice constant.

In a study of these same dielectric samples in a high or superhigh frequency field (from 150 to 3000 MHz/sec) with a field strength from 0.5 to 1.2 V/m one detects no dependence of sample conductivity on field strength. In this case the influence of field strength was determined from the electromagnetic energy absorbed by the sample. The effect of impact ionization in high-frequency fields should be the same as in low-frequency fields and therefore it can be postulated that with an increase in field strength the conductivity of minerals and rocks will increase.

If it is assumed that the length of the free path of electrons in these minerals is 10^2 to 10^3 lattice constants, in this case the width of the energy gap in semiconducting minerals during impact excitation will be considerably less than in the case of thermal excitation. In dielectric minerals, the same assumption being made, the energy gaps for both types of excitation will be approximately equal. Since the change in conductivity during impact excitation /122

is insignificant (within the limits of one order of magnitude), such narrow energy gaps in minerals are created by extrinsic ions.

TABLE 36. WIDTH OF ENERGY GAP

Mineral, rock	Crystal lattice constant, A	Width of energy gap		
		Q_E, J	Q_E, eV	Impure Q, J
Halite	5.62	$4.29 \cdot 10^{-22}$	$2.68 \cdot 10^{-3}$	10^{-20}
Calcite	14,02	$4.62 \cdot 10^{-23}$	$2.79 \cdot 10^{-4}$	$3.28 \cdot 10^{-20}$
Nepheline	10,05	$2,29 \cdot 10^{-23}$	$1,43 \cdot 10^{-4}$	10^{-20}
Apatite	9.62	$2,28 \cdot 10^{-23}$	$1.43 \cdot 10^{-4}$	10^{-20}
Fluorite	5,45	$8,72 \cdot 10^{-24}$	$5,45 \cdot 10^{-5}$	10^{-20}
Quartzite	5.397	$1.149 \cdot 10^{-22}$	$7,17 \cdot 10^{-4}$	10^{-20}
Corundum	13,01	$4.46 \cdot 10^{-22}$	$2,79 \cdot 10^{-3}$	10^{-20}
Oligoclase	10,28	$3,78 \cdot 10^{-22}$	$2,36 \cdot 10^{-3}$	10^{-20}
Hematite	13,73	$9.76 \cdot 10^{-25}$	$6.1 \cdot 10^{-6}$	$2,76 \cdot 10^{-20}$
Sphalerite	5,4	$1.64 \cdot 10^{-24}$	$1,04 \cdot 10^{-5}$	$5,53 \cdot 10^{-20}$
Ilmenite	14,04	$1,4 \cdot 10^{-26}$	$9 \cdot 10^{-8}$	$2,76 \cdot 10^{-20}$
Pyrite	5,4	$1,73 \cdot 10^{-27}$	$1,08 \cdot 10^{-8}$	$1,52 \cdot 10^{-20}$
Galena	5,924	$4,74 \cdot 10^{-27}$	$2,96 \cdot 10^{-8}$	$2,07 \cdot 10^{-21}$

Commas represent decimal points.

Dependence of Conductivity of Minerals and Rocks on Electromagnetic Field Frequency

The conductivity of minerals and rocks at low and intermediate frequencies (up to 200 MHz) is measured in the following way. The samples of minerals and rocks are placed in a plane-parallel capacitor. Then Q-meters are used in measuring the dielectric constant ε and the dielectric loss tangent δ of samples. On the basis of the Maxwell equation

$$\operatorname{rot} \overline{H} = \varepsilon \frac{\partial \overline{E}}{\partial t} + g\overline{E} \qquad \text{(III.53)}$$

we find that if $E = E_0 \sin \omega t$, then

$$\tan \delta = g/\omega\varepsilon', \qquad \text{(III.54)}$$

from which the sample conductivity is determined at the particular frequency

$$g = \omega\varepsilon' \tan \delta. \qquad \text{(III.55)}$$

At frequencies greater than 200 MHz ε' and tan δ are measured in coaxial lines. As mentioned above, the minerals forming the rocks are for the most part ionic compounds. The characteristic frequencies of ion oscillations are in the infrared range and the characteristic frequencies of electron oscillations are in the visible range; accordingly, the relaxation losses to frequencies of about 10^{13} Hz for minerals and rocks are null. However, at different frequencies there is an increase in conductivity of minerals and rocks with an increase in electromagnetic field frequency by several orders of magnitude. /123

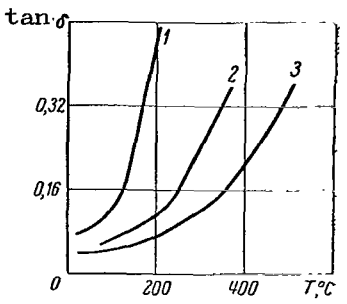

Figure 63. Temperature-frequency dependence of tan δ of granite (based on data from E. N. Parkhomenko [52]): 1- 50 kHz; 2- 500 kHz; 3- 5 kHz.

A study of the heating of minerals and rocks in high-frequency fields shows that with an increase in field frequency the heating intensity increases. This can explain the increase in conductivity of minerals having a low conductivity in constant fields (below 10^2 ohm$^{-1}\cdot$m^{-1}).

As is well known, conductivity is determined by the number of current carriers in a unit volume and their mobility, as well as the charge of the current carriers. D. Barlow [50] demonstrated that the Hall constant in fields from 0 to 10^{10} Hz is not dependent on frequency. This means that the number of current carriers and their charge do not change in fields with the indicated frequency. C. Kittel [51] feels that ion and electron mobility is not dependent on the frequency of electromagnetic oscillations up to the infrared frequencies (10^{13} Hz). This means that conductivity in the frequency range from 0 to 10^{13} Hz is not dependent on frequency. Accordingly, the heating of rocks in high-frequency fields does not originate from Joule heat, but from other losses of electromagnetic energy in minerals (Figure 63).

Investigations of the coefficient of electromagnetic wave attenuation in minerals and rocks as a function of frequency revealed that with an increase in frequency the attenuation coefficient increases linearly (in logarithmic coordinates). However, if it is assumed that conductivity increases linearly with

a frequency increase, the nature of the dependence of the absorption coefficient on frequency will be the same as in the case of invariable conductivity (in logarithmic coordinates only the slope of the straight line changes). Accordingly, it is impossible to determine the change in conductivity from the absorption coefficient.

The minerals become polarized in an electric field. This polarization can be regarded as a deformation of the crystal lattice under the influence of electricity:

$$F = neE, \tag{III.56}$$

where

ne is the ion charge;

e is the electron charge ($e = 1.6 \cdot 10^{-19}$ coulomb).

The elastic deformation energy for an elementary crystal cell is /124

$$W = \frac{1}{2} \cdot \frac{\sigma^2}{E_j}, \tag{III.57}$$

where

σ is the mechanical stress;

E_j is the elastic modulus.

An "elementary cell" is the volume within which the particular ion falls.

The mechanical stress σ is determined using the formula

$$\sigma = \frac{F}{S} = \frac{neE}{S}, \tag{III.58}$$

where

S is the crystal area.

With a constant electric field strength the energy of elastic deformation of an elementary crystal cell is

$$W = \frac{1}{2} \frac{n^2 e^2 E^2}{S^2 E_j}. \tag{III.59}$$

If the electric field changes with a change in frequency f, the energy of elastic deformation per second is

$$W = f \cdot \frac{n^2 e^2 E^2}{S^2 E_j}. \tag{III.60}$$

Some of the energy of elastic deformation is transformed into potential crystal energy and is expended during return of a displaced ion to a state of equilibrium. Some of this energy remains in the crystal in the form of heat. We will assume that the latter part is equal to P. If several ions are incorporated into the crystal, expression (III.60) is generalized:

$$W = Pf \sum_{i=1}^{m} \frac{kn_i^2 e^2 E^2}{S_i^2 E_j}, \qquad \text{(III.61)}$$

where

k is the number of elements in a unit volume of the crystal.

The heat losses during elastic deformation can be written as Joule heat:

$$\Delta g E^2 = Pf \sum_{i=1}^{m} \frac{kn_i^2 e^2 E^2}{S_i^2 E_j t}. \qquad \text{(III.62)}$$

Using expression (III.62) it is possible to determine what degree of increase in mineral conductivity should accompany such losses:

$$\Delta g = Pf \sum_{i=1}^{m} \frac{kn_i^2 e^2}{S_i^2 E_j t}. \qquad \text{(III.63)}$$

This means that losses of electromagnetic energy of any nature can be re- /125
presented in the form of Joule heat. This will mean that with an increase in frequency, the mineral conductivity increases linearly.

Thus, mineral and rock conductivity is composed of two constituents:

$$g = g_{ohm} + Pf \sum_{i=1}^{m} \frac{kn_i^2 e^2}{S_i^2 E_j t}. \qquad \text{(III.64)}$$

The first component, ohmic conductivity, is created by the free charges of any particular mineral and is not dependent on electromagnetic field frequency; the second is the imaginary conductivity Δg, dependent on electromagnetic field energy. Expression (III.64) is convenient to use in computations. If one of the terms in (III.64) is greater than the other by an order of magnitude, the value of the latter term can be neglected. If it is assumed that the ion charge is equal to the electron charge, $S = 25\ \text{Å}^2$, $E_j = 5 \cdot 10^5$ kg/cm^2, $f = 3 \cdot 10^9$ Hz, with $P = 1$, we obtain $\Delta g = 1.8 \cdot 10^{30}$ (ohm·cm)$^{-1}$. Accordingly, P is about $10^{-34} - 10^{-35}$, that is, for the most part crystal deformation is elastic.

If the ohmic part of the conductivity, g_{con}, increases exponentially

with a temperature increase, the imaginary part of the conductivity Δg also increases, but not significantly (within the limits of one order of magnitude).

Ion inertia begins to exert an effect at frequencies of the order of the characteristic frequencies of ion oscillations. In a field of such a frequency the electromagnetic field quantum energy becomes equal to the electron activation energy and therefore the electron can be transferred into the conductivity band. In this case an emission quantum will be absorbed. The condition for electron transfer into the conductivity band can be expressed by the inequality

$$hf \geq Q, \qquad \text{(III.65)}$$

where

h is the Planck constant.

For example, for an activation energy $Q = 1 \cdot 10^{-20}$ J the quantum frequency must be equal to or exceed $1.5 \cdot 10^{13}$ Hz, that is, must be equal to the frequency of infrared radiation.

This phenomenon, called photoconductivity, is discovered during the heating of samples in superhigh-frequency fields with their simultaneous irradiation. In this process there is an increase in the number of free charges and more intensive heating. The experimental results are given in Table 37. Illumination was with a 1 kW incandescent lamp. The heating was registered separately from the lamp, in a superhigh-frequency field with a generator power of 2.5 kW, and in a superhigh-frequency field with simultaneous illumination. The data in Table 37 show that illumination leads to additional heating of the samples; this can be attributed only to an increase in the release of Joule heat in the superhigh-frequency field due to an increase in the number of free charges /126 expelled by light quanta.

Direct measurements of the increase in conductivity during irradiation of minerals and rocks with visible light or X-rays revealed that it is impossible to detect additional conductivity because considerable errors arise due to excitation of the insulating medium. These errors can be eliminated only with joint irradiation and heating in superhigh-frequency fields.

TABLE 37. HEATING TEMPERATURE DURING ILLUMINATION

Mineral, rock	Irradiation time, minutes	Heating temperature, degrees		
		illumination	superhigh frequency field	combined irradiation
Halite	2	10	10	15
Calcite	2	40	0	60
Quartz	2	30	0	35
Gypsum	2	30	0	30
Magnetite	0.5	10	50	100
Hematite	0.5	10	40	85
Galena	0.5	15	70	90
Labradorite	1	25	20	70
Microcline	2.5	30	15	50
Siderite	2	35	30	85
Limonite	1	20	40	80
Sandstone	2	40	150	230

Dependence of Mineral Conductivity on Sample Deformation

Under uniaxial compression (or hydrostatic pressure) mineral conductivity changes in directions perpendicular and parallel to the applied force. Semiconducting (galena, chalcopyrite, pyrite, magnetite, sphalerite, ilmenite, and labradorite) and dielectric minerals (halite, calcite and fluorite) were investigated for determining the dependence of mineral conductivity on deformation. These investigations revealed that the resistances of all samples decrease under small compressive strains. With further deformation the sample resistances increase.

A particularly strong increase in sample resistance is observed immediately prior to their fracturing, that is, during the period of plastic deformation (Figure 64). At this time the change in resistance is one or two orders of magnitude. During elastic deformation of samples the change in resistance is proportional to sample deformation. The change in resistance during plastic deformation can be attributed to the fact that the current carriers (electrons

and ions) are attracted and held by charged dislocation steps. As noted by J. Gilman [53], the number of dislocations is directly proportional to the relative deformation ε of the sample, for example, for halite (NaCl) the number of dislocations is 10^9 ε. /127

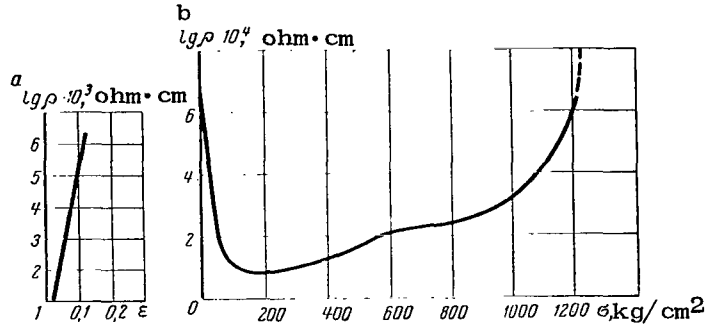

Figure 64. Graph showing dependence of resistivity of labradorite on relative deformation (a) and stress (b) of a sample (the dashed curve corresponds to the sample fracturing process).

On the basis of the dependence of conductivity on relative deformation it can be assumed that the number of charged dislocations is also proportional to the relative deformation of the sample. In the case of halite the number of charged dislocations should be of the same order as the number of current carriers, that is, 10^8, since the number of current carriers for halite is about 10^7. If the number of charged dislocations is greater than this value, the conductivity of minerals should change more sharply, and vice versa.

Controlling Rock Conductivity

In electrothermal methods for fracturing rocks it is necessary to control the electric properties of rocks and especially the conductivity, because electromagnetic energy is transformed into thermal energy by means of conductivity. Different methods can be used for controlling rock conductivity. The following are the most readily available means for external modification of rocks which are employed in the electrothermal destruction of samples:

change in rock temperature: thermal excitation or slowing of the charge carriers;

increase in electromagnetic field strength: force or impact excitation of charge carriers;

mechanical deformation of the rock: creation of traps for charge carriers;

different kinds of ionizing radiation: excitation of charge carriers during capture of a radiation quantum.

Now we will determine the energy capacity of different types of excitation of charge carriers. /128

Thermal excitation or slowing. Assume that the quantity of energy W is expended on the heating or cooling of a unit volume of rock. The rock temperature changes by $\Delta T = W/cm$ degrees, where c is heat capacity, J/g·degree and m is density, g/cm^3; accordingly, there is a change in conductivity by

$$\Delta g = A \exp\left(-\frac{Q}{2k\frac{W}{cm}}\right). \qquad \text{(III.66)}$$

Force or impact excitation. We will introduce into a unit volume of rock some quantity of energy W in the form of electric field energy:

$$W = \frac{\varepsilon \Delta E^2}{2}.$$

This causes the electric field strength to increase by $\Delta E = \left(\frac{2W}{\varepsilon}\right)^{1/2}$; this causes an increase in conductivity by

$$\Delta g = B \exp\left(-\frac{Q_\varepsilon}{ae\left(\frac{2W}{\varepsilon}\right)^{\frac{1}{2}}}\right), \qquad \text{(III.67)}$$

where

Q_E is the width of the energy gap in the case of force excitation (see Table 36).

Formation of charge traps during rock deformation. If the quantity of energy W is introduced into a unit volume of rock in the form of the energy of elastic deformation

$$W = \frac{1}{2}\sigma\varepsilon,$$

a unit volume of rock is deformed by $\varepsilon = 2W/\sigma$. As demonstrated above, the rock conductivity is proportional to its deformation: $g = k/\varepsilon$, where k is a proportionality factor. Accordingly, the decrease in conductivity is

$$\Delta g = \frac{k\sigma}{2W}. \qquad \text{(III.68)}$$

The increase (or decrease) in conductivity can be computed for each specific rock on the basis of the derived expressions; then, comparing the results, one determines which of the methods is most effective with respect to energy.

Thermoelectromotive force in rocks. With a change in the contact temperature for two minerals a thermoelectromotive force appears. The strength of the thermoelectromotive force is dependent on the conductivity of the contacting minerals. The greatest intensity of the thermoelectromotive force (up to 40-45 mV) at a contact temperature of about 200°C is observed in a pair of sulfides, for example, in the galena-pyrite pair. The thermoelectromotive force is investigated in an instrument in which one of the minerals is maintained at a constant temperature and the other is heated. /129

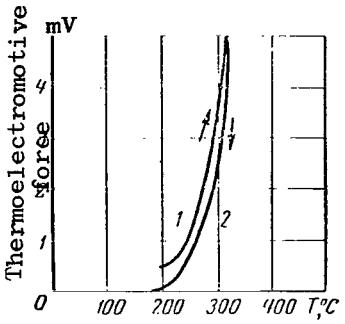

Figure 65. Graph showing the dependence of the thermoelectromotive force for a hematite-magnetite pair on the contact temperature of minerals; 1- heating; 2- cooling.

Figure 65 illustrates the dependence of the thermoelectromotive force for the pair hematite-magnetite on the contact temperature of minerals.

The appearing thermoelectromotive force is relatively small, but under natural conditions, the individual emfs being added together, can give rise to stray currents, induce electrolysis of water solutions, and other phenomena.

Dielectric Constant of Rocks as a Function of the Mineralogical Composition of a Rock and the Dielectric Constant of Minerals

Different researchers have proposed many formulas which make it possible to determine the dielectric constant of heterogeneous media as a function of the concentration of their component substances and their dielectric constants. In general, these formulas are suitable for two-component media with a definite configuration of particles and a definite regularity in their distribution in the mass. Each formula has its own limit of applicability, within which it gives good agreement with the experimental data.

It appears desirable to estimate the effect of the concentration of minerals in a rock and their dielectric constants on energy distribution in minerals.

The energy of a volume of rock in an electric field is determined from the equation

$$\frac{1}{2}\varepsilon E^2 V = \frac{1}{2}(\varepsilon_1 V_1 + \varepsilon_2 V_2 + \ldots + \varepsilon_i V_i) E^2, \qquad \text{(III.69)}$$

where

ε is the dielectric constant of the rock in the volume V;

E is electric field strength;

$\varepsilon_1, \ldots, \varepsilon_i$ are the dielectric constants of the minerals forming the rock;

$V_1, \ldots, V_i$ are the volumes of the minerals in the volume V of rock.

We will write expression (III.69) in the form <130

$$\frac{1}{2}\varepsilon E^2 V = \frac{1}{2} V \left(\varepsilon_1 \frac{V_1}{V} + \varepsilon_2 \frac{V_2}{V} + \ldots + \varepsilon_i \frac{V_i}{V}\right) E^2 \qquad \text{(III.70)}$$

and use the notation

$$\frac{V_1}{V} = c_1; \quad \frac{V_2}{V} = c_2; \quad \frac{V_i}{V} = c_i,$$

where

$c_1, c_2, \ldots, c_i$ are the contents of the particular minerals in the rock.

Expression (III.70) assumes the form

$$\varepsilon = \sum_{i=1}^{n} \varepsilon_i c_i. \qquad \text{(III.71)}$$

For a number of rocks, expression (III.71) gives good agreement with experimental data (for example, for sulfide ores). For other rocks there are deviations from this dependence; this can be attributed to the presence of local electric fields of mineral grains.

In general, it can be asserted that the dielectric constant of a rock is a function (in the simplest case, linear) of the rock composition and the properties of minerals.

Dependence of Dielectric Constant of Minerals and Rocks on Electromagnetic Field Frequency

Experiments show that the dielectric constant of minerals and rocks, when

measured at different frequencies, has different values; for some rocks these differences are insignificant in a broad frequency range, whereas for others they are extremely significant. This indicates that the dielectric constant of minerals and rocks is a function of electromagnetic field frequency. Accordingly, the dependence of the dielectric constant on temperature must be measured at a definite frequency.

In order to determine the dependence of the dielectric constant on frequency the dielectric constant is measured at different frequencies. Then curves of this dependence are constructed.

Analysis of these curves reveals that the dielectric constant of minerals and rocks decreases with an increase in electromagnetic field frequency. A decrease in the dielectric constant can be attributed to the inertia of ions. The dielectric constant therefore tends to the square of the refractive index for light in the particular medium.

In order to evaluate the dependence of the dielectric constant of minerals on electromagnetic field frequency we write an equation for the forces acting on the charge (ion or electron):

$$m\frac{\partial^2 S}{\partial t^2}+P\frac{\partial S}{\partial t}+kS=qE_0\sin\omega t, \qquad \text{(III.72)}$$

where

m is charge mass, kg; /131

S is charge displacement relative to the position of equilibrium, m;

$m\frac{\partial^2 S}{\partial t^2}$ is inertial force, N;

p is a factor taking into account resistance to movement of a charge on the part of the charges surrounding it (the P factor is similar to the friction factor), kg/sec;

$P\frac{\partial S}{\partial t}$ is the force of resistance, N;

k is the elasticity coefficient, kg/sec^2;

kS is the restoring force, N;

E_0 is the amplitude of electric field strength, V/m;

ω is the angular frequency of electric field change, 1/sec;

t is time, sec;

$qE_0 \sin \omega t$ is an external force acting on the charge q.

By solving Eq. (III.72) we obtain

$$S = A \sin \omega t, \tag{III.73}$$

where

A is the amplitude of charge displacement.

By replacing S in (III.72) by A sin ωt, we obtain

$$A = \frac{qE_0 \sin \omega t}{-m\omega^2 \sin \omega t + P\omega \cos \omega t + k \sin \omega t}. \tag{III.74}$$

From the expression

$$B = qS = \beta E_0 \sin \omega t, \tag{III.75}$$

where

B is the dipole moment of the charges, coulomb·m;

β is the polarizability of the charges, km^2/V,

and using expression (III.74) we determine the polarizability of the charges

$$\beta = \frac{q^2}{P\omega \cos \omega t + k \sin \omega t - m\omega^2 \sin \omega t}. \tag{III.76}$$

In the denominator we take the time-averaged value for the period of field change using the formula

$$\psi\ (t)_{mean} = \frac{4}{T} \int_0^{\frac{T}{4}} \psi\ (t)\, dt, \tag{III.77}$$

where

T is the period of charge oscillations, sec.

With the mean value taken into account, expression (III.76) assumes the form

$$\beta_{mean} = \frac{q^2}{4\left(\frac{k}{\pi} + 2Pf + 4\pi m f^2\right)}, \tag{III.78}$$

where

f is linear frequency, Hz.

By knowing the polarizability of charges for a particular mineral it is possible to determine its dielectric constant. /132

With Eq. (III.78) taken into account, and also knowing that the mineral is an ionic compound having ion and electron polarizabilities, we determine the

dielectric constant of the mineral

$$\varepsilon' = 1 + \frac{N}{\varepsilon_0}(\beta_i + \beta_e) = 1 + \frac{N_e}{4\varepsilon_0}\left(\frac{e^2}{\frac{k_e}{\pi} + P_e f + 4m_e \pi f^2}\right) + \frac{N_i}{4\varepsilon_0}\left(\frac{(ne)^2}{\frac{k_i}{\pi} + 2P_i f + 4\pi m_i f^2}\right), \quad \text{(III.79)}$$

where

N is the number of charges in a unit volume, $1/cm^3$;

ε_0 is the dielectric constant of a vacuum in the international system;

β_i and β_e are ion and electron polarizabilities;

e is electron charge, coulomb;

ne is ion charge, coulomb.

The subscript "i" applies to ions.

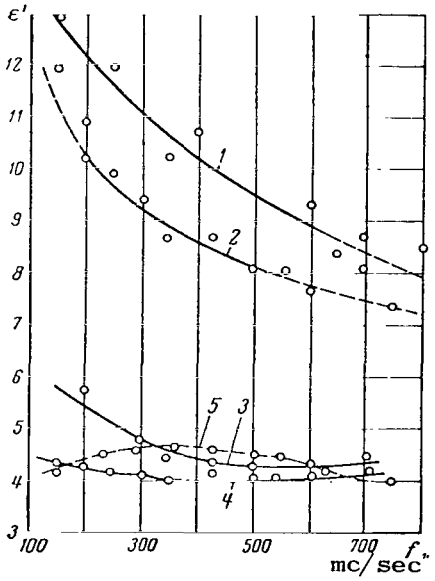

Figure 66. Graph of the dependence of relative dielectric constant of rocks and minerals of electromagnetic field frequency; 1- hematite; 2- ferruginous (hematitic) quartzite; 3- labradorite; 4- halite; 5- granite.

With an increase in frequency the dielectric constant decreases; this decrease is most strongly expressed for heavy minerals (Figure 66). With an increase in frequency the dielectric constant is increasingly affected by electron polarizability. At superhigh frequencies the dielectric constant tends to the square of the refractive index, whereas at low frequencies ion polarizability exerts a considerable effect on the dielectric constant.

A marked decrease in ε' is observed for semiconducting minerals having a high dielectric constant at low frequencies. In dielectric minerals and rocks the decrease in the dielectric constant with an increase in electric field frequency

by several orders of magnitude is only 15-25%. In semiconducting minerals at low frequencies entire regions are evidently polarized.

The dielectric constant of rocks is dependent on the dielectric constants of its component minerals and their quantitative relationship in the rock. For example, in ferruginous quartzite the main influence on its dielectric constant is many times greater than for quartz. With an increase in frequency the dielectric constant of rocks also increases. /133

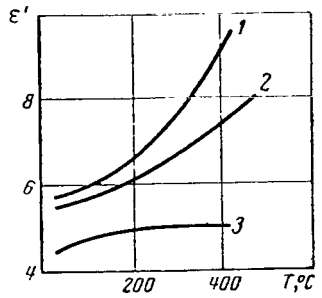

Figure 67. Graph of the dependence of the relative dielectric constant of minerals on temperature; 1- siderite; 2- halite; 3- microline.

Dependence of Dielectric Constant of Minerals and Rocks on Temperature

The dependence of the dielectric constant of minerals and rocks on temperature can be investigated only at intermediate frequencies. The measurements are made with a Q-meter. After determining the dielectric constant at different temperatures, curves are constructed for representing the dependence of the dielectric constant on temperature. With a change in temperature the dielectric constant should change linearly [54], but this law is not satisfied even for a crystal with a cubic lattice (Figure 67, curve 2). The increase in the dielectric constant with an increase in temperature can be attributed to an increase in crystal volume during thermal expansion.

In order to determine the dependence of ε' on temperature one introduces the dielectric constant temperature coefficient TKε'

$$TK\varepsilon' = \frac{1}{\varepsilon'} \cdot \frac{\partial \varepsilon'}{\partial T}.$$

The Clausius-Mossotti formula is used for estimating TKε'

$$\frac{\varepsilon' - 1}{\varepsilon' + 2} = \frac{4}{3} \pi N (\alpha_1 + \alpha_2 + \ldots + \alpha_i), \qquad \text{(III.80)}$$

where

N is the number of pairs of ions in 1 cm^3 of minerals;

α_1 and α_2 is the electron polarizability of ions;

α_i is ion polarizability.

We differentiate formula (III.80) for T and then determine TKε':

$$\frac{1}{\varepsilon'} \cdot \frac{\partial \varepsilon'}{\partial T} = \left[-3 \frac{\varepsilon' - 1}{\varepsilon' + 2} \beta_{\text{lin}} + \frac{4\pi N}{3} \cdot \frac{\partial \alpha_i}{\partial T} \right] \frac{(\varepsilon' + 2)^2}{3\varepsilon'}. \qquad \text{(III.81)}$$

With an increase in temperature the mineral expands; accordingly, the volume occupied by one ion increases. In this case the electron polarizability of the mineral is reduced by the value $\left(-3 \frac{\varepsilon' - 1}{\varepsilon' + 2} \beta_{\text{lin}}\right)$, since the specific density of electrons in 1cm^3 decreases. However, ion polarizability increases because ion displacement increases. Here β_{lin} is the coefficient of linear expansion. /134

The conductivity of minerals increases exponentially with a temperature increase. The free charges in the electric field are more mobile than the bound charges and therefore they exert a greater influence on the dielectric constant of minerals than an increase in volume during thermal expansion. If it is assumed that the influence of free charges on the dielectric constant is $\frac{\varepsilon' N_1}{N_0}$, where N_1 is the number of free charges in a unit volume of the mineral; N_0 is the number of ions in a unit volume, including free charges, with a temperature increase the number of free charges in a unit volume of the mineral increases exponentially and therefore the dielectric constant also increases exponentially:

$$|\varepsilon^*| = \sqrt{\varepsilon'^2 + \left[\frac{A}{\omega} \exp\left(-\frac{Q}{2kT} \right) \right]^2}. \qquad \text{(III.82)}$$

The exponential nature of the dependence of the dielectric constant corresponds to experimental data.

During the cooling of minerals and rocks the dielectric constant decreases insignificantly in comparison with the dielectric constant at room temperature.

Dependence of Dielectric Loss Tangent on Temperature

With a temperature increase the dielectric loss tangent (tan δ) increases exponentially because with an increase in temperature the rock conductivity increases exponentially. However, the nature of the tan δ change is dependent on frequency (see Figure 63). This can be attributed to the fact that with an

increase in frequency there is an increase in the role of the imaginary part of conductivity in the vector admittance, whereas the imaginary part of conductivity increases relatively slightly with a temperature increase (within the limits of one order of magnitude); however, within this same temperature range vector admittance changes by several orders of magnitude. The dielectric constant (real part) changes with a temperature increase within the range of one or two orders of magnitude and therefore with a temperature increase tan δ increases exponentially and this increase occurs for the most part due to an exponential increase in the real part of conductivity:

$$\tan \delta = \frac{\left| ig'' + A \exp\left(-\frac{Q}{2kT}\right) \right|}{\omega \varepsilon'}. \qquad \text{(III.83)}$$

Here, g'' is the imaginary part of conductivity.

With a temperature increase the ohmic part of conductivity increases exponentially. However, at a definite temperature its absolute value is less than the absolute value of the imaginary part of vector admittance. Accordingly, in this temperature range tan δ increases slightly, but as soon as the value of the real part of conductivity attains the value of the imaginary part, tan δ begins to increase exponentially with a temperature increase. /135

Magnetic Permeability and Rock Magnetization as a Function of Mineralogical Composition and Temperature

Most minerals are para- or diamagnetic and their magnetic permeability is approximately equal to unity. The rocks consisting of these minerals are also para- or diamagnetic and their magnetic permeability is also close to unity. A small number of minerals, the most common of which are magnetite, pyrrhotite, and titanomagnetite, are ferromagnetics whose permeability differs appreciably from unity. The magnetic permeability of the rocks in which these minerals are found is greater than unity; the magnetic permeability of the rock is dependent on its content of a ferromagnetic mineral.

We will write the energy of a ferromagnetic in the magnetic field

$$\frac{\mu H^2}{2} V = \frac{1}{2} (\mu_1 V_1 + \mu_2 V_2 + \ldots + \mu_i V_i) H^2, \qquad \text{(III.84)}$$

where

μ is the magnetic permeability of a volume V of rock;

$\mu_1, \mu_2, \ldots, \mu_i$ are the magnetic permeabilities of the minerals making up the rock;

$V_1, V_2, \ldots, V_i$ are the volumes of minerals forming the volume V with the corresponding magnetic permeabilities.

Eq. (III.84) can be written as follows:

$$\frac{1}{2}\mu H^2 V = \frac{1}{2}\left(\mu_1 \frac{V_1}{V} + \mu_2 \frac{V_2}{V} + \ldots + \mu_i \frac{V_i}{V}\right) V H^2, \tag{III.85}$$

then

$$\mu = \mu_1 \frac{V_1}{V} + \mu_2 \frac{V_2}{V} + \ldots + \mu_i \frac{V_i}{V}. \tag{III.86}$$

We assume

$$\frac{V_1}{V} = c_1; \quad \frac{V_2}{V} = c_2; \quad \ldots; \quad \frac{V_i}{V} = c_i, \tag{III.87}$$

where

$c_1, c_2, \ldots, c_i$ are the contents of a mineral with the magnetic permeabilities $\mu_1, \mu_2, \ldots, \mu_i$ in the volume V.

Then Eq. (III.86) assumes the form

$$\mu = \mu_1 c_1 + \mu_2 c_2 + \ldots + \mu_i c_i = \sum_{i=1}^{n} \mu_i c_i. \tag{III.88}$$

For example, if $\mu_1 c_1$ pertains to a ferromagnetic mineral, whereas the other /136
terms apply to para- and diamagnetic minerals, accordingly, the greater the content of a ferromagnetic mineral in a rock, the greater is its magnetic permeability.

Experiments show that the linear dependence (III.88) of magnetic permeability of a rock on its content of ferromagnetic minerals is well satisfied when the magnetite content is up to 60%. With greater magnetite contents there is a deviation from this behavior, attributable to the influence of the local magnetic fields of individual magnetite grains on the magnetization of adjacent grains.

Table 38 gives some measurement results. The data in the table show that only magnetite and pyrrhotite, as well as the rock incorporating these minerals, have a magnetic permeability different from unity.

Magnetic permeability increases and becomes constant if the magnetic mineral or rock are magnetized with saturation of the particular mineral.

The magnetic permeability of rocks in which magnetic minerals are incorporated increases with an increase in the content of the magnetic mineral in the rock.

With a temperature increase magnetic induction decreases and accordingly there is a decrease in the magnetic permeability of a ferromagnetic. This can be attributed to the fact that the magnetic field tends to set all the domains and magnetic moments of atoms in the direction of the magnetic field, but thermal motion tends to destroy this order.

TABLE 38. RELATIVE MAGNETIC PERMEABILITY OF SOME MINERALS AND ROCKS

No. of sample	Mineral, rock	Relative magnetic permeability
1	Ferruginous quartzite (Olenegorskoye deposit)	1.05
2	Magnetite (Dashkesanskoye deposit)	1.755
3	Pyrrhotite	1.027
4	Sphalerite	0.9998
5	Quartz	1.0001
6	Ore-free quartzite	0.9999
7	Ferruginous quartzite (Zheleznogorskoye deposit)	1.00022
8	Granite	1.000
9	Ferruginous quartzite, calcined (Olenegorskoye deposit)	1.3876
10	Ferruginous quartzite, magnetized	1.4417

At some temperature (Curie point) the magnetic permeability approaches unity. It is interesting to note that under the influence of the earth's magnetic field ferromagnetic minerals are remagnetized after heating. Iron oxides, such as FeO and Fe_2O_3, are magnetized after heating and their magnetic permeability is ·/137 increased. They are evidently restored to magnetite with a corresponding restructuring. With such restructuring there is a considerable increase in the conductivity of minerals and rocks containing iron.

Thus, by magnetizing a particular rock or mineral it is possible to attain an increase in their magnetic permeability (see Table 38, samples Nos. 9 and 10), and vice versa, by demagnetization or heating of minerals or rocks it is possible to bring about a decrease in their magnetic permeability.

4. Examples of the Use of the Electric and Magnetic Properties of Minerals and Rocks

The electric and magnetic properties of rocks can be successfully used in mineral extraction for obtaining information on the condition of the rock mass and also for modifying the rock mass for changing the rock properties in the required direction.

Determining the Mineralogical Composition of Rocks Using Electromagnetic Waves

It is known that the reflection of electromagnetic waves from a discontinuity between two media is dependent on the electric and magnetic properties of these media. The reflection coefficient is

$$k_{refl} = \frac{\rho_1 - \rho_2}{\rho_1 + \rho_2}, \qquad \text{(III.89)}$$

where

ρ_1 and ρ_2 are the wave resistances of the first and second media.

Since minerals and rocks have a low conductivity, the wave resistance of minerals and rocks is expressed by the equation [55]

$$\rho = \sqrt{\frac{\mu}{\varepsilon}}, \qquad \text{(III.90)}$$

where

ρ is the wave resistance of the medium.

We will assume that an electromagnetic wave is propagated through the air ($\rho_1 = 1$) and is incident on a rock mass and is partially reflected from it. In this case the coefficient is

$$k_{refl} = \frac{1 - \rho_2}{1 + \rho_2}, \qquad \text{(III.91)}$$

where

ρ_2 is the wave resistance of the rock.

The reflected wave is added to the incident wave. A standing wave is formed /138

in the air, that is, in the first medium; it is characterized by the standing wave ratio:

$$r = \frac{U_{max}}{U_{min}}, \qquad \text{(III.92)}$$

where

U_{max} is the wave strength at the antinode;

U_{min} is wave strength at the node.

The standing wave ratio r is related to the reflection coefficient k_{refl} as follows:

$$r = \frac{1 + k_{refl}}{1 - k_{refl}}. \qquad \text{(III.93)}$$

Accordingly, by measuring r it is possible to determine the rock wave resistance:

$$\rho_2 = r^{-1}. \qquad \text{(III.94)}$$

If $\mu_2 = 1$, which is characteristic for most rocks, from Eqs. (III.90) and (III.91) we obtain

$$\epsilon_2 = r^2, \qquad \text{(III.95)}$$

where

ϵ_2 and μ_2 are the dielectric and magnetic permeabilities of the rock.

In this case (with $\mu_2 = 1$), the standing wave ratio can be used in determining the dielectric constant of the rock.

Assuming that the wave resistance ρ_1 of the rock layer at the surface is known from the standing wave ratio, that is, from the reflected wave from the second rock layer, it is possible to determine the wave resistance of the second layer. In accordance with Eqs. (III.93) and (III.89), we have

$$\rho_2 = \frac{\rho_1}{r}. \qquad \text{(III.96)}$$

If the magnetic permeability of rocks in the second layer is $\mu = 1$, a direct determination can be made of the dielectric constant for rocks in the second layer:

$$\epsilon_2 = \epsilon_1 r^2. \qquad \text{(III.97)}$$

In addition to the dielectric constant of rocks in the mass their conductivity is also determined. The conductivity of rocks in the complex is determined from their heating temperature in the field of an electromagnetic wave; this requires measurement of the rock temperature during a definite time t of irradiation. The rock temperature can be used in computing conductivity at a particular frequency:

$$g = \frac{2W\alpha}{E_0^2 St}, \qquad \text{(III.98)}$$

where

W is electromagnetic field intensity, W;

α is the coefficient of electromagnetic wave attenuation, 1/cm;

S is the area of a unit surface, cm^2.

It is possible to determine whether the rock is a semiconductor or a dielectric from the rate of rock heating in the electromagnetic wave field. /139

The dielectric constant and conductivity of the rock are determined by remote control. By knowing these parameters it is possible to predict the thermal and mechanical properties of the rock.

Determining Deformations of Rock Complex

As is well known, the conductivity of minerals and rocks changes during their deformation. By measuring the conductivity of rock in some sector in the intact rock, such as by use of ohmmeters, remote observations of the rock mass deformations can be made. In this case, deformations are determined from the calibration curve showing the dependence of conductivity of a particular rock on the degree of deformation.

In order to determine deformation of the rock within the mass by this method it is necessary to drill test holes in the mass; this considerably changes the picture of deformations in the complex.

The deformation of the rock mass in some part of its volume can be determined from the absorption of electromagnetic energy by the rock, that is, by measuring the intensity of the electromagnetic wave passing through the rock. This method for determining rock deformation is contactless and remote. In this case the change in the intensity of the electromagnetic wave occurs as a

result of change in rock conductivity during its deformation:

$$\Delta E = E_0 - E_0 \exp(-\alpha x) = E_0 [1 - \exp(-\alpha x)]. \qquad \text{(III.99)}$$

In Eq. (III.99), the electromagnetic wave attenuation coefficient is dependent on rock deformation ε', $\alpha = f(\varepsilon')$. In radiowave control "by transillumination" the receiver used is placed on one side of the block and the transmitter, emitting electric waves propagating into the block, is placed on the opposite side. In this case E_0 is the strength of the wave entering the rock and $E_0 \exp(-\alpha x)$ is the strength of the wave entering the receiver.

The deformations of an "infinite" mass are determined using waves reflected from the block; these are added to the direct (incident) wave forming a standing wave in the block. With a change in rock conductivity in the deformation process the standing wave ratio changes. By measuring the standing wave ratio from the calibration curve, rock deformation can be determined.

During rock deformation the appearance of fractures can also be determined.

Control of Rock Strength

As mentioned above, minerals for the most part are ionic compounds and the charges in them are carried by both electrons and ions. The ions, passing into a free state, impair the crystal lattice of the mineral and thereby change the strength of the mineral and rock which form them. /140

We will assume that the strength of a particular rock with an ideal crystal lattice is σ_0; 1 cm^2 of cross section of this mineral contains

$$N_0 = \frac{10^{16}}{ab} \text{ ions}, \qquad \text{(III.100)}$$

where

a and b are the crystal lattice parameters in the particular cross section, Å.

We will assume that if several ions are eliminated in this cross section the rock strength is reduced. We will assume further that the strength change $\Delta\sigma$ is proportional to the existing strength and the decrease ΔN in the number

of ions in the particular crystal section, that is

$$\Delta\sigma = \sigma\left(-\frac{\Delta N}{N_0}\right). \tag{III.101}$$

The minus sign in the parentheses means that the number of particles in this section has decreased.

Decreasing the $\Delta\sigma$ value, and differentiating Eq. (III.101), we obtain the following differential equation:

$$\partial\sigma = \sigma\left(-\frac{\partial N}{N_0}\right) \tag{III.102}$$

or after separation of the variables

$$\frac{\partial\sigma}{\sigma} = -\frac{\partial N}{N_0}. \tag{III.103}$$

After integrating Eq. (III.103), we obtain

$$\ln\sigma - \ln c = -\frac{N}{N_0}, \tag{III.104}$$

where

c is the integration constant.

When $N_0 = 0$ $\sigma = \sigma_0$ and accordingly

$$\ln c = \ln \sigma_0.$$

Then in place of Eq. (III.04), we obtain

$$\ln\sigma - \ln\sigma_0 = -\frac{N}{N_0} \tag{III.105}$$

or

$$\ln\frac{\sigma}{\sigma_0} = -\frac{N}{N_0}. \tag{III.106}$$

After involution we obtain

$$\sigma = \sigma_0 e^{-\frac{N}{N_0}} = \sigma_0 \exp\left(-\frac{N}{N_0}\right). \tag{III.107}$$

In accordance with the Faraday law /141

$$N = \frac{kIt}{en}, \tag{III.108}$$

where

k is the fraction of the ionic current in the particular crystal, %;

I is the current passing through the mineral (crystal), a;

t is the time of current passage, sec;

e is electron charge, coulomb;

n is ion valency.

Eq. (III.107) assumes the form

$$\sigma = \sigma_0 \exp\left(-\frac{kIt}{enN_0}\right). \qquad \text{(III.109)}$$

Accordingly, under the influence of a constant field the rock strength decreases as a result of ion movement.

This phenomenon is actually experimentally observed [56]; for example, with an initial compressive strength of 600 kg/cm^2 the sample strength after passage of a charge of about 10^6 coulomb is reduced to 200 kg/cm^2. In this experiment the sample temperature was maintained at room temperature and the percentage of the ionic current was about 2% of the current in the circuit.

We note that with an increase in temperature the percentage of the ionic current is increased. In an electric field among the ionic crystals, consisting of two species of ions, such as galena crystals, in general it is the ion with the lesser radius which moves.

If it is assumed that half the ions move, the strength in this case should be reduced by e times, that is, by a factor of 2.73.

The rock strength can also increase. In the real crystal lattice there are always vacancies of the same ion. Therefore, in order to increase the rock strength it is necessary to fill the vacancies with the particular ion. This is accomplished by introducing the necessary ions into the rock under the influence of an applied voltage. The increase in rock strength is also described by Eq. (III.109). In this case there will be a plus sign in the parentheses.

The rock can be strengthened by growing metal "whiskers" in it. The growing occurs by diffusion of metal ions from the electrodes under the influence of the applied voltage. In this case the metal is selected in such a way that the dimensions of its ions will be less than the crystal lattice constant of the minerals in the particular rock. The strength of the metal "whiskers" is several orders of magnitude greater than the strength of the metal from which they are formed and therefore the "whiskers" grown in the rock considerably increase its strength [54].

Thus, using the ionic conductivity of minerals and rocks and acting on the rocks with a constant voltage, their strength can be controlled.

Ionic conductivity can also be used for extracting the useful component from the rock mass or from the rock melt: when a dc voltage is applied to the rock, together with the charges and masses of ions, the rock components separate /142 out at the electrodes. The extraction or segregation of minerals or rocks into components can be in both the solid and liquid states.

The laws controlling these processes are described by the Faraday electrolysis laws:

$$M = \frac{AIt}{Fm}, \qquad \text{(III.110)}$$

where

M is mass, tons;

A is the atomic weight of an ion, g;

F is the Faraday number (F = 96,496), coulomb;

m is the ionic valency.

In order to reduce the energy input in the process it is necessary to increase the percentage of the ionic current; this requires an increase in rock temperature. As is well known, the energy of an electric source is W = IUt, and therefore for increasing the current the voltage across the electrodes must be reduced. This requires that the rock resistance between the electrodes be reduced. In the last analysis, one finds that it is more advantageous to work with a rock melt. Eq. (III.110) is used in determining the energy input in separating the minerals and rocks into components:

$$E = \frac{FmU}{A}. \qquad \text{(III.111)}$$

Using this expression, for the segregation of galena with a voltage of 10 V across the electrodes, we obtain for lead an energy input of 2,570 kW·hour/ton and for sulfur 16,670 kW·hour/ton with the fraction of the ionic current being 100%. These figures show that with respect to energy input it is desirable to obtain electrolysis elements from a melt.

Determining the Content of a Magnetic Mineral in a Rock

In the process of extracting minerals and enriching minerals there is a need for determining the content of the useful component. The content of a magnetic mineral in a nonmagnetic rock can be determined from the magnetic permeability of the particular rock. This is done by measuring solenoid inductance:

$$L = \mu \frac{4\pi N^2 S}{l}. \qquad \text{(III.112)}$$

Here the quantity $4\pi N^2 S/l = c$, 1/m is a constant for the particular solenoid, determined by its parameters (N is the number of turns, S is the turn cross-sectional area, l is solenoid length). Accordingly, in place of Eq. (III.112) we can write

$$L = c\mu, \qquad \text{(III.113)}$$

that is, solenoid inductance is dependent on the magnetic permeability of the rock. In turn, the magnetic permeability of a rock is dependent on its content of magnetic mineral. Thus, by measuring the inductance of a solenoid with a particular rock which contains an unknown quantity of magnetic mineral, using /143 earlier constructed calibration curves it is possible to determine the content of magnetic mineral in the rock. The calibration curves are constructed from the results of measurements of the magnetic permeability of samples of the particular rock with a known content of magnetic mineral.

In order to check the theoretical premises we determined the magnetite content in ferruginous quartzite and in the enrichment products, in an ore concentrate and in tailings. Inductance was measured with a Maxwell bridge or with a Ye12-1 instrument. The calibration curves were constructed from the products of an ore-enrichment plant with a known magnetite content. The investigations revealed that in this way it is possible to measure the content of magnetic mineral with an error to a tenth of a percent; the measurements can be made in the field and on an ore-concentration plant conveyer. The measurements can be made on rocks with both high and low contents of magnetic mineral [57].

Hall pickups can be used for this same purpose if the magnetic material is first magnetized. In this case the Hall emf is dependent on rock magnetic

field induction. The degree of induction is in turn dependent on the content of magnetic mineral in the rock.

Determining Rock Temperature from Its Conductivity

In some engineering problems, and also when investigating some processes, the rock temperature must be determined. For example, the rock temperature must be known when there are underground fires; since the rock temperature increases during a fire, its resistivity is accordingly reduced. The decrease in rock resistivity can be used in determining the center of a fire hidden in the rock mass. In investigating thermal drilling processes one must make precise measurements of rock temperature at the time of its destruction; this is also done from measurements of rock resistivity.

Knowing the parameters A and Q of a particular rock, as well as its resistivity, Eq. (III.32) can be used in determining rock temperature

$$T^0 = \frac{Q}{2k(\ln \rho - \ln A)}. \qquad \text{(III.114)}$$

By constructing calibration curves of the dependence of rock resistivity on temperature and measuring the rock resistivity it is possible to determine its temperature at any moment.

The dependence of rock resistivity on time can be registered in the form of an oscillogram and the time of onset of temperature change can be determined; at any time the resistivity can be used in determining rock temperature. Such an oscillogram makes it possible to trace temporal development of a process, for example, during the course of an underground fire.

The same method can be used in solving the inverse problem: determining the rock content of a finely impregnated conducting or semiconducting mineral. This requires a chemical analysis which involves a great time expenditure. The /144
problem can also be solved by other methods: in a study of the absorption of electromagnetic waves of short length in a piece of rock of definite mass; from the heating of a piece of rock in a superhigh-frequency generator of considerable power (more than 200 W). The absorption of electromagnetic energy and the heating of rock in a superhigh-frequency field in both cases are

dependent for the most part on the conductivity of the mineral and on its content in the particular rock. These methods for determining mineral content are extremely simple and require little time (two to five minutes). They ensure a high measurement accuracy.

Electric Method for Heating Rock

The conductivity of rocks makes it possible to transform the energy of an electromagnetic field into thermal energy and thereby to heat the rock. The picture of rock heating is dependent on the electromagnetic field heating: Joule heat is released in constant and quasiconstant electromagnetic fields

$$W = gE^2t, \tag{III.115}$$

whose value is determined by the real part of vector admittance (that is, conductivity with a constant field strength). In a high-frequency electromagnetic field the quantity of released heat is increased due to a loss of electromagnetic energy expended on the oscillation of ions, that is, due to an increase in the imaginary part of conductivity, or its equivalent, an increase in rock vector admittance with a frequency increase. The quantity of released heat, computed using the formula

$$W = \omega\varepsilon' \operatorname{tg}\delta E^2 t, \tag{III.116}$$

is equivalent to the quantity of heat determined using Eq. (III.115). Substituting the $\tan\delta = g/\omega\varepsilon'$ value into Eq. (III.116), we obtain Eq. (III.115). In this case g represents the rock vector admittance, a function of electromagnetic field frequency.

A frequency increase therefore leads to an intensification of rock heating, but the reflected wave carries off part of the energy, creates radio interference and has a harmful effect on the health of workers.

The amplitude of the reflected wave is dependent on the dielectric constant and magnetic permeability. The reflection coefficient is determined from the expression

$$k_{refl} = \frac{\sqrt{\frac{\mu_1}{\varepsilon_1}} - \sqrt{\frac{\mu_2}{\varepsilon_2}}}{\sqrt{\frac{\mu_1}{\varepsilon_1}} + \sqrt{\frac{\mu_2}{\varepsilon_2}}}, \tag{III.117}$$

where

μ_1 and ϵ_1 are magnetic permeability and the dielectric constant of the medium from which the electromagnetic wave is exposed to the rock. /145

With an increase in rock temperature there is an increase in its dielectric constant and a decrease in magnetic permeability. Accordingly, there is an increase in the reflection coefficient, that is, with an increase in rock temperature an increasingly smaller part of the electromagnetic energy enters it. The distribution of electromagnetic energy in the rock mass is described by the expression

$$W = gSE_0^2 \frac{t}{2\alpha} e^{-2\alpha l}, \qquad \text{(III.118)}$$

where

S is the surface through which the electromagnetic wave enters the rock;

α is the electromagnetic wave attenuation coefficient, being a function of field frequency and the electric characteristics $\alpha = f(g, \epsilon, \mu, \omega)$;

l is the distance from the rock surface to the observation point.

When the rock is heated g and α increase; accordingly, the energy of the electromagnetic wave, having an exponential distribution in the direction of wave movement, is concentrated in an increasingly lesser rock volume which is intensively heated. Using a high-frequency field it is possible to heat a considerable rock volume at the same time. This heating is not dependent on rock heat conductivity and occurs rather rapidly. However, the effectiveness of high-frequency fields is manifested under conditions corresponding to the particular frequency.

Electric heating of a rock is used for the electrothermal destruction of rocks, weakening their strength, thawing permafrost, and in other cases.

During the electrothermal destruction of rocks a small part of the rock mass or profile is heated to an average temperature of 600-700°C. The heated part of the rock expands and mechanical stresses appear in it; at some points these exceed the tensile strength of the rock and it is destroyed. Since in this case the rock destruction occurs due to dilatational stresses, the energy expenditures on destruction are small (up to 3 to 5 kW·hour/m^3). The effectiveness

of such destruction is determined by the combination of mechanical, thermal and electric properties of the rock, in this case being a function of temperature.

Rock strength is weakened by means of thermomechanical stresses produced during the local heating of rock and also due to the difference in the physical properties of the minerals forming the rock.

APPENDIX 1

PETROGRAPHIC DESCRIPTION OF ROCKS

Deposit	Rock	Mineralogical and chemical composition, %						Structure
		SiO_2	Al_2O_3	Fe_2O_3	FeO	MgO	Others	
Quartzite deposit of Pervoural'skoye Dinas (refractory brick) Plant	Bluish-gray quartzite; γ = 2.62 g/cm^3, P = 0.0%	98.72	0.53	0.46	0.08	0.14	0.15	Foliated structure granoblastic texture.
	Porous ferroginous quartzite. γ = 2.24 g/cm^3, P = 20%	97.26	1.05	0.96	0.28	0.18	0.11	Same
Olenegorskoye iron-ore deposit	Gneiss γ = 2.8 g/cm^3, P = 0.8%	Plagioclase 53.73, zoisite 30.97, biotite 14.56, quartz 0.54, zircon 0.20.						Gneissose structure, granular-flaky structure.
	Ferruginous quartzite. γ = 3.44 g/cm^3, P = 2.6%	Quartz 38.92, ore 53.58, pyroxene 3.05, amphibole 2.05, biotite 1.32, microcline-apatite 1.08.						Fine-banded structure, granular texture.
	Ore-free quartzite γ = 3.07 g/cm^3, P = 1.3%	Quartz 74.24, ore 16.32, pyroxene 5.06, calcite 2.38, biotite 1.95, apatite 0.05.						Fine-banded structure, equigranular texture.
	Pegmatite γ = 2.62 g/cm^3, P = 2.3%	Plagioclase 53.07, microcline 28.43 quartz 10.35, muscovite 5.43, pyroxene - garnet - chlorite - carbonate - epidote 2.3, apatite - sphene - tourmaline 0.35.						Uneven coarse-grained texture.

Appendix 1, continued

Deposit	Rock	Mineralogical and chemical composition, %									Structure
Shartashskoye granite deposit	Granite γ = 2.64 g/cm^3, P = 0.56%	Plagioclase 55, potassic feldspar 15.5, quartz 23.6, biotite 5.9.									Medium-grained texture.
	Granite γ = 2.64 g/cm^3, P = 0%	Plagioclase 51, quartz 24, microcline 18.8, biotite 6, accessory 0.2.									Fine-grained texture.
		SiO_2	TiO_2	Al_2O_3	Fe_2O_3	FeO	MnO	MgO	CaO	K_2O	Na_2O
		69.5	0.43	16.6	0.85	1.15	0.04	0.98	2.3	3.0	4.6
		70.0	0.26	17.0	0.7	1.0	0.03	0.45	2.05	2.72	5.0
Smolinskoye granite deposit	Granodiorite γ = 2.74 g/cm^3, P = 0.7%	Acidic plagioclase 55, quartz 18, potassic feldspar 6.7, dark-colored 19.8.									Coarse-grained texture.
	Gneissous granite γ = 2.62 g/cm^3 P = 0.8%	Quartz 28.5, potassic feldspar 32.5, plagioclase 34, biotite 5.									Gneissous structure, granoblastic texture.
		SiO_2	TiO_2	Al_2O_3	Fe_2O_3	FeO	MnO	MgO	CaO	K_2O	Na_2O
		61.6	0.54	17.32	2.01	2.9	0.07	4.9	4.5	2.2	3.7
		73.3	0.26	15.48	0.48	0.94	0.05	0.4	1.3	4.3	3.6
Rovnenskoye granite deposit	Granite γ = 2.68 g/cm^3 P = 0.6%	Plagioclase		Quartz		Microcline		Biotite, chlorite, etc.			Fine-grained texture.
		39.68		28.25		28.8		9.27			
	Granite γ = 2.69 g/cm^3, P = 0.6%	50.57		22.75		16.26		10.42			Fine-grained texture.

Appendix 1, continued

Deposit	Rock	Mineralogical and chemical composition, %								Structure
Rovnenskoye granite deposit	Granite γ = 2.68 g/cm^3, P = 0.4%	39.41		25.23		23.29		12.09		Coarse-grained texture
		SiO_2	Al_2O_3	CaO	Na_2O	Ka_2O	FeO	MgO	MnO	
		69.7	16.49	3.14	5.3	2.75	1.52	0.97	0.05	
		70.16	15.55	1.91	4.5	3.71	1.77	1.12	0.06	
		72.01	15.03	1.88	4.47	3.71	1.35	0.86	0.04	
Zhdanovskoye deposit	Granite γ = 3.11 g/cm^3, P = 1.0%	Pyroxene 45.13, olivine 25.67, plagioclase 15.35, horneblende - chlorite 14.85, ore 1.15.								Trachytoid structure, poikilitic texture.
	Mineralized serpentinized peridotite γ = 3.08 g/cm^3 P = 0.7%	Olivine 26.38, pyroxene 5.43, serpentine 45.22, biotite 4.25, chlorite 5.35, calcite 1.07, ore 12.30.								Massive structure, sideronitic texture.
	Mineralized serpentinized peridotite γ = 2.92 g/cm^3 P = 0.7%	Pyroxene 28.06, biotite 5.13, horneblende 8.16, serpentinite 14.22, olivine 31.15, ore 3.38.								Massive structure, sideronitic texture.
Bakal'skoye deposit	Microquartzite γ = 2.60 g/cm^3 P = 0.0%	SiO_2 98.								Equigranular texture
	Dolomite γ = 2.8 g/cm^3, P = 0.7%	Magnetite 1.05, carbonate 94.7, quartz 3.3.								Massive structure, granular texture.

Appendix 1, continued

Deposit	Rock	Mineralogical and chemical composition, %	Structure
	Diabase $\gamma = 2.65$ g/cm^3, P = 1.0%	Plagioclase 43.67, pyroxene 21.12, horneblende 17.31 biotite 4.57, olivine 8.67.	Massive structure, diabasic texture.
	Shale $\gamma = 2.72$ g/cm^3, P = 1.1%.	Chlorite 35.4, talc 14.86, carbonate 27.7, quartz 18.8.	Porphyroblastic texture.
YuGOK quarry (horizon ±0 m)	Ferruginous quartzite $\gamma = 3.53$ g/cm^3, P = 2.75%	Quartz 36.4, ore 51.32, biotite 1.2,	Fine-banded structure, granular texture.
Mikhaylovskoye deposit of the Kursk Magnetic Anomaly	Semioxidized ferruginous quartzite $\gamma = 3.534$ g/cm^3, P = 18%	Quartz 24, hematite 45, magnetite 15, carbonate 2, pyrite 13.	Banded structure, granular texture.
	Oxidized ferruginous quartzite. $\gamma = 3.8$ g/cm^3, P = 28%	Quartzite 25 - 28, brown iron hydroxides 70 - 72, carbonate 2 - 3.	Banded structure, irregular granular texture.
Lebedinskoye deposit of Kursk Magnetic Anomaly	Martite-magnetite ferruginous quartzite (semioxidized) $\gamma = 3.58$ g/cm^3 P = 34%.	Quartz 38.1, magnetite 25, hematite 24.77, geothite-hydrogoethite 2.86, pyrite 0.04, carbonate 2.16, kaolinite 3.83.	Banded structure, granular texture.

Appendix 1, *continued*

Deposit	Rock	Mineralogical and chemical composition, %	Structure
Lebedinskoye deposit of Kursk Magnetic Anomaly	Amphibole-magnetite ferruginous quartzite (unoxidized). γ = 3.6 g/cm^3, P = 13%	Magnetite 32.9, quartz 31.8, cummingtonite 12.6, carbonate 5.1, kaolinite 3.2, muscovite 0.78.	Same

APPENDIX 2

INDICES OF THERMAL PROPERTIES OF ROCKS AS A FUNCTION OF TEMPERATURE

Rock	Rock constants	Indices of Thermal Properties of Rocks at Temperature, °C												
		18	50	100	150	200	250	300	350	400	450	500	550	575	600
Medium and fine-grained granite (Rovnenskoye deposit)	$a \cdot 10^{-3}$	5,36	4,43	3,75	3,16	2,76	2,68	2,58	2,48	2,38	2,91	—	—	—	—
	λ	2,15	2.05	1,87	1,75	1,69	1,65	1,62	1,6	1,57	1,55	—	—	—	—
	c	0,401	0,464	0,6	0,554	0,61	0,619	0,63	0,646	0,674	0,7	—	—	—	—
	$\beta \cdot 10^{-5}$	—	—	—	1.05	1,35	1,5	1,6	1,75	2,1	2,6	2,7	3,1	3,3	4,1
	$E \cdot 10^5$	6,6	5,6	5,0	4,0	3,4	3,2	3,0	2,75	2,55	2,25	2,15	2,0	1,9	1,5
Coarse-grained granite	$a \cdot 10^{-3}$	4,7	3,8	3,25	3,0	2,48	2,41	2,31	2,26	2,16	2,06	—	—	—	—
	λ	1,93	1.82	1,62	1,59	1,52	1,49	1,48	1,47	1,46	1,45	—	—	—	—
	c	0,41	0,47	0,5	0,53	0,615	0 619	0,64	0,65	0,675	0,706	—	—	—	—
	$\beta \cdot 10^{-5}$	—	—	—	0,7	0,9	1,2	1,4	1,6	1,92	2,26	2,8	3,4	5,2	6,55
	$E \cdot 10^5$	9,05	9,98	8,75	6,25	5,2	4,15	3,55	3,1	2,19	1,87	1,55	1,2	0,75	0,6
Gray granite (Rovnenskoye deposit)	$a \cdot 10^{-3}$	6,26	5,0	3,65	3,28	2,9	2,8	2,68	2,61	2,51	2,35	—	—	—	—
	λ	2,45	2,25	1,85	1,75	1,75	1,7	1,67	1,665	1,66	1,6	—	—	—	—
	c	0,39	0,45	0,507	0 534	0,604	0,608	0,625	0,639	0,662	0,68	—	—	—	—
	$\beta \cdot 10^{-5}$	—	—	—	0,95	1,1	1,35	1,6	1,75	1,6	2,05	2,45	2,95	3,76	4,0
	$E \cdot 10^5$	7,0	6,8	6,5	5,7	5,2	4,35	3,65	2,95	2,65	2,25	1,8	1,45	1,18	1,1
Medium-grained granite (Shartashskoye deposit)	$a \cdot 10^{-3}$	2,44	2,12	1,8	1,47	1,3	1,23	1,2	1,17	1,111	1,18	—	—	—	—
	λ	1,02	0,98	0,9	0,82	0,78	0,762	0,756	0,75	0,748	0,745	—	—	—	—
	c	0,42	0,46	0,5	0,556	0,601	0,618	0,029	0,642	0,675	0 692	—	—	—	—
	$\beta \cdot 10^{-5}$	—	—	—	0,9	0,95	1,0	1,3	1,5	1,75	1,89	2,15	2,55	3,0	4,0
	$E \cdot 10^5$	3.25	3,15	3,0	2,75	2,65	2,4	2,3	2,1	1,95	1,65	1,45	1,25	1,0	0,9
Microquartzite (Bakal'skoye deposit)	$a \cdot 10^{-3}$	5,27	4,5	4,12	3,6	3,1	3,18	2,8	2,7	2,56	2,37	—	—	—	—
	λ	2,4	2,25	2,2	2,0	1,8	1,95	1,8	1,8	1,75	1,7	—	—	—	—
	c	0,455	0,5	0,534	0,557	0,58	0,612	0,642	0,666	0,685	0,719	—	—	—	—
	$\beta \cdot 10^{-5}$	—	—	—	1,15	1,35	1,7	1,9	2,1	2,2	2,55	3,05	3,0	8,5	4,5
	$E \cdot 10^5$	7,1	6,7	6,5	6,2	6,15	5,8	5,2	4,8	4,3	4,0	3,5	3,0	2,5	3,0
Dolomite (Bakal'skoye deposit)	$a \cdot 10^{-3}$	6,04	5,25	4,76	4,51	4,34	3,83	3,82	3,54	3,57	3,23	—	—	—	—
Dolomite (Bakal'skoye deposit)	λ	3,65	3,28	3,03	2,9	2,91	2,7	2,76	2,6	2,73	2,55	—	—	—	—
	c	0,605	0,625	0,635	0,643	0,67	0,705	0,723	0,735	0,765	0,79	—	—	—	—
	$\beta \cdot 10^{-5}$	—	—	—	1,45	1,7	1,9	2,3	2,5	2,7	2,85	—	—	—	—
	$E \cdot 10^5$	4,15	3,78	3,65	3,3	2,9	2,66	2,3	2,12	1,95	1,8	—	—	—	—
Pegmatite (Olenegorskoye deposit)	$a \cdot 10^{-3}$	6,27	4,72	3,57	2,85	2,62	2,59	2,49	1,84	1,86	1,25	—	—	—	—
	λ	3,27	2,64	2,03	1,71	1,66	1,7	1,68	1,27	1,37	0,95	—	—	—	—
	c	0,52	0,56	0,57	0,6	0,635	0,655	0,676	0,63	0,734	0,758	—	—	—	—
	$\beta \cdot 10^{-5}$	—	—	—	1,1	1,3	1,5	1,6	1,7	1,8	1,98	2,2	2,45	3,1	4,2
	$E \cdot 10^5$	4,1	3,9	3,6	3,55	3,45	3,15	2,9	2,65	2,55	2,38	2,05	2,85	2,65	1,55
Gabbro (Zhdanovskoye deposit)	$a \cdot 10^{-3}$	4,52	3,85	3,23	2,71	2,56	2,48	2,36	2,27	2,13	2,07	—	—	—	—
	λ	2,8	2,5	2,2	1,9	1,89	1,86	1,84	1,82	1,81	1,8	—	—	—	—
	c	0,62	0,65	0,68	0,7	0,74	0,75	0,78	0,8	0,85	0,87	—	—	—	—
	$\beta \cdot 10^{-5}$	—	—	—	0,5	0,65	0,6	0,7	0,74	0,78	0,83	0,9	0,95	1,0	1,04	1,06
	$E \cdot 10^5$	10,2	9,78	9,5	9,0	8,4	7,2	6,95	6,6	6,25	5,9	5,85	5,8	5,78	5,72

Appendix 2, continued

Rock	Rock constants	Indices of Thermal Properties of Rocks at Temperature, °C												
		18	50	100	150	200	250	300	350	400	450	500	550	575	600
Mineralized serpentinized peridotite	$a \cdot 10^{-3}$	5,2	4,69	4,3	3,97	3,64	3,53	3,38	3,27	3,13	2,74	—	—	—	—
	λ	3,2	3,0	2 83	2,7	2,6	2,6	2,55	2,54	2,5	2,3	—	—	—	—
	c	0,616	0,64	0,66	0,68	0,716	0,736	0,755	0,38	0,8	0,84	—	—	—	—
	$\beta \cdot 10^{-5}$	—	—	0,45	0,45	0,5	0,57	0,6	0,65	0,68	0,7	0,72	0,75	0,78	0,8
	$E \cdot 10^{5}$	10,8	10,8	10,75	9,5	8,45	6,0	5,75	5,3	5,33	5,3	5,28	5,27	5,25	5,25
Diabase (Bakal'skoye deposit)	$a \cdot 10^{-3}$	4,95	4,3	3,87	3,3	3,08	2,9	2,84	2,76	2,65	2,44	—	—	—	—
	λ	2,4	2,1	1,9	1,85	1,82	1,8	1,18	1,78	1,75	1,7	—	—	—	—
	c	0,486	0,49	0,5	0,56	0,59	0,62	0,635	0,645	0,66	0,685	—	—	—	—
	$\beta \cdot 10^{-5}$	—	—	—	0,9	0,95	1,05	1,1	1,15	1,2	1,4	1,45	1,5	1,55	1,60
	$E \cdot 10^{5}$	4,45	4,43	4,4	4,3	4,15	4,05	4,0	3,9	3,8	3,78	3,6	3,5	3,45	3,3
Shale (Bakal'skoye deposit)	$a \cdot 10^{-3}$	8,5	6,85	6,0	5,3	5,14	5,0	4,8	4,62	4,45	4,21	—	—	—	—
	λ	4,2	3,9	3,6	3,4	3 4	3,35	3,32	3,3	3,25	3,2	—	—	—	—
	c	0,495	0,57	0,6	0,643	0,665	0,673	0,69	0,71	0,73	0,76	—	—	—	—
	$\beta \cdot 10^{-5}$					0,9	0,95	1,05	1,1	1,15	1,2	1,25	1,3	1,35	1,4
	$E \cdot 10^{5}$	4,2	4,18	4,17	4,16	4,15	4,13	4,11	4,09	4,05	4,0	3,95	3,9	3,85	3,8
Ferruginous quartzite ⊥ to stratification (Olenegorskoye deposit)	$a \cdot 10^{-3}$	7,4	6,85	6,12	5,57	5,28	5,0	4,66	4,55	4,55	4,29	—	—	—	—
	λ	4,03	3,9	3,882	3,81	3,78	3,74	3,73	3,75	3,8	3,7	—	—	—	—
	c	0,545	0,57	0,635	0,685	0,716	0,75	0,8	0,823	0,87	0,863	—	—	—	—
	$\beta \cdot 10^{-5}$	—	—	—	0,45	0,53	0,61	0,8	0,9	1 05	1,2	1,65	2,2	2,65	3,0
	$E \cdot 10^{5}$	5,0	4,7	4,5	7,1	3,5	3,1	2,8	2,4	2,15	1,75	1,55	1,42	1,2	1,0
Ferruginous quartzite ‖ to stratification	$a \cdot 10^{-3}$	7,86	7,44	6,54	6,09	5,6	5,25	4,89	4,79	4,71	4,59	—	—	—	—
	λ	4,32	4,22	4,17	4,14	4,0	3,97	3,95	3,93	3,94	3,945	—	—	—	—
	c	0,55	0,568	0,64	0,68	0,715	0,755	0,81	0,82	0,836	0,86	—	—	—	—
	$\beta \cdot 10^{-5}$	—	—	—	1,5	1,5	1,52	1,6	1,68	1,75	2,0	2,3	3,55	4,2	6,7
	$E \cdot 10^{5}$	5,6	5,5	5,45	5,1	4,75	3,6	3,5	3,3	3,0	2,62	2,55	2,05	1,75	1,78
Serpentinized peridotite	$a \cdot 10^{-3}$	3,9	3,59	3,27	3,0	2,8	2,42	2,32	2,27	2,19	2,14	—	—	—	—
	λ	2,4	2,3	2,2	2,1	2,05	1,86	1,86	1,84	1,85	1,86	—	—	—	—
	c	0,615	0,64	0,673	0,7	0,73	0,76	0,8	0,81	0,845	0,867	—	—	—	—
	$\beta \cdot 10^{-5}$	—	—	0,45	0,47	0,49	0,5	0,53	0,55	0,58	0,65	0,68	0,73	0,75	0,75
	$E \cdot 10^{5}$	10,25	9,8	9,45	9,2	8,85	8,3	8,05	7,75	7,5	7,2	7,15	7,1	7,0	6,95
Ferruginous quartzite (Pervoural'skoye deposit)	$a \cdot 10^{-3}$	3,12	2,91	2,72	2,67	2,56	2,45	2,4	2,36	2,26	2,18	—	—	—	—
	λ	1,31	1,28	1,25	1,24	1,23	1,23	1,22	1,215	1,21	1,2	—	—	—	—
	c	0,42	0,44	0,46	0,465	0,48	0,5	0,507	0,515	0,535	0,55	—	—	—	—
	$\beta \cdot 10^{-5}$	—	—	—	0,9	1,2	1,2	1,25	1,26	1,3	1,27	1,4	1 42	1,5	1,55
	$E \cdot 10^{5}$	3,15	2,91	2,76	2,75	2,75	2,75	2,73	2,61	2,5	2,48	2,25	2,0	2,0	1,85
Ore-free quartzite ⊥ to stratification (Olenegorskoye deposit)	$a \cdot 10^{-3}$	5,46	4,66	4,07	3,73	3,35	3,24	3,14	3,04	2,97	2,86	—	—	—	—
	λ	2,85	2,6	2,5	2,45	2,432	2,4	2,38	2,37	2,375	2,371	—	—	—	—
	c	0,523	0,556	0,61	0,655	0,705	0,74	0,756	0,78	0,8	0,83	—	—	—	—
	$\beta \cdot 10^{-5}$	—	—	—	1,0	1,2	1 33	1,5	1,65	2,0	2,6	3,2	3,9	5,3	5,0
	$E \cdot 10^{5}$	8,5	7,95	7,75	7,15	5,62	5,12	4,6	4,2	4,0	3,1	2,8	2,5	2,2	2,1
Ore-free quartzite ‖ to stratification	$a \cdot 10^{-3}$	6,1	5,42	4,84	4,37	3,84	3,72	3,67	3,6	3,44	3,2	—	—	—	—
	λ	3,2	3,04	2,98	2,87	2,8	2,83	2,8	2,79	2,75	2,72	—	—	—	—
	c	0,525	0,56	0,615	0,665	0,73	0,76	0,763	0,78	0,8	0,85	—	—	—	—
	$\beta \cdot 10^{-5}$	—	—	—	1,2	1,31	1,53	1,72	2,1	2,5	3,0	5,5	6,5	3,3	2,8
	$E \cdot 10^{5}$	9,0	8,7	8,5	7,1	6,22	5,73	5,31	5,15	4,85	4,45	4,15	3,75	3,5	3,1

Appendix 2, continued

Rock	Rock constants	Indices of Thermal Properties of Rocks at Temperature, °C												
		18	50	100	150	200	250	300	350	400	450	500	550	575	600
Gneiss ⊥ to stratification (Olenegorskoye deposit)	$a \cdot 10^{-3}$	4,4	3,81	3,33	3,05	2,71	2,5	2,34	2,25	2,18	2,05	—	—	—	—
	λ	2,24	2,09	2,0	1,98	1,9	1,87	1,86	1,865	1,85	1,84	—	—	—	—
	c	0,51	0,55	0,6	0,65	0,7	0,75	0,795	0,83	0,85	0,9	—	—	—	—
	$\beta \cdot 10^{-5}$	—	—	—	—	0,75	1,0	1,25	1,5	1,8	2,1	2,5	3,0	3,25	3,9
	$E \cdot 10^{5}$	5,76	5,42	5,2	4,5	4,0	3,8	3,4	2,9	2,5	2,1	1,85	1,4	1,1	0,95
Gneiss ‖ to stratification	$a \cdot 10^{-3}$	4,82	4,12	3,64	3,34	3,11	3,0	2,76	2,59	2,55	2,41	—	—	—	—
	λ	2,48	2,39	2,36	2,3	2,28	2,25	2,2	2,15	2,18	2,16	—	—	—	—
	c	0,515	0,582	0,646	0,689	0,735	0,75	0,795	0,83	0,854	0,896	—	—	—	—
	$\beta \cdot 10^{-5}$	—	—	—	0,95	1,35	1,63	1,8	1,95	2,15	2,35	2,55	2,9	—	—
	$E \cdot 10^{5}$	6,6	6,5	6,4	6,1	4,2	3,8	3,6	3,5	3,4	3,35	3,3	3,28	3,26	3,2
Fine-grained granite (Shartashskoye deposit)	$a \cdot 10^{-3}$	1,89	1,64	1,49	1,33	1,15	1,1	1,07	1,01	0,97	0,94	—	—	—	—
	λ	0,786	0,756	0,75	0,74	0,694	0,68	0,67	0,66	0,655	0,65	—	—	—	—
	c	0,415	0,462	0,503	0,557	0,602	0,82	0,628	0,65	0,675	0,69	—	—	—	—
	$\beta \cdot 10^{-5}$	—	—	—	0,99	1,05	1,15	1,35	1,4	1,5	1,8	1,9	2,1	2,4	2,75
	$E \cdot 10^{5}$	4,2	4,1	4,0	3,88	3,6	3,3	3,0	2,85	2,7	2,4	2,1	1,85	1,65	1,45
Granodiorite (Smolinskoye deposit)	$a \cdot 10^{-3}$	3,13	2,76	2,37	1,98	1,8	1,74	1,76	1,7	1,65	1,61	—	—	—	—
	λ	1,5	1,46	1,35	1,21	1,17	1,17	1,2	1,2	1,198	1,19	—	—	—	—
	c	0,48	0,53	0,57	0,61	0,65	0,672	0,684	0,706	0,725	0,74	—	—	—	—
	$\beta \cdot 10^{-5}$	—	—	—	—	1,35	1,45	1,54	1,72	1,95	2,1	2,45	3,0	3,4	3,8
	$E \cdot 10^{5}$	3,9	3,89	3,85	3,75	3,68	3,45	3,3	3,0	2,8	2,6	2,2	2,0	1,8	1,7
Granite gneiss (Smolinskoye deposit)	$a \cdot 10^{-3}$	6,9	5,88	5,62	5,0	4,22	4,54	3,98	3,91	3,78	3,66	—	—	—	—
	λ	2,9	2,9	2,97	2,81	2,6	2,83	2,6	2,6	2,58	2,55	—	—	—	—
	c	0,419	0,494	0,53	0,562	0,616	0,623	0,654	0,665	0,683	0,698	—	—	—	—
	$\beta \cdot 10^{-5}$	—	—	—	1,0	1,02	1,0	1,1	1,3	1,4	1,5	1,7	2,3	2,7	3,15
	$E \cdot 10^{5}$	4,6	4,58	4,55	4,45	4,15	4,1	3,8	3,6	3,35	3,1	2,75	2,4	2,25	2,1
Quartzite (Pervoural'skoye deposit)	$a \cdot 10^{-3}$	5,64	4,92	4,07	3,82	3,53	3,37	3,06	3,05	3,14	2,92	—	—	—	—
	λ	2,65	2,45	2,2	2,16	2,14	2,1	2,02	2,06	2,18	2,1	—	—	—	—
	c	0,47	0,5	0,54	0,565	0,605	0,625	0,662	0,675	0,695	0,72	—	—	—	—
	$\beta \cdot 10^{-5}$	—	—	—	—	1,35	1,51	1,75	1,9	2,1	2,3	2,5	3,1	3,5	4,0
	$E \cdot 10^{5}$	6,7	6,68	6,65	6,28	6,15	5,9	5,6	5,35	5,15	4,75	4,0	3,75	3,5	3,25
Martite-magnetite ferruginous semioxidized quartzite ‖ to stratification (Lebedinskiy quarry, Kursk Magnetic Anomaly	$a \cdot 10^{-3}$	1,63	1,7	1,52	1,49	1,2	1,04	0,89	0,79	0,81	1,14	0,8	0,74	0,555	0,603
	λ	0,894	0,962	0,95	1,006	0,89	0,782	0,714	0,65	0,676	1,005	0,715	0,668	0,503	0,561
	c	0,548	0,564	0,622	0,673	0,738	0,752	0,801	0,822	0,835	0,878	0,893	0,900	0,908	0,923
	$\beta \cdot 10^{-5}$	—	—	0,88	0,90	0,96	1,06	1,63	1,98	2,21	2,35	4,64	3,59	13,8	4,7
	$E \cdot 10^{5}$	5,85	—	6,41	6,44	6,02	6,44	6,02	5,78	5,6	5,2	4,48	3,62	2,89	2,77
Same, ⊥ to stratification	$a \cdot 10^{-3}$	2,02	1,95	1,75	1,62	1,4	1,37	1,215	1,2	1,09	1,01	0,91	0,865	0,85	0,826
	λ	1,1	1,1	1,1	1,084	1,032	1,032	0,974	0,99	0,93	0,881	0,815	0,776	0,761	0,761
	c	0,544	0,565	0,623	0,679	0,740	0,754	0,802	0,892	0,85	0,872	0,892	0,899	0,902	0,921
	$\beta \cdot 10^{-5}$	—	—	1,12	0,97	0,91	1,42	1,42	1,56	1,96	2,99	3,89	6,87	12,8	17,5
	$E \cdot 10^{5}$	1,6	—	1,71	1,73	1,72	1,69	1,65	1,58	1,48	1,33	1,29	0,985	0 826	0,68

Appendix 2, continued

Rock	Rock constants	Indices of Thermal Properties of Rocks at Temperature, °C													
		18	50	100	150	200	250	300	350	400	450	500	550	575	600
Amphibole-magnetite ferruginous unoxidized quartzite ∥ to stratification (Lebedinskiy quarry, Kursk Magnetic Anomaly)	$a \cdot 10^{-3}$	5,74	5,54	5,2	4,81	4,32	4,2	3,57	3,22	2,56	2,71	2,94	3,13	3,22	3,18
	λ	3,318	3,46	3,56	3,598	3,41	3,43	3,075	2,85	2,32	2,499	2,758	3,017	3,177	3,177
	c	0,58	0,625	0,686	0,745	0,79	0,82	0,86	0,887	0,905	0,92	0,94	0,962	0,98	0,997
	$\beta \cdot 10^{-5}$	—	—	0,62	0,75	0,84	1,07	1,39	1,39	2,35	2,01	2,96	3,84	9,4	9,2
	$E \cdot 10^{5}$	7,13	—	7,44	6,6	6,07	5,34	4,98	4,98	4,67	4,39	4,25	3,79	2,91	2,39
Same, ⊥ to stratification	$a \cdot 10^{-3}$	2,26	2,07	1,89	1,7	1,6	1,5	1,42	1,35	1,3	1,23	1,18	1,15	1,12	1,11
	λ	1,31	1,296	1,286	1,26	1,254	1,23	1,218	1,187	1,174	1,136	1,112	1,101	1,109	1,211
	c	0,58	0,625	0,683	0,744	0,785	0,892	0,815	0,882	0,902	0,922	0,945	0,963	0,987	0,999
	$\beta \cdot 10^{-5}$	—	—	0,95	1,11	1,11	1,22	1,34	1,77	1,95	2,81	2,67	3,18	7,29	4,15
	$E \cdot 10^{5}$	4,69	—	5,36	5,36	5,18	5,08	4,97	4,94	4,8	4,52	4,37	3,89	3,02	2,89
Oxidized ferruginous quartzite ⊥ to stratification (Mikhaylovskiy quarry, Kursk Magnetic Anomaly)	$a \cdot 10^{-3}$	3,91	—	2,57	—	2,1	—	1,94	—	1,8	Cracked		—	—	—
	λ	2,03	—	1,76	—	1,7	—	1,67	—	1,63	—	—	—	—	—
	c	0,52	—	0,685	—	0,81	—	0,86	—	0,304	—	—	—	—	—
	$\beta \cdot 10^{-5}$	—	—	—	1,2	—	1,7	—	2,2	—	2 24	—	6,3	12,0	6,0
	$E \cdot 10^{5}$	3,9	—	4,2	—	3,9	—	3,6	—	3,0	—	2,4	—	1,2	1,4
Same, ∥ to stratification	$a \cdot 10^{-3}$	3,53	—	2,12	1,96		Cracked			—	—	—	—	—	—
	λ	1,87	—	1,46	1,385	—	—	—	—	—	—	—	—	—	—
	c	0,53	—	0,69	0,709	—	—	—	—	—	—	—	—	—	—
	$\beta \cdot 10^{-5}$	—	—	—	1,05	—	1,52	—	1,6	—	2,1	—	6,2	10,5	2,3
	$E \cdot 10^{5}$	7,5	—	8,2	8,4	8,3	—	8,0	—	7,2	—	6,0	—	3,1	4,0
Semioxidized ferruginous quartzite ⊥ to stratification (Mikhaylovskiy quarry, Kursk Magnetic Anomaly)	$a \cdot 10^{-3}$	2,12	1,41	1,67	1,46	1,33	1,2	1,07	1,13	1,04	1,01	—	—	—	—
	λ	1,1	0,83	1,08	1,04	1,0	0,94	0,875	0,94	0,89	0,88	—	—	—	—
	c	0,52	0,586	0,646	0,715	0,755	0,785	0,816	0,83	0,855	0,868	—	—	—	—
	$\beta \cdot 10^{-5}$	—	—	—	1,12	1,36	1,45	—	1,62	1,7	—	2,2	3,6	7,9	4,2
	$E \cdot 10^{5}$	6,8	6,65	6,3	6,2	6,0	—	5,6	—	4,9	4,6	—	—	2,5	2,45

Note: The data given in the appendix have the following measurement units:
a - m^2/hour; c - Cal/m^3·degree; E - kg/cm^2; λ - Cal/m·hour·degree; β - degree^{-1}.

APPENDIX 3

THERMAL EFFECTS OF SOME ROCKS AND MINERALS

[35, 37]

Rock, mineral	Temperature of effect, °C	Nature of effect
Aragonite	450	Monotropic transformation
	900	Dissociation (44%)
Anhydrite	1450	Fusion
Anorthite	1500-1550	Same
Aluminum	660	Same
Albite	1100-1250	Same
Azurite	200	Decomposition
Arsenopyrite	675	Volatization
Bauxite (mixture of kaolinite and diaspore)	285-310	Dehydration
Beryl	1420	Fusion
Biotite	1100	Lattice breakdown
Bromine	58.6	Boiling
Barite	1580	Fusion
Barium	710	Same
Hydrohematite	120-140	Dehydration
	340	"
Hydromuscovite (mica group)	140-180	"
	600-650	"
	1100	"
	130-170	"
Glauconite (mica group)	550-600	"
Hematite	1390	Fusion
Halite	800	Same
Galena	1130	Fusion
	110-120	Dehydration (15.8%)
	170-190	Same
Gypsum	360	Lattice restructuring
	730-740	Disintegration of dolomite
Diopside	1391	Fusion
Dolomite	900	Dissociation
Serpentine	130-170	Dehydration
Serpentine (second type)	650-730	Same
	900	Dissociation
Iodine	113.5	Fusion
Calcite	1025	Same
	550-600	Dehydration
Kaolinite	960	Lattice restructuring
Cassiterite	1625	Fusion
Corundum	2050 ± 10	Same
Quartz	1470	Fusion

Appendix 3, continued

Rock, mineral	Temperature of effect, °C	Nature of effect
Cerargyrite	455 ± 5	Same
Covellite	501 + 10	Dissociation
Carnallite	125	Fusion
Cinnabar	1450	Same
Magnesite	373-540	Dissociation
Muscovite	125	Loss of hygroscopic water
	450-650	Loss of constitution water
	850-900	Lattice destruction
Magnetite	1590	Fusion
Manganese	1254	Same
Molybdite	795 ± 2	Fusion
Magnesium	659	Same
Malachite	200	Decomposition
Arsenic	604	Volatization
Nepheline	1526	Fusion
Olivine	1208	Same
Orthoclase	1170 ± 10	"
Pyrite	1200	"
Plagioclase	1100-1550	"
Sopiolite (talc group)	130-150	Loss of adsorption water
	800-850	Loss of constitution water
Antimony	413	Transition
	630.5	Fusion
	1640	Boiling
Siderite	350-450	Dissociation
	1000	
Sphalerite	1020 ± 10	Fusion
Smithsonite	296	Dissociation
Sulphur	96.5	Fusion
Selenium	217.4	Same
Sylvite	770	Same
Sylvite	800-840	Decomposition
Zircon	2430 ± 20	Fusion
Zinc	419	Same
Cerussite	285	Dissociation
Chalcocite	1110 ± 20	Fusion
Chrysoberyl	1820	Same
Chlorapatite	1580	Fusion
Fluorite	1392	Same
Phosphorus	280.5	Boiling
Fluorapatite	1660	Fusion

/156

APPENDIX 4

HEAT OF POLYMORPHIC TRANSFORMATIONS AND FUSION OF PRINCIPAL ROCK-FORMING MINERALS [35]

Compound	Mineral	Phase change	Temperature, °C	Δh, J/degree
Al_2O_3	Corundum	γ → α	20	0.41
		Solid → liquid	2045	1070
Au	Gold	Solid → liquid	1063	65 ± 4
$BaCO_3$	Witherite	α → β	810	97.5
$BaSO_4$	Barite	Solid → liquid	1350	174
$CaAl_2Si_2O_8$	Anorthite	Solid → liquid	1550	440
$CaCO_3$	Calcite	→ Aragonite		-21
$CaFe_2$	Fluorite	Solid → liquid	1392	220
$CaSO_4$	Anhydrite	Solid → liquid	1297	201
Cu	Copper	Solid → liquid	1084	200
CuO	Tenorite	Solid → liquid	1447	148
Cu_2O	Cuprite	Solid → liquid	1230	391
Cu_2S	Chalcocite	α → β	103	35.2
Fe	Iron	α → β	755	No data
		β → γ	903	16.36
		γ → δ	1401	78.6
		Solid → liquid	1530	279
Fe_3O_4	Magnetite	Curie point	576	No data
Fe_2O_3	Hematite	Amorphous → α	33	341
H_2O	Ice	Solid → liquid	0	32
KCl	Sylvite	Solid → liquid	770	360
KNO_3	Niter	α → β	128	58.5
		Solid → liquid	338	117.5
NaCl	Halite	Solid → liquid	80	530
$NaAlSi_3O_8$	Albite	Solid → liquid	1105	203
PbS	Galena	Solid → liquid	1114	73
S	Sulfur	Rhombic → monocline	95	11 + 1
		Microcline → liquid	119.6	38.5
		Liquid → viscous	160	11.5

/157

Appendix 4, continued

Compound	Mineral	Phase change	Temperature, °C	Δh, J/degree
Sb_2S_3		Solid → liquid	546	123
SiO_2	Stibnite	α-quartz → β-quartz	575	14.6
		α-cristobalite → β-cristobalite	250	1, 3, 2
		β-cristobalite → α-quartz	77	-117
		Quartz → liquid	1470	244
		Cristobalite → liquid	1713	142
TiO_2	Rutile	Solid → liquid	1825	597
ZnS	Sphalerite	Solid → liquid	1645	391

APPENDIX 5

DENSITY OF MINERALS AND ROCKS AT HIGH TEMPERATURE [35]

Mineral, rock	Temperature, °C	Density, g/cm3		Density difference*, %
		Crystalline state	Liquid state	
Diabase	1200	2.89-2.88	2.6-2.64	9.9-8.4
Basalt	1250	2.98	2.63	11.7
Diorite	1250	2.839	2.6	8.45
Plagioclase	1480	2.63	2.519	4.2
Copper	1083**	8.29	7.96	3.9
Pure iron	1535**	7.30	7.25	0.68
Common salt	804**	1.9	1.55	18.6
Sylvite	776**	1.766	1.524	13.6
Akermanite	1458**	2.94	2.724	7.5
Diopside	1391**	3.14	2.671	14.8

*The density difference is equal to the difference in densities of the crystalline and liquid states at the indicated temperature in % relative to density of the crystalline state.

**Melting point.

REFERENCES

1. Shreyner, L.A., Petrova, O.P., Yakushev, V.P., et al., Mekhanicheskiye i abrazivnyye svoystva gornykh porod, [Mechanical and Abrasive Properties of Rocks], Gostoptekhizdat, 1958. /158

2. Baron, L.I., Voblikov, V., "The Effect of Temperature on the Resistance of Rocks to Mechanical Destruction," IN: Fiziko-mekhanicheskiye svoystva, davleniye i razrusheniye gornykh porod, [Physico-Mechanical Properties, Pressure and Destruction of Rocks], No. 2, Izd-vo AN SSSR, 1963.

3. Suptelya, V.V., "The Study of the Dependence of Rock Strength under Uniaxial Compression from Temperature," IN: Fizika gornykh porod i protsessov, [The Physics of Rocks and Processes], Scientific Works of the MGI, No. 55, Izd-vo "Nedra", 1967.

4. Nikolin, V.I., Dudushkina, K.I., "The Strength of Sedimentary Rocks Under the Influence of Temperature," Nauchnyye trudy Magnitogorskogo gornometallurgicheskogo instituta, No. 35, 1965.

5. Yamshchikov, V.S., Viglin, V.Ye., Yegurnov, V.G., "An Apparatus for Testing 'Load-Deformation' Automatically in Compression Tests on Rocks," Zavodskaya Laboratoriya, No. 5, 1965.

6. Protod'yakonov, M.M., Koyfman, M.I., et al., Pasporta prochnosti gornykh porod o metody ikh opredeleniya, [Certification of Rock Strength and Methods of Determining it], Nauka Press, 1964.

7. Mel'nichuk, I.P., Fokeyev, V.M., "The Study of the Effects of Temperature on the Mechanical Properties of Rocks," Geologiya i razvedka, No. 7, Izv. VUZov, 1966.

8. Fokeyev, V.M., Mel'nichuk, I.P., "Some Causes of Change in the Mechanical Properties of Rocks under the Influence of Heat and Subsequent Cooling," Izv. VUZov, Geologiya i razvedka, No. 5, 1965.

9. Baydyuk, B.V., Mekhanicheskiye svoystva gornykh porod pri vysokikh temperaturakh, [Mechanical Properties of Rocks at High Temperatures], Gostoptekhizdat, 1963.

10. Griggs, D., Turner, F., Heard, H., "Deformation of Rocks at 500°C to 800°C," The Geol. Soc. Amer. Mem. No. 79, 1960.

11. Rozanov, L.N., Fiziko-mekhanicheskiye usloviya obrazovaniya tektonicheskikh struktur platformennogo tipa, [Physicomechanical Conditions for the Formation of Tectonic Structures of the Platform Type], Izd-vo Nedra, 1965.

12. Handin, J., Hager, R.V., "Experimental Deformation of Sedimentary Rocks under Confining Pressure: Tests at High Temperature," Bull. of the American Association of Petroleum, Geologists, Vol. 42, No. 12, 1958.

13. Kranse, Y., "Differential Path Method for Measuring Ultrasonic Velocities in Classes at High Temperatures," Journal Aconts. Soc. America, Vol. 35, No. 1, 1963.

14. Volarovich, M.P., Gurvich, A.S., "Study of the Dynamic Elastic Modulus of Rocks as a Function of Temperature," Izv. AN SSSR, Geofizicheskaya Seriya, No. 4, 1957.

15. Yamshchikov, V.S., Ul'trazvukovyye i zvukovyye metody issledovaniya gornykh porod, [Ultrasonic and Sonic Methods for Investigating Rocks], Izd. MIRGEN, 1964.

16. Mukhin, L.M., "Dynamic Methods for Determining Elastic Constants of Materials at High Temperatures," Zavodskaya Laboratoriya, No. 2, 1964.

17. Kalugin, B.A., Mikhaylov, I.G., "New Ultrasonic Method for Measuring the Elastic Properties of Solid Bodies at High Temperatures," Akusticheskiy Zhurnal, No. 2, 1961.

18. Yamshchikov, V.S., "Study of the Dependence of the Elastic Modulus of Rocks on Temperature," Izv. AN SSSR, Fizika Zemli, No. 10, 1965.

19. Silayeva, O.I., "Use of ultrasound for Studying the Propagation Velocities of Elastic Waves and Elastic Parameters in Rock Samples under Unilateral Pressure," Trudy Instituta Fizika Zemli imeni O. Yu. Schmidt, No. 27, 1962.

20. Rzhevskaya, V.V., Vaynshteyn, I.S., Yamshchikov, V.S., "Ultrasonic Pulse Instrument for Studying Rocks," Gornyy Zhurnal, No. 1, 1965.

21. Yamshchikov, V.S., Dobrovol'skiy, G.N., "Method for the Joint Determination of Young's Modulus and the Coefficient of Thermal Linear Expansion of Rocks," Izv. VUZov, Gornyy Zhurnal, No. 9, 1965.

22. Ziner, K., "Elasticity and Inelasticity of Metals," IN: Uprugost' i neuprugost' metallov, [Elasticity and Inelasticity of Metals], Translated from English, Metallurgizdat, 1954.

23. K'uo T'ing-sui, "Relaxation of Stresses at the Boundaries of Grains in Metals," IN: Uprugost' i neuprogost' metallov, [Elasticity and Inelasticity of Metals], Metallurgizdat, 1954.

24. Dmitriyev, A.P., Yamshchikov, V.S., "Effect of Rock Elasticity on Their Drillability by the Thermal Method," Izv. VUZov, Gornyy Zhurnal, No. 7, 1965.

25. Kuzyayev, L.S., Protasov, Yu. I., "Measuring the Surface Temperature of Rock During Thermal Drilling," Inzhenerno-Fizicheskiy Zhurnal, No. 9, 1964. /159

26. Agroskin, A.A., Fizika Uglya, [Physics of Coal], Metallurgizdat, 1965.

27. Mikheyev, M.A., Osnovy Teploperedachi, [Principles of Heat Transfer], Energoizdat, 1947.

28. Rzhevskiy, V.V., Novik, G.Ya., Osnovy Fiziki Gornykh Porod,[Principles of Rock Physics], Izd-vo Nedra, 1967.

29. Kondrat'yev, G.M., Teplovyye Izmereniya, [Heat Measurements], Mashgiz, 1957.

30. Livshits, B.G., Fizicheskiye Svoystva Splavov, [Physical Properties of Alloys], Metallurgizdat, 1946.

31. Verzhinskaya, A.B., "The Constant Intensity Source Method," IN: Teplo- i massoperenos, [Heat and Mass Transfer], Vol. 1, AN BSSR, 1962.

32. Kulakov, M.V., "Problems in Heat Conductivity with a Heat Source," IN: Teplo- i massoperenos, [Heat and Mass Transfer], Vol. 1, Izd-vo AN BSSR, 1962.

33. Dmitriyev, A.P., Dobrovol'skiy, G.N., Kuzyayev, L.S., Tret'yakov, O.N., Yamshchikov, V.S., "Determination of Some Physical Properties of Rocks for Evaluating Their Drillability by the Thermal Method," Izvestiya VUZov Gornyy Zhurnal, No. 8, 1964.

34. Tokhtuyev, G.V., Borisenko, V.G., Titlyakov, A.A., Fiziko-mekhanicheskiye svoystva gornykh porod Krivbassa, [Physicomechanical Properties of Rocks in the Krivoy Rog Basin], GITL UkrSSR, 1962.

35. Berch, F., Sherer, D., Spayser, G., Spravochnik dlya geologov po fizicheskim konstantam, [Handbook of Physical Constants for Geologists], IIL, 1949.

36. Mironov, N.P., "Thermal Characteristics of Dry and Moist Coal," IN: Doklad na vsesoyuznoy konferentsii po fizike gornykh porod i protsessov, [Report at the All-Union Conference on Rock Physics and Processes], Izd-vo MIRGEM, 1965.

37. Berg, L.G., Termografiya [Thermography], Izd-vo AN SSSR, 1960.

38. Rybakov, V.M., Voshchanov, K.P., Tekhnologiya Rudnoy Dugovoy Svarki, [Technology of Ore Arc Welding], Mashgiz, 1953.

39. Borisov, V.N., Zasetskiy, L.P., "Principal Physicochemical Properties of Sulfur. Native Sulfur," Trudy GIGKhS, No. 6, Izd-vo GIGKhS, 1960.

40. Lakhtionov, M.O., Tarkhov, A.G., "Experience in Thermal Prospecting in the Copper Pyrite Deposits of the Urals," Izv. VUZov, Geologiya i razvedka, No. 5, 1967.

41. Dmitriyev, A.P., Kuzyayev, L.S., Termodinamicheskiye protsessy v gornykh porodakh, [Thermodynamic Processes in Rocks], No. 1, Izd-vo MGI, 1967.

42. Lyubimov, I.S., "Phase Transformations and the Polymorphism Phenomenon in Rocks," Nauchnyye Trudy MIRGEN, No. 52, Izd-vo MIRGEM, 1964.

43. Arens, V.Zh., Novik, G.Ya., Shostak, A.G., Podzemnaya vyplavka şery, [Underground Sulfur Extraction], Izd-vo Naukova Dumka, 1967.

44. Ostrin, Yu.F., "Possibility of Measuring Hall emf by the Two Current Methods," FTT, Vol. 6, No. 9, Izd-vo AN SSSR, 1964.

45. Brandt, A.A., Issledovaniye dielektrikov na sverkhvysokikh chastotakh, [Study of Dielectrics at Superhigh Frequencies], Izd-vo Fiz.-Mat. Lit., 1963.

46. "Physics of Dielectrics", Trudy konferentsii, Izd-vo AN SSSR, 1956.

47. Tisher, F., Tekhnika izmereniy na sverkhvysokikh chastotakh, [Techniques for Measurements at Superhigh Frequencies], Izd-vo Fiz.-Mat. Lit., 1963.

48. Tamm, I.Ye., Osnovy teorii elektrichestva, [Principles of the Theory of Electricity], Izd-vo Fiz.-Mat. Lit., 1962.

49. Kobranova, V.N., Fizicheskiye svoystva gornykh porod, [Physical Properties of Rocks], Gostoptekhizdat, 1962.

50. Smith, R., Poluprovodniki, [Semiconductors], Izd-vo Fiz.-Mat. Lit., 1963.

51. Kittel', C., Vvedeniye v fiziku tverdogo tela, [Introduction to Solid State Physics], Izd.vo Fiz.-Mat. Lit., 1962.

52. Parkhomenko, E.I., Elektricheskiye svoystva gornykh porod, [Electric Properties of Rocks], Izd-vo Nauka, 1965.

53. Gilman, J., "Mechanical Properties of Ionic Crystals," UFN, Vol. XXX, No. 3, IIL, 1964.

54. Skanavi, G.I., Fizika dielektrikov, [Physics of Dielectrics], Part 1, Izd-vo Tekhn.-Teor. Lit., 1949.

55. Stratton, J., Teoriya elektromagnetizma, [Theory of Electromagnetism], Izd-vo Tekhn.-Teor. Lit., 1950.

56. Belen'kiy, P.G., Protasov, Yu.I., Ushakov, Yu.A., "Effect of Mass Transfer on Crystal Strength," IN: Fizika gornykh porod i protsessov, [Physics of Rocks and Processes], MIRGEN, Izd-vo Nedra, 1965.

57. Kuzyayev, L.S., Protasov, Yu. I., "Determination of the Iron Content from Magnetic Permeability in a Magnetite-Silica Mixture," IN: Fiziko-tekhnicheskiye problemy razrabotki poleznykh iskopayemykh, [Physical-Technical Problems in Mineral Extraction], No. 2, 1967.

Translated for the National Aeronautics and Space Administration under contract No. NASw-2038 by Translation Consultants, Ltd., 944 South Wakefield Street, Arlington, Virginia 22204.

"The aeronautical and space activities of the United States shall be conducted so as to contribute . . . to the expansion of human knowledge of phenomena in the atmosphere and space. The Administration shall provide for the widest practicable and appropriate dissemination of information concerning its activities and the results thereof."

—NATIONAL AERONAUTICS AND SPACE ACT OF 1958

NASA SCIENTIFIC AND TECHNICAL PUBLICATIONS

TECHNICAL REPORTS: Scientific and technical information considered important, complete, and a lasting contribution to existing knowledge.

TECHNICAL NOTES: Information less broad in scope but nevertheless of importance as a contribution to existing knowledge.

TECHNICAL MEMORANDUMS: Information receiving limited distribution because of preliminary data, security classification, or other reasons.

CONTRACTOR REPORTS: Scientific and technical information generated under a NASA contract or grant and considered an important contribution to existing knowledge.

TECHNICAL TRANSLATIONS: Information published in a foreign language considered to merit NASA distribution in English.

SPECIAL PUBLICATIONS: Information derived from or of value to NASA activities. Publications include conference proceedings, monographs, data compilations, handbooks, sourcebooks, and special bibliographies.

TECHNOLOGY UTILIZATION PUBLICATIONS: Information on technology used by NASA that may be of particular interest in commercial and other non-aerospace applications. Publications include Tech Briefs, Technology Utilization Reports and Technology Surveys.

Details on the availability of these publications may be obtained from:

SCIENTIFIC AND TECHNICAL INFORMATION OFFICE

NATIONAL AERONAUTICS AND SPACE ADMINISTRATION

Washington, D.C. 20546